Towards Sustainable Additive Manufacturing: Assessment of Cost, Greenhouse Gas Emission, and Recyclability

A Dissertation Submitted to

The University of Texas at Arlington

by

Lei Di

In partial fulfillment of the requirements for the degree of

Doctor of Philosophy, Industrial Engineering

August 2023

Department of Industrial, Manufacturing, and Systems Engineering

Dissertation Committee:

Committee Chair: Dr. Emma Yang
Ph.D. Program Advisor: Dr. Victoria Chen, Director of Doctoral Studies
Committee Members: Dr. Shouyi Wang, Dr. Chen Kan, Dr. Narges Shayesteh

Acknowledgment

In the beginning, I would say thanks to my supervisor Professor Emma Yang to guide me well throughout the research work from the title's selection to finding the results. Her immense knowledge, motivation, and patience have given me more power and spirit to excel in research writing. Conducting the academic study regarding such a difficult topic couldn't be as simple as she made this for me. She is my mentor and a better advisor for my doctoral study beyond the imagination.

Apart from my Supervisor, I won't forget to express my gratitude to the rest of the Committee team: Professor Victoria Chen, Professor Shouyi Wang, Professor Chen Kan, and Professor Narges Shayesteh, for giving encouragement and sharing insightful suggestions. They all have played a major role in polishing my research writing skills. Their endless guidance is hard to forget throughout my life.

I would always remember my fellow lab mates too for the fun time we spent together, the sleepless nights that gave us the courage to complete tasks before deadlines and for stimulating the discussions. I would also like to thank my friends from the University of Texas at Arlington.

In the end, I am grateful to my parents, friends, and all the family. I consider myself nothing without them. They gave me enough moral support, encouragement, and motivation to accomplish my personal goals. My parents have always supported me financially so that I only pay attention to my studies and achieve my objective without any obstacles in the way.

Abstract

Additive Manufacturing technologies fabricate 3D objects layer by layer following a predesigned CAD model. Owing to the unique layer-wise production method, additive manufacturing offers competitive advantages in comparison with traditional subtractive manufacturing, such as shortened production time, increased design freedom, improved manufacturing capability and complexity, and reduced manufacturing waste. Numerous research studies have been conducted to design, understand, and improve additive manufacturing technologies in order to facilitate the implementation in the supply chain. On the other hand, with the rapid growth of additive manufacturing, sustainability issues that exist on both process level and supply chain level have started to receive increasing public interest. The current literature on additive manufacturing sustainability is mostly focused on process energy consumption, emission, and cost evaluation, towards establishing the life cycle inventory for additive manufacturing and life cycle assessment. Research questions on how to evaluate the recyclability of additive manufacturing waste and how to evaluate the feasibility of additive manufacturing implementation in the supply chain in terms of cost and greenhouse gas emission have not yet been investigated. A comprehensive understanding of material recyclability and additive manufacturing supply chain performance is critical to evaluate the feasibility of large-scale implementation of additive manufacturing towards the circular economy.

To fill the knowledge gaps mentioned above, this Ph.D. dissertation aims to establish mathematical models to quantify the cost and greenhouse gas emission of additive manufacturing supply chains and improve performance through supply chain structure innovation and delivery route optimization. Case study results suggest that the overall supply chain cost can be reduced by up to 25.75% and the greenhouse gas emission can be reduced by up to 26.43% when using additive manufacturing in the supply chain. Results also indicate the potential to achieve same-day delivery

with less than $20 per order and over 90% delivery rate in 3 hours by properly coordinating the visiting/fabricating sequence. In addition, this Ph.D. dissertation also aims to develop a framework to evaluate the recyclability of additive manufacturing thermoplastic wastes, embedded with quantified tools to investigate the process parameters and their impact on material recyclability in terms of fabrication quality, mechanical properties, and molecular weight distributions. Experimental results indicate that ultimate tensile strength degradation after each round of recycling varies from 27% to 50%, the surface roughness increases by 29.54% after three rounds of recycling, and molecular weight distribution of recycled material demonstrates an obvious shift in each round of recycling.

The results generated from this Ph.D. dissertation will help additive manufacturing designers, manufacturers, and users better understand the waste recycling process and design/optimization of additive manufacturing supply chain. The ultimate goal of this research is to facilitate the large-scale implementation of additive manufacturing while achieving circular economy and enabling sustainable additive manufacturing.

Content

List of Tables

List of Figures

Chapter I. Introduction

1.1 Introduction on Additive Manufacturing Technologies

Additive Manufacturing (AM), also known as 3D printing, rapid manufacturing, or rapid prototyping, refers to a collection of technologies that fabricate parts by joining materials layer upon layer based on the three-dimensional computer-aided design model data. Compared with traditional substrative manufacturing, AM presented advantages on saving production time and cost, reducing human interaction, increasing geometry complexity, and improving manufacturing quality. As the popularity of AM expand in the world and the demand for AM machines increase since the 1990s, various AM technologies have been invented and commercialized based on different principles, materials, and mechanisms, including photopolymerization, binder jetting, extrusion-based, powder bed fusion, sheet lamination, and direct energy deposition. All the processes have a common feature: the model is fabricated by adding layer by layer from raw material, rather than removing or deforming materials through machining, milling, curving, and shaping as in the conventional manufacturing process.

Owing to the unique characteristics ensured by the layer-wise fabrication technique, AM technologies have been implemented for a wide range of applications. The major applications of AM technologies are extended to different modern industries including manufacturing, medicine, electronics industry, aerospace industry, and other fields. In particular, the major applications of AM technologies include prototyping for products in development, medical models, and computer hardware, building concept models in early stages, fabricating lightweight parts for aerospace with complex geometries, and repairing and overhauling for aerospace, defense, and biomedical applications. Numerous research studies have been performed to investigate the advantages and challenges of adopting AM in place of traditional manufacturing (TM) systems [1]–[3].

With the enhanced manufacturing capabilities offered by AM technologies, the global market of AM industries is and will be significantly increasing for decades. According to Wohler's Report 2022, even with the impact of the Covid-19 pandemic, the global AM products and services grew by 19.5% in 2021 to more than $15.2 billion [4]. With the huge potential in the global market, AM is fast becoming integrated with mainstream manufacturing in the world prominent companies, such as Airbus, Boeing, GE, Ford, and Siemens, are attempting a leap into Industry 4.0 [5]. In the worldwide range, AM is taking an important position in both national and supranational agendas to achieve higher international influence as indicated in Figure 1 [6]. For example, the United States (U.S.) of America is now adopting AM in almost every manufacturing sector by leading industries. AM has offered a great opportunity of consolidating its competitiveness in progressing U.S. innovation. Within the global AM revenue share, the U.S. takes around 35% as a result of the massive adoption of AM in different industries [4]. In European Union, AM has offered the value of creating 1.6 million jobs and an amount of 11% of production [7]. In addition, Asia Pacific is gradually increasing its competitiveness with embark on AM through research investment [5]. Continuous support, investment, and all other necessary resources from both public and private sectors have made Asia Pacific a potential manufacturing hub in the upcoming decades [8].

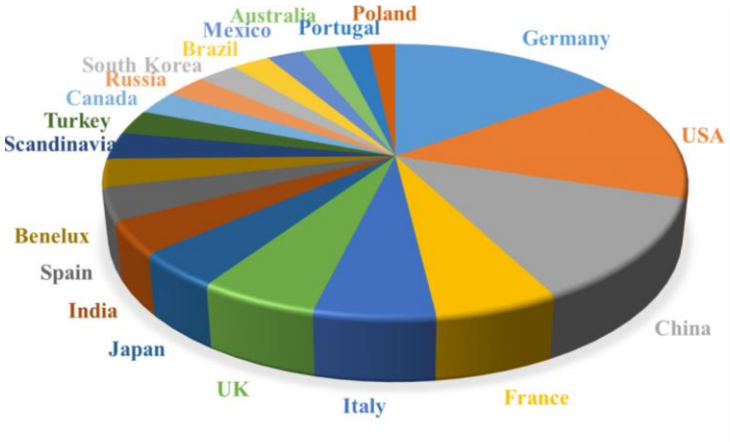

Figure 1. Top 20 global AM markets [6]

Despite the tremendous growth of AM market, some limitations still need to be overcome for further implementation in various industries unconditional acceptance in mission-critical industries. First, AM is more suitable for high-value low volume productions but no proper for large-scale mass manufacturing. Although research efforts have been made to explore the potentiality of large-scale AM [9]–[11], it will still take some time to fully replace conventional manufacturing with AM. Second, certain specific AM processes have limitations on the type of materials, the need for post-processing, generating the greenhouse gas (GHG) emission, the possible consumption of energy, and the requirement of accurate and precise 3D model data, etc. In addition, environmental and economic sustainability issue caused by waste in AM has raised increasing concerns. Potential opportunities in recycling waste make AM a driving technology enabling cleaner production.

1.2 Introduction on Sustainability Issues in Additive Manufacturing

With the increasing development and application, the sustainability issues of AM process require to be carefully evaluated and controlled. The impact of AM on current supply chain models focuses on the supply chain network structure and the supply chain costs [12]–[14].

Although AM has shown to be cost-effective for manufacturing small batches with continued centralized manufacturing [15], some limitations in AM cost can be a problem in the process of replacing conventional manufacturing for mass production in the supply chain for the future. Potential cost issues in AM include high machine and material costs, high energy costs caused by parts geometry complexity, and training costs for the labor to manipulate the AM machines, etc.

Environmental issues of including energy consumption, GHG emissions, and AM process emissions. Some specific AM processes apply high energy-intensive components, for example, laser unit or heating modulus, that can possibly lead to high electricity consumption. This will lead to an increase in GHG emissions and lead environmental problems. As indicated in Figure 2 [16],

the transportation in AM supply chain is another important contribution to GHG emissions. In addition, certain types of AM material, such as acrylonitrile butadiene styrene (ABS), polylactic acid (PLA), and nylon, may be vaporized and cause particulate matter emissions as well as toxic gas emissions during the printing process.

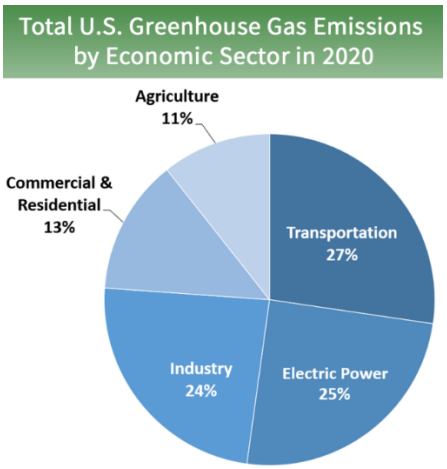

Figure 2. Total U.S. Greenhouse Gas emissions by economic sector in 2020 [16]

AM waste is another sustainability issue. Multiple reasons cause AM waste include fail parts, inappropriate geometry designs or process parameter settings, removed support structures, wasted filament in case of machine misfunctions, abandoned parts, used parts because of insufficient property or functionality, etc. Specifically, AM waste generates in different stages of AM process including fabrication, use, and end-of-life phase. Without proper treatment, the AM waste can be a tremendous problem with the application of AM in various industries.

This dissertation aims to answer three research questions proposed as follows.

RQ1. Is it cost-effective to adopt AM technologies in the manufacturing supply chain, in comparison with traditional manufacturing? If yes, how to achieve the optimal route design in order to save supply chain costs?

Traditional supply chain models used by e-commerce platforms such as Amazon in the U.S. and JD in China can accommodate the same-day deliveries of products stored in the front warehouse,

but they cannot be directly used to handle the highly customized goods due to the long production time and transportation. The same-day delivery of customized goods, however, can be achieved with the capabilities of AM by leveraging the production-inventory-transportation (PIT) structure. This new supply chain structure has received increasing research interest. For example, the supply chain costs of a local PIT structure were mathematically modeled and compared in cases of AM or traditional manufacturing [17]; In addition, the greenhouse gas emission generated throughout the PIT structure was thoroughly studied [18]. The results suggest that the overall costs and GHG emissions can be significantly reduced by adopting the unique PIT structure. Moreover, this mobile structure was adopted in a supply chain that consists of disassembly centers and remanufacturing centers for end-of-life products [19]. In this dissertation, the disassembly line balancing problem and routing problem were mathematically formulated as Nonlinear Programming and solved by GAMS/SCIP, resulting in the conclusion that the mobile AM supply chain can lead to reduced inventory costs.

RQ2. Is it environmentally friendly to adopt AM technologies in the manufacturing supply chain?

The impact of AM on current supply chain models is attributed to the unique capabilities of AM to fabricate highly customized products, reduction in the number of sequential operations or processes that need to be performed during production, and opportunities for more robust logistic models. In current literature, numerous analysis-driven, comparative studies on AM and TM supply chains, which use data collected from existing literature as the primary data source and survey information from industry experts as the secondary data source, have been conducted [20]–[22]. It has been revealed that various aspects of the traditional supply chain such as inventory and logistics, mass customization and portable manufacturing, the relevance of digital supply chains, and future supply chain trends like cloud manufacturing, will be influenced by AM [20]. Also,

AM has demonstrated the capability of reducing the cost of mass customization, leading consumers to become micro-manufacturers, and enabling less lead time [21]. This indicates the potential of AM for enabling more local, globally-connected, and efficient supply chain structures. Integrating AM with the supply chain has shown the potential in reducing inventory and transportation costs, owing to the change from make-to-stock to a make-on-demand product cycle [22].

RQ3. To enable a circular economy in AM, how to achieve high-quality waste recycling?

With the rapid growth of the AM market, potential sustainability issues caused by AM waste have raised increasing attention. Different reasons that lead to potential waste in AM include failed parts, inappropriate geometry designs, and process parameter settings, removed support structures, wasted original material based on machine misfunctions, and use of parts because of insufficient property or functionality. AM waste generates in different stages of AM process including fabrication, use, and end-of-life phase. To recycle waste materials and reuse them back to 3D printing, especially for polymer wastes, a mechanical process was developed to process waste pellets into reusable filaments for extrusion-based AM [23]. Similarly, unused metal powder for AM is collected and recycled after the seizing process for further production. The such closed-loop material flow will increase material efficiency and reduce the potential adverse environmental impact of AM thermoplastics. Plastic waste usually persists on earth for at least decades [24] and causes serious environmental damage. In addition, facilitating closed-loop material flow in AM also has economic benefits, as indicated in a research study that recycling polymer-based AM waste presents great economic potential, especially in the case of customized or commercial sporting goods [25]. To enable the circular economy, the potential opportunity lies in recycling AM waste with high quality.

Chapter II. Literature Review

In this Chapter, an overview of current literature on the sustainability issues of AM, including the impact on supply chain and AM waste recycling, is illustrated. More specifically, a comprehensive literature review on AM supply chain cost is presented in Section 2.1.1. A literature review on GHG emissions for AM supply chain is discussed in Section 2.1.2. The current studies on route design for AM supply chain is reviewed in Section 2.1.3. The existing academic research studies are reviewed and discussed in detail in Section 2.2.

In current literature, numerous analysis-driven, comparative studies on AM and TM supply chains, which use data collected from exist literature as the primary data source and survey information from industry experts as the secondary data source, have been conducted [20]–[22]. It has been revealed that various aspects of the traditional supply chain such as inventory and logistics, mass customization and portable manufacturing, the relevance of digital supply chains, and future supply chain trends like cloud manufacturing, will be influenced by AM [20]. Also, AM has demonstrated the capability of reducing the cost of mass customization, leading consumers to become micro-manufacturers, and enabling less lead time [21]. This indicates the potential of AM for enabling more local, globally connected, and efficient supply chain structures. Integrating AM with the supply chain has shown potential in reducing inventory and transportation costs, owing to the change from make-to-stock to make-on-demand product cycle [22].

2.1 Literature Review on Additive/Traditional Manufacturing Supply Chain

2.1.1 Cost of Additive Manufacturing Supply Chain

In the current literature, several detailed analyses on the AM supply chain have been conducted. For example, a systematic analysis has been performed to explore the effects of AM technology adoption on supply chain management in an engineer-to-order environment [26], leading to the conclusion that a change to AM technique affects both internal processes (e.g., manufacturing

order fulfillment) and external processes (e.g., supply chain). Also, different types of commercial AM technologies (e.g., stereolithography, fused deposition modeling, selective laser sintering, etc.) and their impacts on supply chain logistics costs have been investigated and the results have shown that different AM processes have substantial impacts on both upstream supply chain and downstream customer orders [12]; which, in turn, leads to reduced warehousing and shipping, increased mass customization, and reduced logistics cost. Furthermore, an action research method has been adopted to study the effect on cost and revenue of companies who invest in 3D printing considering multiple supply chain processes such as source, make, deliver, and return [27].

Alongside the analysis-based literature, simulation and analytical based studies have been conducted to better understand the difference between TM and AM supply chains. For example, a simulation model has been developed to compare the supply chain networks of TM and AM [28] by performing case studies in healthcare applications. This work shows that shortened lead time and an increased number of customer orders could be achieved through 3D printing enabled supply chain networks. Another simulation-based method has also been developed to model an AM supply chain in the lamp industry [29], and the results show that AM can improve the lead time and total supply chain cost. Meanwhile, a more detailed model has been established which shows different conditional parameters under which low part demands are economically satisfied using on-demand selective laser sintering rather than conventional injection molding [30]. Also, a regression model has been developed to formulate the supply chain cost of products manufactured by AM using the Mean Absolute Percent Error of 16% [31]. Meanwhile, a stochastic cost model that leverages the customized Sample Average Algorithm has been established to quantify the cost associated with the production [32] and the system-level costs such as inventory and transportation.

In addition to the benefits of the AM supply chain, it is important to consider how supply chain performance would change considering the different supply chain structures enabled by AM. In current literature, comparative studies have been performed to evaluate centralized and distributed supply chain configurations of AM and TM [15], [33]–[37]. For example, it has been found that adopting rapid manufacturing in centralized structure results in a reduction in the inventory holding cost, while distributed structure eliminates inventory holding and transportation, and reduces the response time in the spare parts supply chain [33]. Another systematic and quantitative analysis has been conducted to explore the structure of AM research domains in the scope of management, business, and economics [34], and has concluded that though distributed structure shows potential advantages (improved service and reduced inventory), the centralized structure is still the most feasible option. AM has shown to be cost-effective for manufacturing small batches with continued centralized manufacturing. However, with an increasing level of automation, distributed production may become more cost-effective [15].

The current literature has suggested that integrating AM with the supply chain has a positive and significant impact, as it can lead to a reduction in the total cost compared to TM [13], [38]. Most of the existing studies on the AM supply chain are comparative case studies aiming to analyze the benefits and challenges in the AM supply chain. Comprehensive theoretical models on AM supply chain costs have not yet been sufficiently studied, resulting in the lack of abilities in cost evaluation and optimization. Besides, the current literature is mainly focused on two types of supply chain structures, i.e., centralized and distributed; while neglecting a unique, AM-enabled supply chain structure where production, inventory, and transportation stages are combined into one, owing to the capabilities of AM in quick, simplified production and less need for labor involvement.

2.1.2 GHG Emissions of Additive Manufacturing Supply Chain

The current GHG emission issue has been obtaining increasing public attention due to its impact on accelerating the rate of climate change [39]. Research studies show that GHG emission can affect the global temperature [40], soil quality [41], and agriculture [42]. The major economic sectors contributing to the U.S. GHG emission are transportation (28%), electricity (27%), and industry (27%) [43], and they are closely related to the manufacturing supply chain. Researchers have been studying the GHG emissions from TM since 1996 [44]–[48]. Efforts have been dedicated to exploring the potential of reducing GHG emissions and the associated supply chain profitability [49]. A three-dimensional carbon footprint model of the supply chain is proposed for the practice of green supply chain management [50]. A conceptual framework for measuring and analyzing the carbon footprint in the supply chain for the purpose of reducing CO_2 emission and improving efficiency is proposed [51].

Most GHG emission studies in the current literature are focused on the production process. A systematic approach is presented to estimate the GHG emission during manufacturing using data from concrete manufacturers [52]. A GHG emission monitoring system is developed to monitor the emission in real-time during the process of building construction [53]. In addition, some studies are focused on establishing models to quantify carbon footprint in the supply chain to reduce GHG emissions. A detailed model of production carbon footprint across the supply chain is proposed in the literature to analyze the supply chain of an agricultural machine [54]. A mathematical model is applied using analytical and finite difference methods to reduce the GHG emission in the food supply chain [55]. A carbon footprint model is proposed considering technical and pricing policies to reduce GHG emissions [56]. A mixed-integer linear programming model is developed to minimize the total cost of the supply chain with reduced GHG emission [57]. The current literature suggests a lack of mathematical models on GHG emission for AM-enabled supply chains. To fill

this research gap, a GHG model will be established in this work, quantifying the potential GHG emissions generated from TM and AM supply chains. Specifically, a unique AM-enabled PIT structure will be explored for its potential of reducing GHG emissions.

2.1.3 Route Design for Supply Chain

The delivery route design is critical to the overall supply chain management as it has an evident impact on delivery time, cost, and overall supply chain capacity. In a traditional supply chain, the delivery route design problem is usually defined as the Travelling Salesman Problem (TSP) or the Vehicle Routing Problem (VRP), where the products are completed at the manufacturing plant and then delivered to the customers by vehicles [58], [59]. In such cases, the delivery routes are optimized in a static environment by minimizing the delivery costs. These combinatorial optimization problems are often formulated as Mixed-Integer Programming (MIP) models and they can be solved by exact methods such as dynamic programming, branch-and-bound, cut plane, and branch-and-price, and heuristic methods such as greedy rules, local search, and meta-heuristics [60]–[65].

On the other hand, in the AM-enabled PIT structure, the route design problem becomes more complicated due to the simultaneous occurrences of delivery and production. Therefore, the visiting sequence to customers and the fabricating sequence of products need to be optimized simultaneously in order to minimize the total cost while completing the delivery as soon as possible and satisfying customers' requirements. In these cases, more decision variables need to be considered in the mathematical model compared with classic TSP or VRP, leading to more constraints that formulate the relationships among different variables. Meanwhile, because the customers' orders can be submitted any time during the workday, the decision (on delivery route design) needs to be made dynamically without the perfect information. To solve this complex problem more efficiently, this dissertation will approach this problem by analyzing the problem

structure first, then establishing the corresponding models for different scenarios, and developing the optimization algorithms accordingly. This work aims to not only generate the delivery routes for known existing customers like classic VRP but also provide solutions for the integrated PIT supply chain in the real-world environment.

2.2 Literature Review on AM Waste Recycling

In current literature, research studies have been conducted focusing on the waste recycling of AM thermoplastics from different perspectives. For example, a unique print head was designed to achieve the functions of fabricating oversized components and recycling wastes from various types of plastic [66]. The mechanical characteristics of AM thermoplastic waste were evaluated and an upgrade processing method for recycling the waste was proposed [67]. Furthermore, the recycling of AM thermoplastic has been investigated in the perspective of the life cycle impact. For example, a life cycle analysis was performed considering recycling polyethylene filament, indicating 80% of energy saved when using properly distributed recycling operation [68]. A life cycle assessment was conducted on recycling PLA waste, showing that waste recycling can achieve significant environmental savings compared to other methods like landfill and incineration [69]. To date, only a limited number of research studies have been dedicated to studying multiple rounds of recycling and characterizing variations of material and mechanical properties of waste materials. An exploratory study was performed to evaluate the tensile properties of PLA waste after multiple recycling rounds and mechanical degradation was observed [23]. Polyamide 12 was tested for its mechanical properties after multiple recycling rounds, and the results show that the overall mechanical behavior was enhanced first and then degraded rapidly after a specific recycling course [70]. The commercial ABS filament compounded with heat stabilizer was investigated focusing on its thermal degradation behavior, indicating good applicability for 3D printing even after multiple recycling rounds [71].

The state-of-the-art research on AM thermoplastic waste recycling suggests a decrease in mechanical properties after one or multiple rounds of recycling, which could be compensated by adjusting the values of process parameters. Numerous research studies indicate that different combinations of process parameters in extrusion-based AM can lead to various levels of fabrication quality and mechanical properties. For example, process parameters including infill density, extruder temperature, raster angle, and layer thickness were found to affect mechanical properties including tensile strength, yield strength, modulus of elasticity, and elongation of PLA parts fabricated by FDM [72]. Process parameters including extruder temperature, platform temperature, and printing speed were found to have a remarkable influence on the adhesion force of fabricated parts [73]. In summary, the current literature confirms the mechanical degradation of thermoplastics caused by the recycling process, and the selection of process parameters can greatly affect the AM fabrication quality. Based on the literature, no efforts have been dedicated to investigating the effect of different combinations of printing parameters in different recycling rounds with the purpose of compensating for the mechanical degradation caused by waste recycling. Furthermore, the root cause for mechanical degradation that occurs in AM waste recycling has not yet been well studied. This indicates a research gap in better understanding the material recyclability of AM thermoplastics. Based on the literature review, questions arisen include how to define and estimate material recyclability in multiple recycling rounds; how the printing parameters affect the recyclability; and how the effects change the material recyclability in multiple rounds.

To address these questions, this dissertation aims to assess the recyclability of AM thermoplastics under multiple rounds of recycling by proposing an assessment framework integrating the manufacturing parameters. In this work, material recyclability is defined as the ability of materials

in terms of being recycled and reused back in 3D printing with satisfactory material properties, fabrication quality, and mechanical properties. To demonstrate the implementation of the framework, experiments are performed to characterize the potential variations of material recyclability of ABS waste undergoing multiple recycling rounds. Different combinations of printing parameters are also explored for their impact on compensating for mechanical degradation caused by waste recycling. The potential causal relationship between molecular weight distribution and mechanical degradation is also investigated. This relationship can be utilized to determine the process parameters in different recycling rounds to compensate for material degradation. This paper serves as a preliminary work for understanding the material recyclability in AM, and the results of this dissertation will help guide high-quality waste recycling in AM towards higher material efficiency and closed-loop material flow. This dissertation also aims to promote awareness of AM recycling and sustainable manufacturing.

Chapter III. Implementation of Additive Manufacturing in Supply Chain: Cost and Greenhouse Gas Emission

Additive manufacturing, according to its advantages in design flexibility, enhanced quality, inventory reduction, and shorten lead times, has been adopted in the supply chain to enhance the operations and improve the customer satisfactions. The game-changing impact of AM on supply chains has been observed in the literature [74]–[76]. In literature, an integrated PIT structure is proposed integrating the production, inventory, and transportation stages in one by installing the AM machine on the vehicle [77]. In the structure, the AM process can be proceeded during the process of delivery. The supply chain structure not only diminishes the need for warehouses to store the inventory for the products awaiting delivery but also reduces the leading time for customers. In the innovative AM integrated PIT supply chain, the total supply chain cost is greatly influenced by saving the response time to customer, reduction in inventory holding cost and the cost of transportation from far off locations. The environmental impact is influenced by the reduction of transportation and production time. It is important to establish cost and GHG emission models to indicate the advantages of an AM integrated PIT supply chain compared with a TM supply chain. This PIT structure takes advantage of the unique capabilities of AM with respect to fast production and reduced or even eliminated need for labor involvement. There is also a potential benefit that, with proper route design, the AM integrated PIT supply chain can enlarge its advantages of delivery efficiency.

In this Chapter, the AM integrated supply chain is investigated in the perspective of cost and greenhouse gas emission analysis. Section 3.1 will focus on the cost model of the traditional supply chain and AM integrated PIT supply chain. Section 3.2 will focus on the route design problem of the AM integrated PIT supply chain. Section 3.3 will focus on the GHG emission analysis of the

traditional and innovative supply chain. Section 3.4 will discuss the contribution and the potential applications of the established models in this Chapter.

3.1 Cost Modeling of the TM Supply Chain and AM Integrated PIT Supply Chain

3.1.1 Cost Modeling of the TM Supply Chain

For manufacturing facilities equipped with traditional manufacturing machines, they rely on 1) the pre-stock of semi-finished components, and 2) on-demand fabrication of customized designs. In this Section, a local manufacturing facility producing the products with high level of customization, such as consumer goods or medical devices, is considered. A typical TM supply chain can be illustrated in Figure 3. In a TM supply chain, orders are submitted to the manufacturers by customers through retailors. The manufacturer organizes the orders and generates a manufacturing plan. The manufacturer takes pre-stocked semi-finished products from the inventory for production. After the production is completed, the final products are delivered to the warehouse for dispatching, packaging, and sorting. Finished products are delivered to retailors for the customers to pick up in the TM supply chain structure. To simply the modeling, a few assumptions are made as follows. Specifically, for customers, it is assumed that 1) customers submit their orders at a retail location that is the closest to their home address w.r.t. distance; and 2) customers can submit their orders to the retailors anytime during the workhour of service. For retailors, it is assumed that they are operated at a fixed work schedule, and they submit their received order to the manufacturer at a fixed schedule. For the manufacturer, 1) the manufacturer receives customization orders solely from its collaborative retail network, and they do not accept individual orders from customers; 2) the manufacturer has a fixed work schedule; 4) the manufacturer handles transportation in-house and has trucks to deliver finished products to retailors, who then inform the customers for pickup; and 5) the manufacturer sends out delivery trucks to the retailors at a fixed schedule.

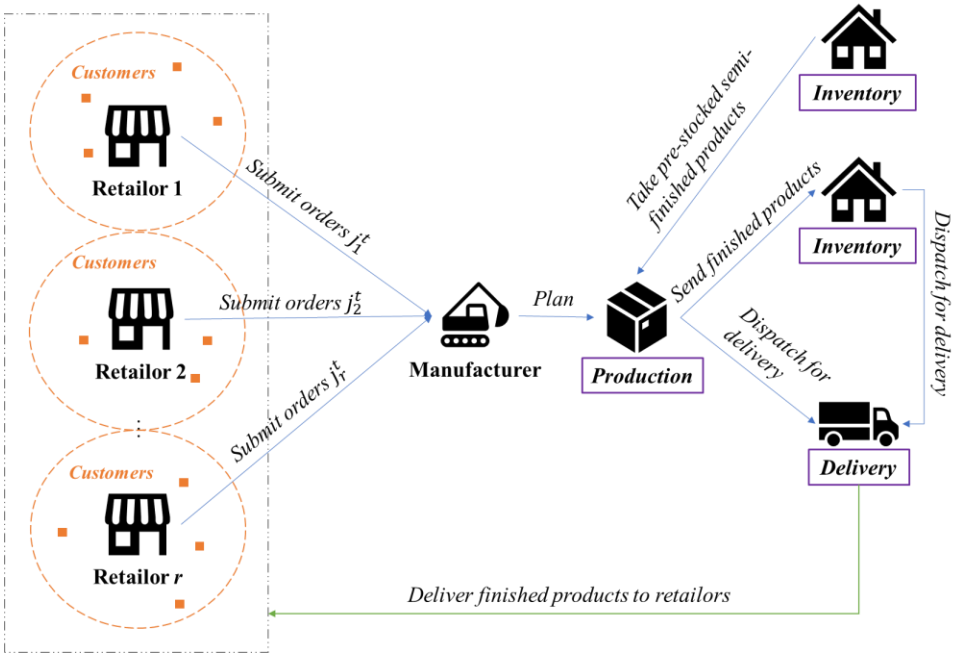

Figure 3. An example of the supply chain structure of a traditional manufacturing facility

The total supply chain cost C_{TM} is contributed by the production cost PC_{TM}, the delivery cost DC_{TM}, and the inventory cost IC_{TM}.

$$C_{TM} = PC_{TM} + DC_{TM} + IC_{TM} \tag{1}$$

Traditional Manufacturing Production Cost

Let r be the index of retailors, $r \in R$, where R represents a set of retailors that are in the manufacturer's retail network. Let t be the index of retailors' workdays (assuming all retailors have the same work schedule), and j_r^t be the index of customized orders submitted to retailor r on day t, $j_r^t \in \{1, J_r^t\}$ where J_r^t denotes the total number of customization orders received at retailor r on day t. Each individual order has different customization levels, which can significantly affect the required processing time. Let $\theta(j_r^t)$ be the customization level of the order j_r^t. The traditional manufacturer handles two types of orders, i.e., new orders submitted from retailors, and rework orders returned from the retailors and customers. In practice, products with higher customization level often have lower satisfaction level comparing to standardized products with no customization

freedom; that requires rework to adjust and/or improve the products based on retailors or customers' feedback. φ is defined to represent the average rework rate of this manufacturer's product and assume for every new order that is submitted to the manufacturer, φ rework order is also requested. Hence, on workday t, the manufacturer receives total J_r^t new orders from retailor r and receives total $(\varphi \times J_r^t)$ rework orders from the same retailor.

It is assumed that this manufacturer only produces one type of product, and this product is assembled with several components. Let n be the index of components required to assemble the final product, and N be the total number of required components. The production cost for a new order j_r^t includes the raw material purchase cost for each component (transportation included) MC_{TM_n}, the processing cost (from raw material to semi-finished parts) for each component SC_{TM_n}, and the final assembling cost $AC_{TM}(j_r^t)$.

$$PC_{TM}(j_r^t) = AC_{TM}(j_r^t) + \sum_{n=1}^{N} \left(MC_{TM\_n} + SC_{TM\_n}\right) \quad (2)$$

The assembling cost $AC_{TM}(j_r^t)$ is considered to be related to the customization level $\theta(j_r^t)$ of the final product and can be formulated as follows.

$$AC_{TM}(j_r^t) = AC_{TM_0} \times (1 + |\theta(j_r^t) - \theta_0|) \quad (3)$$

In this equation, AC_{TM_0} refers to the base assembling cost for a product with no customization requests, and θ_0 represents the complexity level of the product with no customization requests. In this Section, the complexity level is defined as the ratio of product volume and the bounding box volume, which refers to the minimum cuboid that contains a certain 3D model. Note that in current literature, different methods have been used to define the complexity level of a geometry; in this Section, the ratio is selected because it is one of the most popular methods to define the complexity level for 3D printing geometries. AC_{TM_0} can be calculated as the product of hourly pay of

assemblers $HP(A)$ (\$/hr), and the processing time for product with no customization request PT_{TM_0}.

The production cost for a rework order is determined by the difficulty level of the required adjustment or improvement, which is considered to be a certain portion of the original customization level $\theta(j_r^t)$. For model simplification, it is assumed that the average rework cost for rework orders is δ times of $AC_{TM}(j_r^t)$, where δ is assumed to be within the range of $(0,2)$, indicating the rework cost can either be lower or higher than the assembling cost of the initial product $AC_{TM}(j_r^t)$. The production cost for rework orders $RC_{TM}(j_r^t)$ can be formulated as follows.

$$RC_{TM}(j_r^t) = \delta \times AC_{TM}(j_r^t) \tag{4}$$

Let $\tau(j_r^t)$ be a function to indicate if an order j_r^t is a new order or a rework order.

$$\tau(j_r^t) = \begin{Bmatrix} 1 & If\ order\ j_r^t\ is\ returned\ as\ a\ rework\ order \\ 0 & otherwise \end{Bmatrix} \tag{5}$$

The total production cost of this manufacturer during a certain time period T including both new orders and rework orders can then be calculated as follows.

$$PC_{TM}(T) = \sum_{t\in T}\sum_{r\in R}\sum_{j\in j_r^t}[1-\tau(j_r^t)] \times PC_{TM}(j_r^t) + \tau(j_r^t) \times RC_{TM}(j_r^t) \tag{6}$$

Note that after the production stage, new orders and rework orders will be treated with no difference in the inventory and delivery stages.

Traditional Manufacturing Delivery Cost

To quantify the delivery cost, a function y_r^t is defined to represent whether if there is a delivery scheduled for a certain relator on a certain workday, as shown in Equation (7).

$$y_r^t = \begin{Bmatrix} 1 & If\ there\ is\ a\ delivery\ scheduled\ to\ retailor\ r\ on\ day\ t \\ 0 & otherwise \end{Bmatrix} \tag{7}$$

The value of the function y_r^t is determined by the current state of inventory at the end (10 PM) of the workday $(t-1)$. Let CO_{t-1} be the number of completed bulk orders at 10 PM on day $(t-1)$,

and UO_{t-1} be the uncompleted orders that are currently processing or pending for processing at 10 PM on day $(t-1)$. If there is at least one order in CO_{t-1} belongs to retailor r, then $y_r^t = 1$. The transportation cost of delivering the finished orders to retailor r on day t (denoted as $DC_{TM\_r}^t$) is related to the transportation distance TD_r^t on day t to retailor r (in miles), average local traffic speed TS (mile/hr), the hourly pay for the truck driver $HP(TD)$ ($/hr), the mile per gallon MPG of the delivery truck (miles/gallon of fuel), the average fuel price FP ($/gallon of fuel), and the maintenance and repair cost of the delivery truck MC_r^t ($/mile).

$$DC_{TM\_r} = \frac{TD_r^t}{TS} \times HP(TD) + \frac{TD_r^t}{MPG} \times FP + MC_r^t \times TD_r^t \quad (8)$$

The delivery cost of this manufacturer during a certain time period T can be quantified as follows.

$$DC_{TM}(T) = \sum_{t \in T} \sum_{r \in R} \left(DC_{TM\_r} \times y_r^t \right) \quad (9)$$

This formulation is based on the assumption that all the customization orders that are received from retailor r on workday t will be delivered together once they are all finished.

Traditional Manufacturing Inventory Cost

The inventory cost is contributed by two sources: 1) inventory of semi-finished products; and 2) inventory of finished products before they are dispatched for delivery. The inventory of semi-finished products in jointly determined by the expected demand (based on historical data) as well as the fluctuated demand. Let ED_t be the expected demand and FD_t be the fluctuated demand on day t. The inventory cost of semi-finished products on day t can be calculated as follows.

$$IC_{TM}(t) = IC_{TM\_0} \left[\frac{ED_t}{2} + FD_t \right] \quad (10)$$

In this equation, IC_{TM_0} refers to the unit inventory cost ($/unit/day)

Let NUM_t^{CO} be the number of the finished products in completed order set CO_t on day t, and NUM_t^{UO} be the number of finished parts in uncompleted order set UO_t on day t. The inventory cost of this manufacturer during a certain time period T can be formulated as follows.

$$IC_{TM}(T)=\sum_{t\in T}[IC_{TM}+IC_{TM\_0}(NUM_t^{CO}+NUM_t^{UO})] \quad (11)$$

3.1.2 Cost Modeling of the AM Integrated PIT Supply Chain

As different AM technologies have been emerging and adopted in different industries, it is expected that future manufacturing facilities will be equipped with a mix of traditional and additive processes, or even pure AM processes. In this section, an AM integrated PIT supply chain that solely relies on AM is investigated. A typical AM integrated PIT supply chain structure can be illustrated in Figure 4. To fully explore the benefits of adopting AM, a few assumptions in terms of customers' order submission, retailors' work schedule and the manufacturer's work schedule. In this case, two different types of orders and their corresponding delivery schedules are considered, i.e., 1) same-day delivery for rush orders; and 2) regular delivery schedules for other regular orders. Rush orders are only accepted for certain levels of customization $\theta(j_r^t)$. The estimated fabrication time for such orders should be less than or equal to the estimated delivery time. Rush orders are submitted to the manufacturer at the time of order, and the rest of the regular orders are submitted to the manufacturer at a fixed schedule.

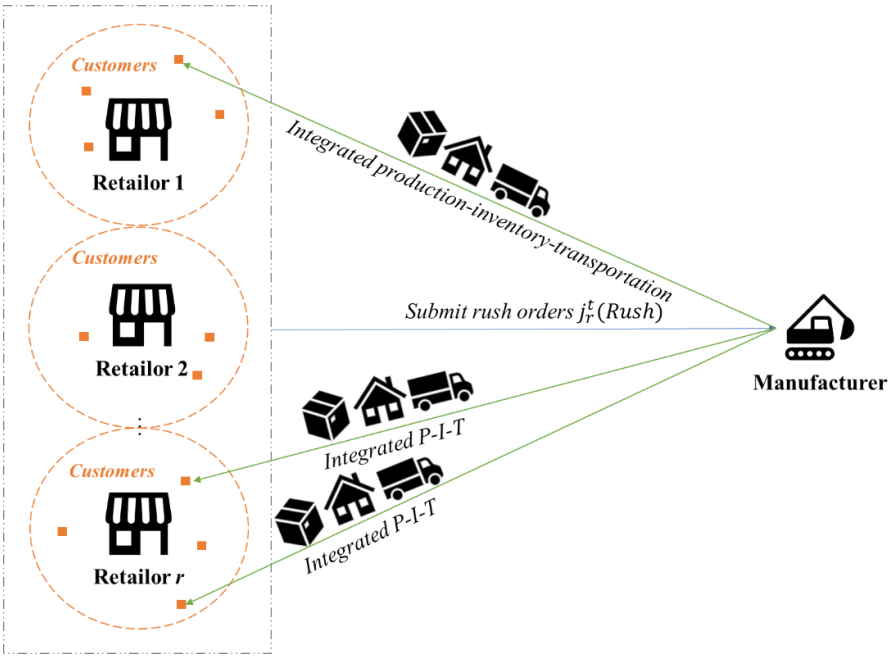

Figure 4. An example of the integrated PIT structure for AM

When three separate supply chain stages, i.e., production, inventory, and transportation, are integrated into one, some extremely complex issues such as delivery sequencing/scheduling and route planning are involved, which requires extensive research efforts and thus will be investigated in future studies. In this section, to simplify the problem, assumptions are made as follows: 1) the delivery sequence is solely based on the sequence of receiving the orders and is not affect by the delivery distance, production time, or any other factors; 2) the delivery truck is equipped with multiple number of 3D printers that can satisfy the average demand of rush orders in the scope of localized supply chain; 3) the 3D printers that are used by the manufacturer are assumed to be well maintained so they have high level of reliability and fabrication quality; and 4) the truck driver has been professionally trained to use the 3D printers.

The total supply chain cost C_{AM} is contributed by the production cost PC_{AM}, the delivery cost DC_{AM}, and the inventory cost IC_{AM}.

$$C_{AM} = PC_{AM} + DC_{AM} + IC_{AM} \tag{12}$$

Additive Manufacturing Production Cost

For retailor r on day t, let $j_r^t(Rush)$ be the index of received rush orders, $j_r^t(rush) \in \{1, J_r^t(rush)\}$ and $j_r^t(reg)$ be the index of other regular orders, $j_r^t(reg) \in \{1, J_r^t(reg)\}$. Traditional manufacturers need to assemble several components together to make the final products, while AM machines are capable of 1) fabricating the final product in one batch with minimum need for assembling, and 2) producing multiple number of products in one single batch. In this section, it is assumed that the AM products can be manufactured in one batch. The production cost of a product fabricated by AM j_r^t is consisted of raw material cost MC_{AM} and processing cost SC_{AM} (which includes labor, electricity, and other costs that are associated with the processing of the product). More specifically, the raw material cost can be calculated as the product of the unit price of the raw material (\$/volume) and the volume of the product, i.e.,

$MC_{AM}(j_r^t) = UP_{AM} \times V(j_r^t)$; the processing cost $SC_{AM}(j_r^t)$ includes the electricity cost $EC_{AM}(j_r^t)$, which can be calculated as the product of the production time $PT_{AM}(j_r^t)$, average electricity price EP (\$/kWh), and the AM machine rated power RP (kW); and the labor cost $LC_{AM}(j_r^t)$ can be formulated as the product of AM technician's hourly pay $HP(AM)$ (\$/hr) and the production time $PT_{AM}(j_r^t)$. The production time $PT_{AM}(j_r^t)$ of a certain geometry fabricated by a certain AM machine has been extensively studied in literature.

$$PC_{AM}(j_r^t) = UP_{AM} \times V(j_r^t) + PT_{AM}(j_r^t) \times EP \times RP + HP(AM) \times PT_{AM}(j_r^t) \quad (13)$$

Therefore, the total production cost of this AM facility during a certain time period T can then be calculated as follows.

$$PC_{AM}(T) = \sum_{t \in T} \sum_{r \in R} \sum_{j \in j_r^t} PC_{AM}(j_r^t) \quad (14)$$

Additive Manufacturing Delivery Cost

For the AM facility, the delivery cost for regular orders can be calculated similar with the traditional manufacturer, and therefore will not be further discussed in this paper. The delivery cost for rush orders, on the other hand, is substantially different, as the manufacturer delivers rush orders to the customers using the integrated PIT structure. To quantify the delivery cost, a new index c_r^t is introduced to denote the customer who submits orders with a certain retailor r on day t, $c_r^t \in C_r^t$ where C_r^t refers to the total number customers who submit orders at retailor r on day t. A function $\beta(c_r^t)$ is defined to represent whether if there is a delivery scheduled to a certain customer c_r^t, who is affiliated with a certain retailor r on day t.

$$\beta(c_r^t) = \begin{cases} 1 & If\ there\ is\ a\ delivery\ scheduled\ to\ customer\ c_r^t \\ 0 & otherwise \end{cases} \quad (15)$$

The transportation cost of delivering the finished orders to customer c_r^t, denoted as $DC_{AM}(c_r^t)$, is related to the transportation distance $TD(c_r^t)$ (in miles), average local traffic speed TS (mile/hr), the hourly pay for the truck driver $HP(TDAM)$, who needs to have sufficient technical training for

operating 3D printers c (\$/hr), the mile per gallon MPG of the delivery truck (miles/gallon of fuel), the average fuel price FP (\$/gallon of fuel), and the maintenance and repair cost of the delivery truck MC_r^t (\$/mile) (same with the maintenance and repair cost for TM delivery truck). Note that the hourly pay for AM truck drivers (for rush orders) is higher than the regular truck drivers (for TM and AM non-rush orders), considering these truck drivers must have basic knowledge on 3D printer and take technical trainings.

$$DC_{AM}(c_r^t) = \frac{TD(c_r^t)}{TS} \times HP(TDAM) + \frac{TD(c_r^t)}{MPG} \times FP + MC_r^t \times TD(c_r^t) \quad (16)$$

The delivery cost of the additive manufacturer during a certain time period T can be formulated as follows.

$$DC_{AM}(T) = \sum_{t \in T} \sum_{r \in R} [DC_{AM}(c_r^t) \times \beta(c_r^t)] \quad (17)$$

Additive Manufacturing Inventory Cost

The regular orders, once they are finished, are stored in warehouses before dispatched for delivery. The rush orders, on the other hand, do not require on-site inventory as they are stored temporarily on the delivery truck. Therefore, the inventory cost for AM fabricated products is considered to be zero.

3.1.3 Case Study Results

Comparison of Traditional and Additive Manufacturing

In this case study, the supply chain cost of orthopedic insoles is investigated using the model established in the previous section, which can be produced using both TM and AM technologies [28]. Traditionally, patients (customers, clients) are examined by orthopedists (retailers), who take a foam print of the patients' foot and send that information to the insole manufacturer along with doctors' notes. The orthopedic insoles are usually assembled from three components, i.e., cork, plastic, and leather. Cork and plastics are used to fabricate the basis of the insoles, and leather is used as a top layer to increase the comfort level. After the insoles are fabricated, they are delivered

to the orthopedists who then perform the final fitting with the customers. If the customers and/or the orthopedists are not satisfied with the fitting results, the insoles can be sent back to the manufacturer for further improvement. Several rounds of adjustments are needed. In this case study, a rework rate of 30% is assumed, which indicates that 30% of the customers/orthopedists are not satisfied with the fitting results and would return the insoles back to the manufacturer for adjustment.

In the case of AM, orthopedists would 3D scan the customers' foot and send that information to the insole manufacturer along with doctors' notes. The patients have two choices: 1) submit regular orders and have the insoles delivered to the orthopedists' office; and 2) submit rush orders and have the insoles delivered directly to their home address on the same day. Generally, 3D printed insoles can provide a perfect fit (at least much better fit than traditionally manufactured insoles) owing to the use of high-accuracy 3D scanning data, which generally does not require additional adjustment; in other words, a return rate of 0% is assumed for AM. Illustrations of the 3D models (adapted from [78]) used in TM and AM are shown in Figure 5.

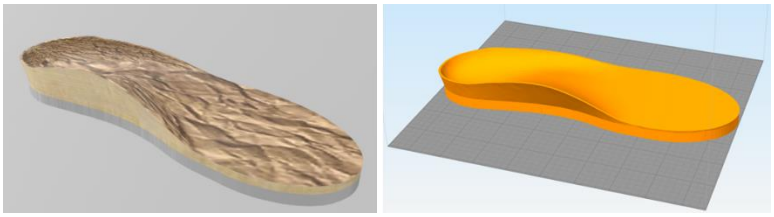

Figure 5. The 3D models used in TM (left) and AM (right)

In this case study, a few assumptions are made as follows to simplify the calculation: 1) the retailors' workhour is assumed to be from 10 AM to 6 PM, Monday-Sunday; 2) the retailers submit their daily orders from customers in bulk at the end of their workhour on each workday (at 6 PM, Monday-Sunday); 3) the manufacturer has a 16-hr daily work schedule, from 8 AM to 10 PM, Monday to Sunday; 4) the manufacturer receives the daily bulk orders from retailers at 6 PM each

day and plans the future production schedule accordingly; 5) the manufacturer sends out delivery trucks at 8 AM on each Monday; and 6) all calculations that are related to distance and transportation time are based on the route and traffic information suggested by Google Map. These assumptions apply to both TM and AM (non-rush orders only). In this case study, it is assumed that the additive manufacturer does not accept rush orders; in other words, the additive manufacturer adopts the exact same supply chain structure as the traditional manufacturer. The supply chain cost that is involved with rush orders will be studied in the next case study.

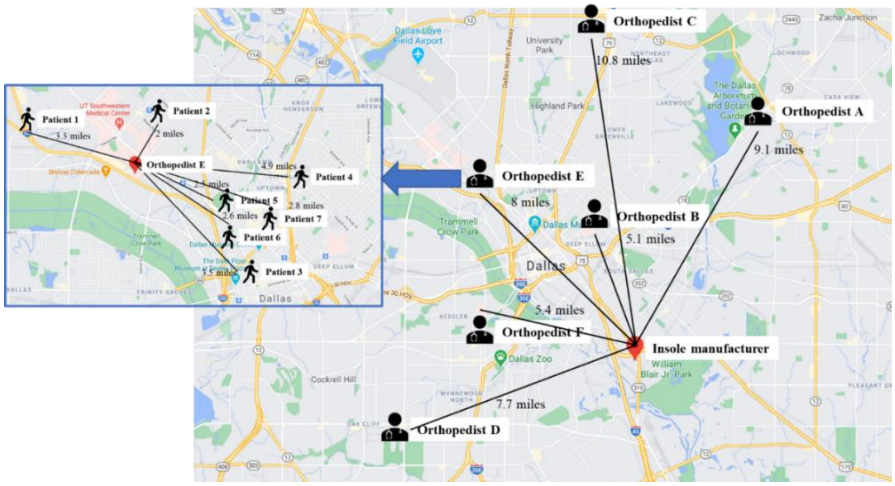

Figure 6. The supply chain network for the traditional insole manufacturer

The location of the insole manufacturer is selected to be in Dallas, Texas. The selection of this location is based on the real-life industry distributions in the area. Also, six orthopedists' offices are selected as the manufacturer's retail network, and they are located within a 15 miles radius from the manufacturer. For each orthopedist's office, a randomly selected number of patients or customers (5-10) is selected, and they are located within 5 miles of radium from the orthopedist's office. An illustration of the supply chain structure is shown in Figure 6. The parameter values and data sources used for this case study are summarized in Table 1. Note that in this case study, the

values of parameters that are related to the location are determined based on local or national statistics.

Table 1. Parameters' values used in model calculation

Parameter	Value	Data source
Traditional manufacturing		
N: the total number of components	3	Current literature [28]
δ: rework cost ratio	Random values taken from $(0, 2)$	Assumed based on experience
MC_{TM_1}: the raw material cost of cork	\$133.07/m^3	Online commercial data [79]
MC_{TM_2}: the raw material cost of plastic	\$4916.23/m^3	Online commercial data [80]
MC_{TM_3}: the raw material cost of leather	\$4.58/ft^2 (thickness: 1.6mm)	Online commercial data [81]
PT_{TM_0}: the processing time for a product with no customization requests	0.33hr	Assumed based on experience
$HP(A)$: the TM worker's hourly pay	\$15.40/hour	Average wage of shoe machine operators, Texas, 2019 [82]
θ_0: the level of complexity of a product with no customization request	16.20%	Calculated in this chapter (geometry is from online) [78]
TS: the local average traffic speed	53 miles/hour	Average truck movement speed, Texas, 2019 [83]
$HP(TD)$: the truck driver's hourly pay	\$21.76/hour	Average wage for truck drivers, Texas, 2019 [84]
MPG: the delivery truck's average fuel consumption in mile per gallon	7.1 miles/gallon	Average fuel consumption of delivery truck, U.S., 2020 [85]
FP: the fuel unit price	\$2.44/gallon	Average retail diesel prices, Texas, 2019 [86]
ED_t: the daily expected demand	30 orders	Calculated in this Section (the number of orders at each retailor is randomly generated from [0,10])
FD_t: the daily fluctuated demand	3.9 orders	Calculated in this chapter (assuming 30% of the expected demand)
IC_{TM_0}: the inventory unit price	\$0.041/unit/day	Online commercial data (in the area of the manufacturer's location) [87]
Additive manufacturing		
UP_{AM} : the unit price of raw material	\$25/kg	Online commercial data [88]
EP: the average electricity price	10.71cents/kWh	Average electric service rate, Texas, 2020 [89]
RP: the machine rate power	0.09kW	Current literature [90]
$HP(AM)$: the AM technician's hourly pay	\$18.48/hour	Calculated in this Section (20% increase from $HP(A)$)
$HP(TDAM)$: the trained truck driver's hourly pay	\$26.11/hour	Calculated in this Section (20% increase from $HP(TD)$)

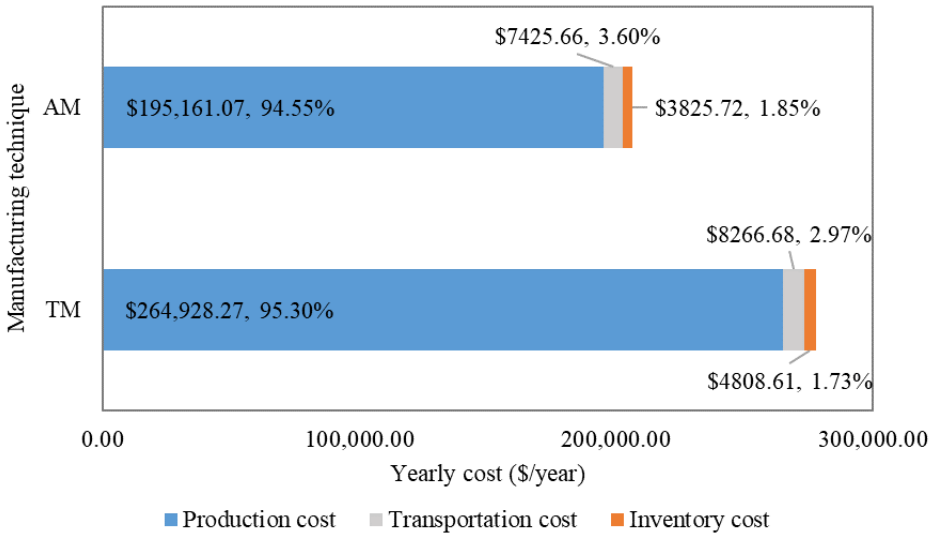

Figure 7. The supply chain costs for TM and AM

The model calculation results for both TM and AM are illustrated in Figure 7. The overall supply chain cost of AM is 25.75% less than that of TM, indicating the cost-saving potentials of adopting AM in this case. Specifically, the AM production cost, delivery cost, and inventory cost are 26.33%, 10.17%, and 20.44% less than those of TM, respectively. The main reasons for the production cost difference between AM and TM are 1) the unique capability of AM in terms of fabricating the entire product in one build without the need for assembling; 2) the reduced average raw material cost of AM comparing to TM; and 3) the reduced labor cost of AM contributed by less production time. Note that in this case study, the 3D model design of the orthopedic insole remains the same for TM and AM, while in practice, a different design for AM geometry can be adopted with less usage of material while achieving the desired structural performance. This indicates additional opportunities for further reducing the AM production time and material consumption. In addition, the cost breakdown of AM and TM shows similar behaviors. The product cost contributes the most to the total supply chain cost (around 95%), where the delivery cost and inventory cost contribute

only around 3% and 2%, respectively. This is caused by the current localized scope of the supply chain designs.

Make-to-Order: Adopting Integrated PIT Structure for AM

In this case study, the benefits of adopting AM with respect to make-to-order or on-demand production are explored. Specifically, the additive manufacturer is investigated on how the integrated PIT structure affects the supply chain cost. For rush orders, the production, inventory, and transportation stages of the supply chain are integrated into the delivery truck. To simplify the calculation, a few assumptions are adopted: 1) rush orders are delivered directly to the customers' address rather than the retailers' location, owing to the 100% fitting satisfaction level ensured by AM; 2) the delivery route is designed by Dijkstra's algorithm in this case study; 3) the rush order delivery capacity is considered sufficient due to the local scope of the supply chain; 4) the AM machine fabricates one order at a time (batch size=1); and 5) the need for on-site warehousing for rush orders is eliminated.

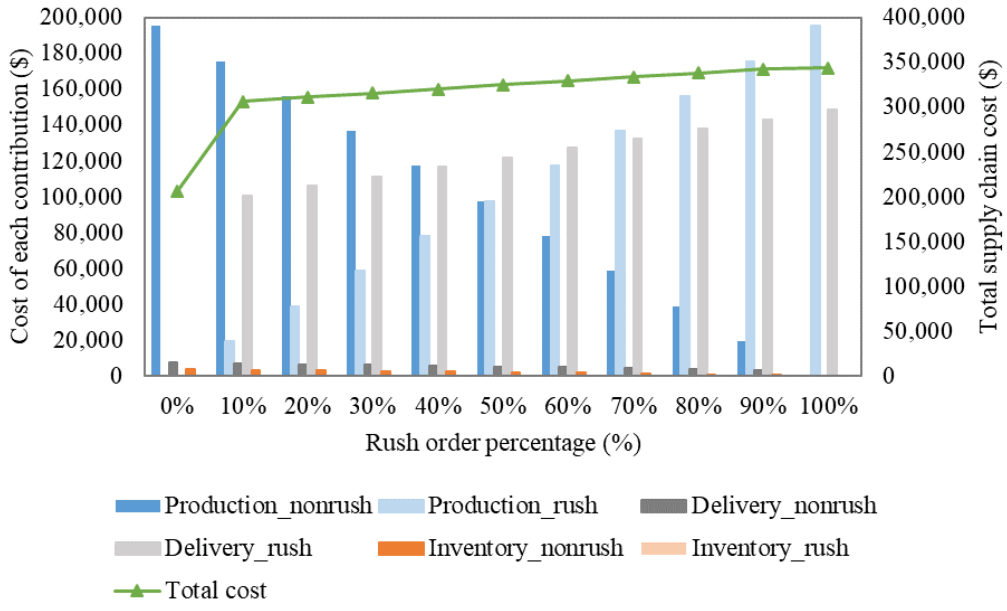

Figure 8. The supply chain cost of AM with varying rush order percentage

The total supply chain cost of AM with varying rush order percentages is shown in Figure 8. As indicated in the figure, the total supply chain cost increases with the growing percentage of rush orders, mainly because the increase in delivery cost for rush orders. An increase from 0% rush order to 10% rush order leads to an increase of 48.48% on total supply chain cost. Also, it can be observed from this figure that the delivery cost for rush orders is extremely higher than that for non-rush orders. This is mainly because that to quantify the delivery cost for rush orders, it is assumed that a professionally trained (with AM knowledge) truck driver must stay by during the entire workday, even when no rush orders are scheduled, to ensure the absolute guarantee on the same-day delivery for rush orders. Another reason for the huge difference between delivery cost of AM and TM is that a 7-day delivery schedule is adopted in TM (8 AM on each Monday). The impact of different delivery schedules on the supply chain cost will be analyzed in Section 3.1.3.3. Note that the inventory cost for rush orders remain zero owing to the use of PIT structure.

Sensitivity Analysis

Variations of some parameter values and assumptions adopted in the supply chain cost model can lead to different cost performance, and they are often 1) external parameters that have fluctuations due to market change (e.g., labor's hourly rate and raw material price), or 2) internal parameters that depend on core assumptions used in the model (e.g., delivery schedule, order rework rate). In this case study, both types of parameters are investigated for their influence on the supply-chain-related costs. Note that in this case study, a rework rate of 30% is used for TM and no rush orders are considered for AM.

Figure 9 shows the effects of raw material price and labor's hourly rate of AM and TM on the AM and TM production cost, respectively. It can be observed from this figure that AM raw material price has a more significant impact on AM production than TM raw material price on TM production cost, while TM labor's hourly rate has a more significant influence on TM production

cost than AM labor's hourly rate on AM production cost. The main reasons are that 1) the production time of AM is less than TM, owing to the unique capability of AM in terms of fabricating the entire product in one build which eliminates the need for assembling and leads to less working hours; and 2) the AM production starts with raw materials rather than semi-finished products in TM, which require additional processing time and also inventory cost.

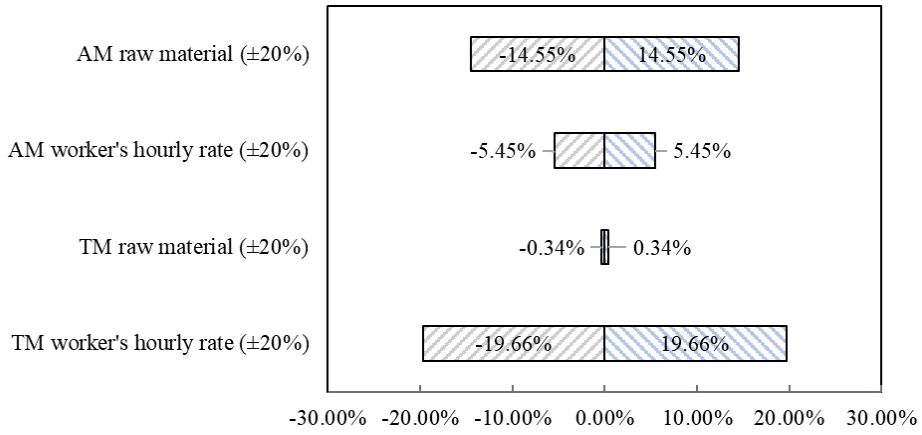

Figure 9. The effects of raw material cost and worker's hourly rate on the production cost for AM and TM

For the traditional manufacturer, the rework rate is a critical factor to evaluate the customers' and the doctors' satisfaction level on the manufactured products, and how the variations of rework rate affect the total supply chain cost is illustrated in Figure 10. Note that in practice, it is common that after the first-time fitting, these highly customized orthopedic insoles need to be sent back to the manufacturer for adjustment or improvement, based on the customers' feedback on comfort and the doctors' notes on functionalities. According to the results, a change from 0% rework rate to 100% rework rate causes a 22.37% increase in the total supply chain cost of TM (from $264,285.80 to $323,404.16).

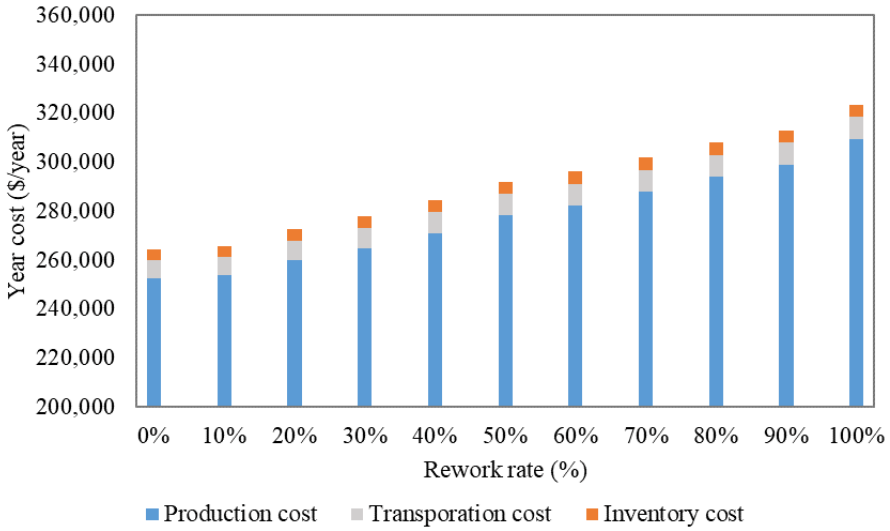

Figure 10 The supply chain cost of TM with varying rework rate

In addition, different delivery schedules can affect the delivery and inventory costs for both AM and TM, as summarized in Table 2. Note that in this comparison, the additive manufacturer does not accept rush orders. The results suggest that changes of TM delivery schedule from every 7 days to every 5 days and from every 7 days to every 3 days, lead to 15.83% and 56.20% reduction in delivery cost, respectively; and 23.90% and 49.37% reduction in inventory cost, respectively. Also, the changes of AM delivery schedule from every 7 days to every 5 days and from every 7 days to every 3 days, lead to 17.74% and 62.78% reduction in delivery cost, respectively; and 25.69% and 46.25% reduction in inventory cost, respectively. It can be observed that a change of delivery schedule affects AM delivery cost more than it affects TM. This is mainly because the AM case entails shorter production time comparing with TM, indicating more dependency on delivery and inventory, and hence is more sensitivity to the change of delivery schedule.

Table 2. The supply chain cost under different delivery schedules for TM and AM

Delivery schedule	*Traditional manufacturing*		*Additive manufacturing*	
	Delivery cost	Inventory cost	Delivery cost	Inventory cost
Every 7 days	$8,266.68	$4,808.01	$7425.66	$3825.72
Every 5 days	$9,575.23	$3,659.39	$8743.28	$2842.83
Every 3 days	$12,912.96	$2,434.55	$12,087.42	$2056.51

3.2 Route Design Problem for AM enabled supply chain

3.2.1 Route design for AM supply chain problem description

The research problem to be formulated in this section is a small-sized PIT structure used by a company that utilizes delivery trucks equipped with 3D printers aiming to provide the same/next-day delivery service of customized goods. Customers can submit orders online anytime; In other words, the company receives the order dynamically with no fixed schedule. However, the delivery trucks only work during certain work hours during the day. Hence, orders received during the night will not be handled until the next morning of a workday; orders received during the workday will be handled immediately. This leads to a hybrid static-dynamic operation. To mathematically formulate the problem, two types of vehicle route design/optimization problems are identified: (1) an offline static problem where the delivery schedule and 3D printing schedule are optimized offline before the start of each workday (i.e., before the delivery vehicle leaves the manufacturing plant), and (2) an online dynamic problem where the delivery schedule and 3D printing schedule are updated dynamically during the work hours based on the received new orders. Note that "delivery schedule" and "3D printing schedule" refer to the sequences of orders to be delivered and to be fabricated, respectively; they are not necessarily the same. In the scope of this research work, the optimal delivery schedule and 3D printing schedule have been proved to be the same in the static problem. This means that when the delivery truck arrives at a certain customer's delivery location, but the order is still being fabricated, the truck driver must wait until the order is fabricated, deliver the order, and then drive to the next customer's address. In a more general setting, the 3D printing sequence can be different from the delivery schedule to save the lead time and enhance the work efficiency even in the static problem, which will be further investigated in future studies.

3.2.2 Model assumptions

Without the loss of generality, the following assumptions are adopted to reasonably simplify the mathematical formulations.

(1) The manufacturer owns one delivery truck that is equipped with one desktop 3D printer. The desktop 3D printer is securely fixed on the truck with a good capability of printing good-quality parts on the route. This represents the most fundamental and simplified vehicle route problem in AM-enabled supply chains and will serve as the baseline case for more complicated scenarios in future studies, e.g., multiple delivery trucks each with multiple numbers of 3D printers (even with different types of 3D printers).

(2) The delivery truck has enough space to store 3D printing raw materials and finished orders on a typical workday. This assumption is to ensure that no additional storage space is needed for AM-enabled supply chains.

(3) The truck driver has been professionally trained to operate and maintain 3D printers, and he/she has a fixed work schedule with no overtime. This means that if for any reason, the truck driver did not finish delivering all the orders on a specific workday, these orders will be accumulated to be delivered on the next workday.

(4) All orders' delivery addresses are assumed to be available for receiving deliveries during the workday. This assumption is to avoid delivery failures.

(5) During the workday, the communication between the manager and truck driver is instant and effective. This assumption is to ensure the implementation of a dynamically updated delivery schedule during the workday.

(6) In the problem formulation, the number of orders received on each workday is assumed to be feasible to be delivered using one truck within a couple of days. In cases of a large number

of orders, more delivery trucks will be required, which is further discussed in the numerical experiments.

3.2.3 Offline Static Problem Formulation

Let t be the index of workdays, $t \in$ {Mon., Tues., Wed., Thurs., Fri., Sat., Sun.}. For day t, the start elapsed time is denoted as T_m and the finish elapsed time is denoted as T_e. in minutes The elapsed time is defined as the time elapsed from the starting time of a workday. Let i be the index of customers. Let j_i^t represent the order that needs to be delivered to customer i on day t. Note that for a specific day t, orders at T_m that need to be delivered might include unfinished orders from the previous day and new orders received before the start elapsed time. The manufacturing plant and all these customers compose a set of locations denoted by V. The static optimization aims to generate a delivery sequence $\boldsymbol{\sigma}$ and printing sequence $\boldsymbol{\tau}$ for workday t at T_m according to the obtained information. In this subsection, $\boldsymbol{\sigma}$ and $\boldsymbol{\tau}$ are considered the same. The proof is shown as follows.

Theorem 1. The optimal visiting sequence $\boldsymbol{\sigma}$ and the optimal printing sequence $\boldsymbol{\tau}$ are the same for the static problem in this Section.

Proof. Assume that the solution $(\boldsymbol{\sigma}^*, \boldsymbol{\tau}^*)$ is the optimal solution to this problem. In $\boldsymbol{\sigma}^*$, customer i is the k^{th} visited customer and customer j is the $(k+1)^{th}$ visited customer. In $\boldsymbol{\tau}^*$, the product of customer i is the $(k+1)^{th}$ printing task and product of customer j is the k^{th} printing task. Let l be the $(k-1)^{th}$ visited customer. Let LT_l be the time that driver leaves customer l. Let P_A be the total printing time of all customer orders from the first to the $(k-1)^{th}$ customer. Let t_{li} be the traveling time between l and i. Let t_{ij} be the traveling time between i and j. Let PT_i and PT_j be the printing time of customer i and j. Then, the delivery time of customer i can be calculated as $DT_i = LT_l + \max(t_{li}, P_A + PT_i + PT_j - LT_l)$. And, we have $DT_j = DT_i + CT + t_{ij}$.

Then, we can find another solution $(\boldsymbol{\sigma}^*, \boldsymbol{\tau}')$. $\boldsymbol{\tau}'$ is the same with $\boldsymbol{\tau}^*$ except that the product of customer i is the k^{th} printing task and the product of customer j is the $(k+1)^{th}$ printing task. The delivered time can be calculated as follows.

$$DT_i' = LT_l + \max(t_{li}, P_A + PT_i - LT_l), \text{ and } DT_j' = DT_i' + CT + \max(t_{ij}, P_A + PT_i + PT_j - DT_i' - CT). \quad (18)$$

Therefore, we have the following relationship.

$$\begin{aligned} DT_j' - DT_j = {} & DT_i' - DT_i + \max\left(t_{ij}, P_A + PT_i + PT_j - DT_i' - CT\right) \\ & - t_{ij} \max(t_{li}, P_A + PT_i - LT_l) \\ & - \max\left(t_{li}, P_A + PT_i + PT_j - LT_l\right) \\ & + \max\left(t_{ij}, P_A + PT_i + PT_j - DT_i' - CT\right) - t_{ij} \leq 0 \end{aligned} \quad (19)$$

For the solution of $(\boldsymbol{\sigma}^*, \boldsymbol{\tau}^*)$, the leaving time of $(k+1)^{th}$ customer equals to $DT_j + CT$. For the solution of $(\boldsymbol{\sigma}^*, \boldsymbol{\tau}')$, the leaving time of $(k+1)^{th}$ customer equals to $DT_j' + CT$. Since $DT_j' \leq DT_j$, then the solution $(\boldsymbol{\sigma}^*, \boldsymbol{\tau}')$ is better than $(\boldsymbol{\sigma}^*, \boldsymbol{\tau}^*)$. Thus, it leads to a contradiction; in other words, the theorem is proven.

The static decision-making problem aims to find the optimized delivery/printing sequence so that the delivery/fabrication of all the orders can be finished as soon as possible. In other words, this optimization problem aims to minimize the elapsed time when the driver returns back to the manufacturing plant from the last customer, defined as ω. Therefore, the mathematical programming model can be established as follows.

$$\text{Objective: Min } \omega \quad (20)$$

The constraints of this optimization problem include Equations (21)-(32).

$$DT_i \geq AT_i \forall i \in V \backslash 0 \quad (21)$$

Equation (21) indicates that the driver will first arrive at the customer's location and then deliver the package. DT_i represents the delivery time to customer i, AT_i denotes the arrival time to customer i.

$$DT_i \geq AT_i \forall i \in V \backslash 0 \quad (22)$$

Equation (22) limits that the driver must deliver the package after the product is fabricated, which means if the fabrication of the product has not yet been finished by the arrival time to the customer,

the driver must wait until the product is fabricated before delivery. FT_i denotes the product finish time (elapsed time) of the order of customer i.

$$LT_i = DT_i + CT \forall i \in V \backslash 0 \tag{23}$$

Equation (23) indicates that there are no other activities between the driver and the customer except product delivery and averaged communication. LT_i represents the elapsed time that the driver leaves customer i, and CT denotes the averaged communication time between the driver and each customer.

$$AT_j \geq x_{ij}\left(LT_i + d_{i,j}/DS\right) \forall i \in V \backslash j; \forall j \in V \backslash 0 \tag{24}$$

Equation (24) limits that the arriving time at customer j equals to the sum of the leave time from customer i and the travel time from customer i to customer j. $d_{i,j}$ denotes the distance between customer i and j, and DS denotes the averaged driving speed. x_{ij} is a binary variable to represent if the driver immediately visits customer j after customer i.

$$x_{ij} = \begin{cases} 1 & the\ driver\ visits\ customer\ j\ right\ after\ i \\ 0 & otherwise \end{cases} \tag{25}$$

This binary variable ensures that customer j is the next customer in sequence right after customer i. i=0 represents the manufacturing plant.

$$\omega \geq x_{i0}\left(LT_i + d_{i,0}/DS\right) \forall i \in V \backslash 0 \tag{26}$$

Equation (26) indicates that the driver returns back to the manufacturing plant after the delivery of the last order. $d_{i,0}$ denotes the distance between customer i and the manufacturing plant.

$$\sum\nolimits_{i \in V, i \neq j} x_{ij} = 1 \forall j \in V \tag{27}$$

$$\sum\nolimits_{i \in V, i \neq j} x_{ji} = 1 \forall j \in V \tag{28}$$

Equations (27) and (28) ensure that each customer is only visited once. Combining with Equation (24), illegal sub-tours can be avoided.

$$LT_0 = T_m \tag{29}$$

Equation (29) limits that the driver leaves the manufacturing plant at the time T_m, which is the start working time of each workday.

$$FT_i = PT_i + P_i \forall i \in V \backslash 0 \tag{30}$$

Equation (30) indicates that the finish time of customer i's order equals to the sum of the printing start time and the printing time required to fabricate order i.

$$PT_j \geq x_{ij} FT_i \; \forall i \in V \backslash j; \forall j \in V \backslash 0 \tag{31}$$

Equation (31) indicates that in this Section, we only consider the one-off production scenario where the printer only fabricates one part in each batch.

$$FT_0 = T_m \tag{32}$$

Equations (32) and (31) ensure that the printing of the first order starts at T_m.

In this static problem, the direct decision variable is x_{ij}, and the auxiliary decision variables include AT_i, DT_i, LT_i, PT_i, and FT_i. In the scope of the offline optimization problem, at the start of each workday t, the set of orders $J^t = \{j_i^t \forall i \in V/0\}$ is checked. The optimal delivery sequence $\boldsymbol{\sigma}$ is obtained by solving the mathematical model and finding the optimal value of $\{x_{ij}\}$ using the algorithms in Section 3.1. The mathematical model established in this section is a variant of the Travelling Salesman Problem with Time Windows (TSPTW). In the classic TSPTW, the time windows of customers are fixed in advance. However, in this Section, the allowed delivered time interval is sequence-dependent, which is affected by the products' fabrication. Thus, the actual delivered time of one customer does not equal the leave time from the last customer plus the traveling time between these two customers; furthermore, the performance of a visiting sequence, e.g., {0,1,2…n-1, n,0}, is different from its reverse sequence {0, n, n-1, …2,1,0}.

3.2.4 Online Dynamic Problem formulation

With the optimized delivery sequence $\boldsymbol{\sigma}$ obtained from the offline problem, the orders J^t will be fabricated and delivered one by one. If no new orders are received during the day, the driver will finish delivering all the orders and return back to the manufacturing plant. When new orders are received during the day, the predetermined sequence will be updated to a new sequence $\boldsymbol{\sigma}'$ and sent to the driver. The driver will not execute the newly updated sequence until he/she finishes the current delivering order. Besides, the plant manager must guarantee that the driver can finish all the orders and return back before T_e when the manager generates a new delivery sequence for the driver. Since the delivery and fabrication are two different things, some orders may be printed on

this day but delivered on the next day, when the remaining time of the day is enough to fabricate the product, but the distance is too far to deliver on this day.

At the time epoch ξ, the original unfinished delivery sequence and unfinished printing sequence are denoted as $\boldsymbol{\sigma}^{\xi}$ and $\boldsymbol{\tau}^{\xi}$. The manufacturing plant and customers in $\boldsymbol{\sigma}^{\xi}$ compose a node set $\boldsymbol{V}^{\xi}$. And, a new customer ϱ arrives at this time. Then, we can get the new set $\boldsymbol{\sigma}^{new} = \{\boldsymbol{\sigma}^{\xi} \cup \varrho\}, \boldsymbol{\tau}^{new} = \{\boldsymbol{\tau}^{\xi} \cup \varrho\}, \boldsymbol{V}^{new} = \{\boldsymbol{V}^{\xi} \cup \varrho\}$. It is obvious that $\boldsymbol{\tau}^{\xi} \subseteq \boldsymbol{\sigma}^{\xi}$. The driver is moving to the first customer in $\boldsymbol{\sigma}^{\xi}$, which is denoted as $\boldsymbol{\sigma}^{\xi 1}$. Similar to the definition in static problem, x_{ij} is a 0/1 variable to indicate whether there is a direct link between node i and node j in $\boldsymbol{V}^{\xi}$. Then, we have the following three equations to constrain that the driver return back to the plant after serving each customer exactly once.

$$\sum\nolimits_{j \in \boldsymbol{V}^{new}, j \neq \boldsymbol{\sigma}^{\xi 1}} x_{\boldsymbol{\sigma}^{\xi 1} j} = 1 \tag{33}$$

$$\sum\nolimits_{j \in \boldsymbol{V}^{new}, j \neq 0} x_{j0} = 1 \tag{34}$$

$$\sum\nolimits_{j \in \boldsymbol{V}^{new}, j \neq i, j \neq \boldsymbol{\sigma}^{\xi 1}} x_{ij} = \sum\nolimits_{j \in \boldsymbol{V}^{new}, j \neq i, j \neq 0} x_{ji} = 1 \forall i \in \boldsymbol{V}^{new}, i \neq 0, i \neq \boldsymbol{\sigma}^{\xi 1} \tag{35}$$

The 3D printer is processing the first order in $\boldsymbol{\tau}^{\xi}$ at ξ, which is denoted as $\boldsymbol{\tau}^{\xi 1}$. Assume that the remaining printing time length of $\boldsymbol{\tau}^{\xi 1}$ is $p^{\tau \xi 1}$. We need to arrange a new printing sequence for orders in $\boldsymbol{\tau}^{new}$. Let $y_{i[k]}$ be the 0/1 variable. $y_{i[k]}$=1 if the customer i is the k^{th} processed job in the 3D printer in the future; otherwise, 0. Then, the finish time FT_i of customer i's product can be obtained by the following five equations.

$$\sum\nolimits_{k} y_{i[k]} = 1 \forall i \in \boldsymbol{\tau}^{new}, i \neq \boldsymbol{\tau}^{\xi 1} \tag{36}$$

$$\sum\nolimits_{i} y_{i[k]} = 1 \forall k \geq 1 \tag{37}$$

$$FT_i = \sum\nolimits_{k} (y_{i[k]} FT_{[k]}) \; \forall i \in \boldsymbol{\tau}^{new}, i \neq \boldsymbol{\tau}^{\xi 1} \tag{38}$$

$$FT_{[k]} = FT_{[k-1]} + \sum\nolimits_{k} \left(y_{i[k]} P_i\right) \forall k \geq 1 \tag{39}$$

$$FT_{[0]} = p^{\tau \xi 1} + \xi \tag{40}$$

Considering that the delivery of one customer is successful after the driver arrives at the customer's place and the customer's product is completely fabricated, the return time ω^{new} can be derived for

$\{x_{ij}\}$ and $\{y_{i[k]}\}$. Finally, it is necessary to constrain that $\omega^{new} \leq T_e$. If the feasible solution space of the above model is not empty, the manager can always find a solution to guide the driver to successfully deliver all orders of $\boldsymbol{\sigma}^{new}$ in this day. Otherwise, the new order ϱ can only be arranged to deliver in the next day.

3.2.5 Solution algorithms

Solution Approach for the Offline Static Problem

The static problem formulated in Section 2.1 can be linearized to a mixed-integer linear mathematical model by introducing the big-M method for Equations (24), (26), and (31). Then, the model can be solved by commercial software such as Cplex and Gurobi. However, only small-sized problems with less than 10 customers can be solved within an acceptable time, since the problem is Np-hard, which can be proved by reducing the classical TSP to our problem. Then, we devise a dynamic programming (DP) approach for the medium-sized problem to get the optimal solution and a heuristic based on local search for the large-sized problem to search the near-optimal solution. In the literature, significant research efforts have been dedicated to addressing the challenge of solving large-sized problems within acceptable computational time using advanced dynamic programming approaches. With the increasing complexity and scale of real-world problems, traditional dynamic programming methods can become computationally infeasible due to the exponential growth of the state and action spaces. To overcome this limitation, researchers have focused on developing novel techniques such as approximate dynamic programming, where function approximation methods, including neural networks, decision trees, or linear regression, are employed to estimate the value or policy functions [91][92]. These advancements enable the efficient handling of large state and action spaces by generalizing from available data, thereby significantly reducing the computational burden while still achieving satisfactory solution quality. By leveraging the power of advanced dynamic programming techniques, researchers have made significant strides in solving large-sized problems in various domains. Although advanced dynamic programming methods have been developed to address complex optimization problems, DP continues to serve as a benchmark in the context of route design problems. Comparing DP with

heuristics provides valuable insights into the performance of different approaches. However, future research endeavors will focus on further developing and applying approximate dynamic programming techniques to tackle both static and dynamic route design problems

Dynamic Programming-based Approach

Consider a network $G = (V, A)$ where V is the set of nodes representing customers and the manufacturing plant, A is the set of feasible arcs among these nodes. Denote $DT(S, i)$ as the earliest delivery time of node i in a path starting at plant 0, passing through every customer of $S \subseteq \{V \backslash 0\}$ exactly once, ending at node $i \in S$. Then the function of $DT(S, i)$ can be calculated by solving the following recurrence equation.

$$DT(S,i) = \min_{j \in S \backslash i} \left\{ \max \left[DT(S \backslash i, j) + CT + \frac{d_{ji}}{DS}, \sum\nolimits_{i \in S} P_i \right] \right\}$$
$$= \max \left\{ \min_{j \in S \backslash i} \left[DT(S \backslash i, j) + CT + \frac{d_{ji}}{DS} \right], \sum\nolimits_{i \in S} P_i \right\} \quad (41)$$
$$\text{for all } S \subseteq \{V \backslash 0\}, i \in S.$$

Equation (41) shows that the system state (S, i) has several immediate preceding states $(S \backslash i, j)$. Then, the arriving time of customer i for state (S, i) equals to the sum of departure time from customer j and the travelling time between i and j. Meanwhile, the delivery time of customer i cannot be earlier than the finish time of his product. The recursion formula is initialized by Equation (42).

$$DT(\{0, i\}, i) = \max\{\tfrac{d_{0i}}{DS} + T_m, P_i + T_m\} \text{ for all } i \in V \backslash 0 \quad (42)$$

The optimal solution of the static problem can be obtained by solving Equation (43).

$$\min_{i \in V \backslash 0} \{DT(V \backslash 0, i) + CT + \frac{d_{i0}}{DS}\} \quad (43)$$

Similar to the classic TSPTW, the difficulty in solving the recursive equations above is the increment of computation time and storage requirements, which is caused by the exponential explosion of system states. For the TSPTW, a lot of states can be eliminated considering the infeasibility caused by fixed time windows. However, in this Section, no state can be eliminated by checking the feasibility of time windows. Meanwhile, the bi-directional technique cannot be

applied to accelerate the computation in this Section since the allowed time window is sequence-dependent. The computation complexity of this algorithm is $O(2^n)$. For our problem, only instances with less than 28 customers can be solved within 5 minutes using a personal computer with 8G RAM and 2.4GHz CPU.

Heuristic Local Search-based Approach

To solve large-sized problems, a fast two-stage heuristic approach is proposed. Stage 1 is the construction stage from nothing to a feasible solution. Stage 2 is the refinement stage from one solution to a better solution.

Stage 1. Greedy insertion.

Step 1.1 Let $i = 0$; define a set $C = V/0$; define a list $L^0 = \Phi$.

Step 1.2 For each customer $j \in C$, calculate the delivery time of j after leaving customer i. Let j^* be the customer whose delivery time is earliest in C.

Step 1.3 Add j^* to the end of the list L^0. Delete j^* from the set C. Let $i \leftarrow j^*$.

Step 1.4 If C is not empty, go to Step 1.2. Otherwise, go to Step 1.5.

Step 1.5 Calculate the return time from customer i to the manufacturing plant, which is denoted as ω^0.

Stage 2. 2-optimal local search.

Step 2.1 For each pair ($i \in V/0, j \in V/0$) in the list L^0, interchange the sequence of i and j to obtain a new list L'. Then, calculate the return time ω' for each L'.

Step 2.2 Choose the smallest ω'. Denote the corresponding solution as ω^* and L^*.

Step 2.3 If $\omega^* < \omega^0$, then let $\omega^0 \leftarrow \omega^*$, let $L^0 \leftarrow L^*$, go to Step 2.1. Otherwise, output ω^0 and L^0, stop.

Although one solution can be obtained quickly through this procedure, it cannot be guaranteed to be the optimal solution. We compare this solution with the optimal solution obtained by DP in the numerical experiments, which shows that the gap is rather small.

Solution Approach for the Online Static Problem

At the start of workday t, a delivering sequence $\boldsymbol{\sigma}$ is stored in the driver's mobile terminal. σ_k is the kth customer in the sequence. The driver will always drive the truck to the customer σ_1, which is stated at the top of sequence $\boldsymbol{\sigma}$. When the order of σ_1 is delivered successfully, σ_1 is deleted from the sequence and the next customer will climb to the top of $\boldsymbol{\sigma}$. Meanwhile, some new orders will be inserted into the sequence $\boldsymbol{\sigma}$ by the manager. It is the manager's job to consider the condition of delivering the system and update delivering sequence. The driver only needs to focus on the top customer of $\boldsymbol{\sigma}$. If the driver delivers that order and finds that the sequence $\boldsymbol{\sigma}$ becomes empty, then he/she will return to the manufacturing plant.

The truck and 3D printer can be viewed as two agents. To get a quick response for the newly arrived order, a simple rule needs to be devised for each agent. For the 3D printer, the basic idea of the agent is that it should fabricate the orders as many as possible without idle. For the truck route, the sequential relationship between any two orders should keep unchanged once it is established; and the newly arrived order should be inserted into an appropriate position such that all the orders can be delivered as soon as possible.

To formulate the driver's condition during a whole day, four different states can be analyzed. (a) The driver is in the plant; no orders need to be delivered at this time. (b) The driver is in the plant; at least one order needs to be delivered. (c) The driver is leaving from one customer; no orders need to be delivered at this time. (d) The driver is leaving from one customer; at least one order needs to be delivered. During the working hours, the driver will transfer from one state to another state in these four states. Therefore, the procedure from the start time T_m to the end time T_e during workday t can be described in detail as follows.

Let DD^t be the driving distance of truck during workday t. It is obvious that DD^t equals to zero at the start of workday t. Let J^{t+1} be the order set containing the orders that cannot be delivered successfully at workday t. And, J^{t+1} is empty at the start of workday t.

Step 0 Set the start_point be the manufacturing plant. Set the leave_time be T_m.

Step 1 The driver leaves the start_point at leave_time and drive to σ_1. He/she will deliver the order at the time DT_{σ_1} and leave this customer at LT_{σ_1}.

Step 2 During the time interval [leave_time, LT_{σ_1}], the number of customers in $\boldsymbol{\sigma}$ is denoted as N_σ, once a new order j_{new} is submitted, the manager will do as follows.

Step 2.1 For each position $k(2 \leq \mathrm{k} \leq N_\sigma + 1)$, try to insert the j_{new} to the of the kth position of $\boldsymbol{\sigma}$, and calculate the corresponding back time of the driver.

Step 2.2 Choose the best insert position and the earliest back time. If this timer is earlier than T_e, then update the sequence $\boldsymbol{\sigma}$. Otherwise, put the j_{new} into the set J^{t+1}.

Step 3 When the driver leaves σ_1 at LT_{σ_1}, let $DD^t \leftarrow DD^t + d_{start\_point,\sigma_1}$, let start_point be σ_1, let leave_time be LT_{σ_1}. Delete σ_1 from $\boldsymbol{\sigma}$. If $\boldsymbol{\sigma}$ is not empty, go to Step1; otherwise, go to Step 4.

Step 4 The driver leaves start_point and drive back to the manufacturing plant, let $DD^t \leftarrow DD^t + d_{start\_point,0}$. Denote the return back time as T_r.

Step 5 During the time interval $[T_r, T_e]$, if no new orders come, the driver waits and gets off work at T_e; otherwise, the driver will try to handle the new orders similarly and gets off work at T_e.

3.2.6 Numerical Case studies

Optimization Algorithms Comparison: DP vs Heuristic Approaches

To evaluate the solution accuracy of the proposed heuristic approach in comparison with DP in the static problem, the ratio δ_1 is proposed to investigate the optimized elapsed time ω that the driver returns to the manufacturing plant after delivering all the orders obtained before T_m. This

ratio is formulated in Equation (27), which directly shows the difference between the heuristic solution and the optimal solution. Note that ω^{DP} represents the optimized elapsed time solved by the DP approach and ω^{H} denotes the optimized elapsed time solved by the heuristic approach.

$$\delta_1=\frac{\omega^H-\omega^{DP}}{\omega^{DP}}\times 100\% \quad (44)$$

Since the delivery sequence obtained in the morning will be updated during the day considering new orders received dynamically, we want to analyze the realized performance of that sequence during the day. Thus, another two indicators are selected, which are the total delivery distance L and the total number of delivered orders M. L^{DP} is the total distance during the day when the driver uses DP to solve the static problem and update the sequence dynamically during the day. M^{DP} is the total number of customers delivered successfully in a whole day. Thus, the two ratios can be calculated as follows.

$$\delta_2=\frac{L^H-L^{DP}}{L^{DP}}\times 100\% \quad (45)$$

$$\delta_3=\frac{M^H-M^{DP}}{M^{DP}}\times 100\% \quad (46)$$

In this case study, we consider a 30-mile radius of the service area with one delivery vehicle. The printing time of orders is randomly set from 6min to 30min. {10, 15, 20} orders are received the day before, and another 20 orders are received during the day. Some parameters that are applicable in case studies as shown in Table 3.

Table 3. Values of parameters used in case studies

Definition	**Values**	**Data source**
Vehicle speed DS	60 mile/h	Assumed in this Section
Start elapsed time T_m	8:00 AM	
Finish elapsed time T_e	8:00 PM	
Service time CT	2min	
Driver's wage	\$24.27/hour	[93]
Diesel price	\$3.35/gallon	[94]
Diesel consumption for a delivery truck	6.5 MPG	[85]

By adopting the values in Table 3, the same static optimization problem is solved by both DP and heuristic methods for comparison reasons. Both optimization algorithms are solved by IntelR CoreTM i5-7200U CPU @ 2.5GHz. To increase the comparison scope, different total numbers of orders and different product customization levels are adopted. Note that the optimization problem is solved for 100 days, and the averaged results of 100 runs using each method are shown in Table 4.

Table 4. Comparison of averaged static problem solutions by DP and heuristic approaches

Total No. of orders	**Product customization level** (print time range)								
	[6min, 10min]			[6min, 20min]			[6min, 30min]		
	δ_1	δ_2	δ_3	δ_1	δ_2	δ_3	δ_1	δ_2	δ_3
30	1.21	-0.19	-0.03	1.88	-0.15	0.04	1.85	0.03	0.03
35	1.69	-0.95	0.00	2.65	-0.95	-0.06	1.14	-0.70	0.03
40	2.19	0.55	0.00	3.00	-1.22	-0.02	0.52	-0.93	-0.02

The following observations are drawn based on the comparison results between DP and heuristic approaches.

(1) All the values of δ_1 are positive small numbers, indicating the optimized elapsed time solved by the heuristic approach ω^H is slightly larger than the result obtained from the DP method. The δ_1 values are less than 3%, and that means the solution accuracy of the heuristic approach in terms of optimized elapsed time is good (>97%).

(2) The absolute values of δ_2 and δ_3 are close to 0, indicating that the optimized solutions from DP and heuristic methods lead to a similar impact with respect to the total delivery distance and the total number of delivered orders. It should be noted that δ_2 even has some negative values; In other words, the total delivery distance obtained by the heuristic approach is shorter than that of the DP method in some cases when the new orders arrive dynamically in the day. It is noted that in some cases, although the vehicle speed is constant, the travel distance can be higher while the total travel time is shorter. The vehicle may arrive at the location while the fabrication on the truck is still in process. The vehicle needs to stay at the customer location until the fabrication is completed to continue the delivery.

(3) The computation time when using the heuristic approach is usually less than 1 second, whereas the computation time when adopting the DP approach increases dramatically based on the complexity of the optimization problem.

Based on the comparison results, in this Section, the DP approach will be used when the number of orders is less than 20, and the heuristic method will be adopted when the number of orders is greater than 20. Note that this logic of selecting optimization algorithms will be applied to all other case studies in this paper.

Optimized Delivery Sequence of a Randomly Selected Workday

The optimized delivery sequence calculated for a randomly selected workday is shown in Figure 11. Only one delivery vehicle is considered. In the figure, the scatter points represent the customers' address in the service radius, where the red dots are the static orders received prior to this workday and the blue dots are the dynamic orders received during the workday. The numbers represent the sequence of orders submitted to the manufacturer. As shown in Figure 1, the delivery truck returns back to the manufacturing plant a few times when no other orders are in the process of handling.

It can be observed from Figure 11 that, unlike other traditional TSP problems, the optimized delivery route obtained in this Section show overlapping routes, e.g., orders 12, 20, and 21, orders 14, 15, and 29, etc. This is caused by the dynamic nature of orders received during the day. In addition, the optimized order delivery sequence shown in Figure 11 is different from the order receiving sequence to reduce the total delivery distance while ensuring the delivery of all orders received from the previous day or night and as many orders received during the workday as possible. Moreover, 4 routes (with different colored lines) are identified in the figure, meaning that the delivery truck returns back to the manufacturer when no new orders need to be delivered and restarts the delivery when new orders are received. As shown in the figure, the 1st route is the longest because of the 10 static orders received prior to the work hours, demonstrating the hybrid nature of the problem formulated in this section.

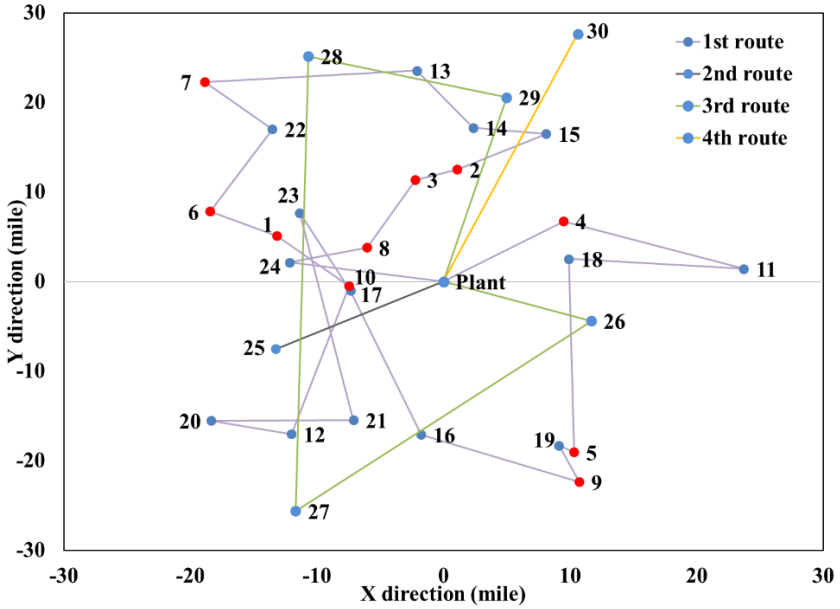

Figure 11. The optimized delivery route for a randomly selected workday (red dots: orders received prior to the work hours; blue dots: orders received during the workday)

Optimized Delivery Sequence Vs. First-Order-First-Deliver Policy

This case study aims to investigate the difference in averaged delivery cost between using the optimized delivery sequence obtained from this case study and the first-order-first-delivery (FOFD) policy when changing the number of orders to be delivered each day. Only one delivery vehicle is considered. The calculation results are shown in Figure 12.

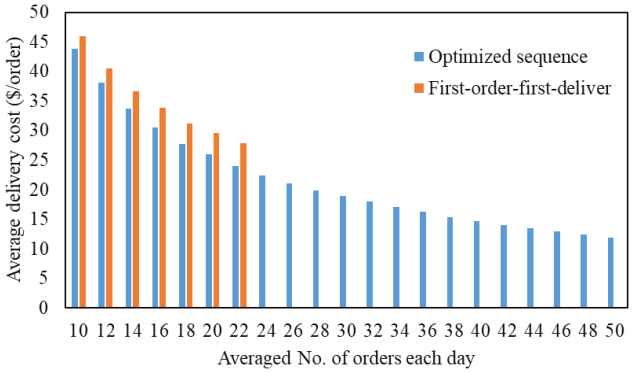

Figure 12. The averaged delivery cost per order calculated by using the optimized sequence vs. first-order-first-deliver policy

As shown in Figure 12, the average delivery cost per order decreases as the average number of orders each day increases. When the average number of orders each day is 24 or higher, one

delivery vehicle is no longer capable of handling all the orders if using the FOFD policy. It can also be observed from the figure that when the average number of orders each day is from 10 to 22, the average delivery cost calculated using the optimized sequence is less than the average delivery cost calculated using the FOFD policy, because the FOFD policy usually involves longer delivery distance.

Reduce Delivery Cost by Changing One Factor at a Time

In this case study, different strategies to potentially reduce the delivery cost are explored one factor at a time, including expanding the service area, increasing the number of customers, enhancing the complexity of the offered product, and increasing the offered customization level. In practice, these strategies can be executed by the manufacturer via advertisement, network expanding and collaboration, research and development, etc. The main objective of this case study is to investigate the influence of each factor on reducing the delivery cost of the investigated supply chain.

This section focuses on investigating if and how enhancing the offered product, e.g., the product complexity level and customization level, can potentially affect the delivery cost. In 3D printing, a higher product complexity level generally indicates a longer fabrication time; a higher customization level usually means a higher complexity level. In this case study, printing time is used to represent the product complexity and customization level. Specifically, the minimum printing time under a fixed range (i.e., the maximum is always three times the minimum) is used to present the product complexity level, where the minimum printing time means the printing time of the product with no customization request. This is applicable when different categories of products are offered. For example, the minimum printing time for a 5cm radius coaster is less than the minimum printing time for a pair of glass frames. Figure 13 shows that the average delivery cost per order increases when the product complexity level increases. When the printing time is [7,21], the average delivery cost per order shows a sudden decrease and then an increase again, which is caused by the random generation of orders.

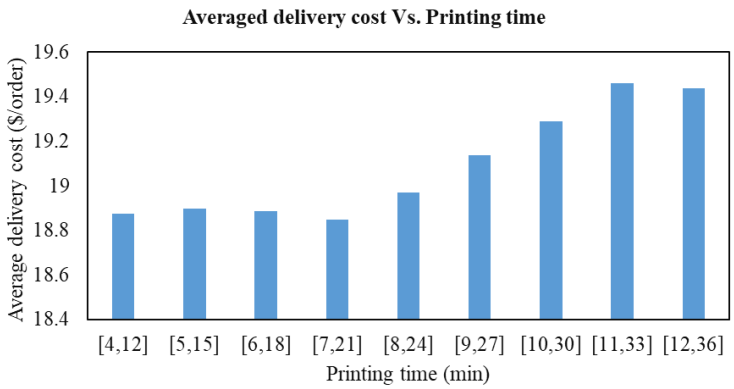

Figure 13. Reduce the delivery cost per order by changing one factor at a time: changing the offered product complexity level

The delivery details of changing the product complexity level are shown in Figure 14, in terms of the percentages of orders delivered within 30mins, within 60mins, within 120mins, within 360mins, and delivered on the same day. The delivery time has a direct relationship with the customer satisfaction level. As shown in the figure, the delivery details do not vary much when the printing time range is from [4,12] to [10,30], but demonstrate a sudden decrease right after [10.30]. This indicates that when the product complexity level is higher and the printing time for each order is longer, the delivery time is correspondingly longer, leading to a lower customer satisfaction level. Although increasing the product complexity level can reduce the average delivery cost per order, it can cause the loss of customers due to lowered customer satisfaction. Hence, solely increasing the offered product complexity level is not a beneficial method.

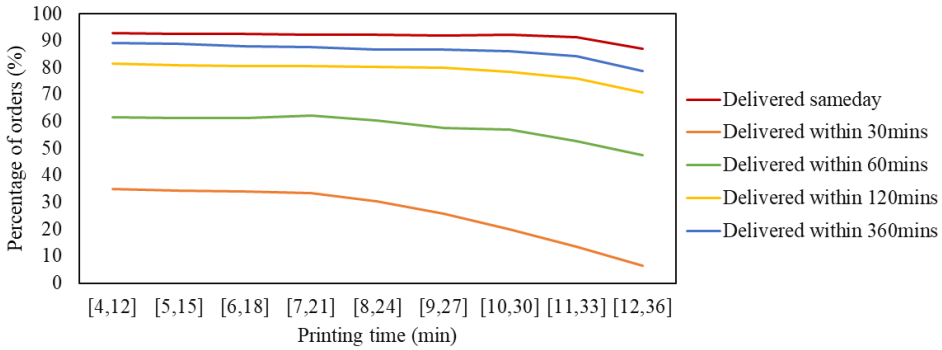

Figure 14. The detailed results in delivery when changing the product complexity level percentage of delivery orders according to the printing time

On the other hand, with the same minimum printing time (product with no customization level), the maximum printing time (product with the highest customization level) is used to represent the offered product customization level. The averaged delivery cost per order and the delivery details with increasing product customization levels are shown in Figure 15 and Figure 16. In this case, the minimum printing time for a product without customization is fixed to be 10min. As shown in Figure 15, when the highest customization level is around 12-18mins, the average delivery cost per order does not change much. When the customization level continues to increase, the average delivery cost per order starts to increase and then decreases after the maximum printing time reaches 34 min. A similar observation can be made from the delivery details when changing the maximum customization level shown in Figure 16.

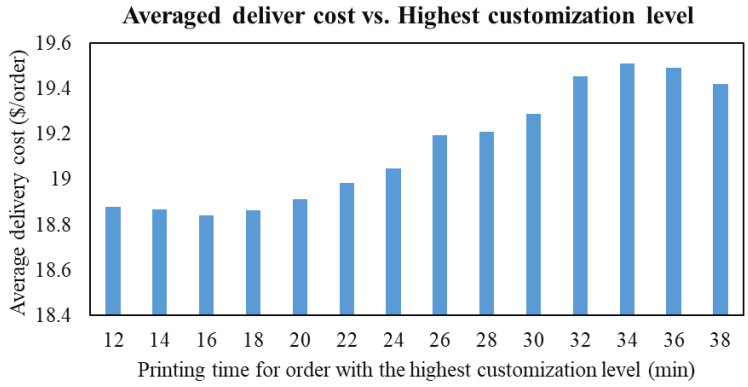

Figure 15. Reduce the delivery cost per order by changing one factor at a time: changing the offered product customization level

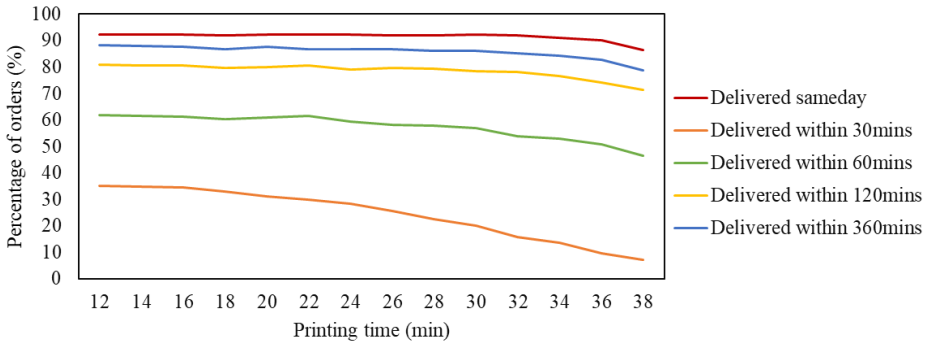

Figure 16. The detailed results in delivery when changing the product customization level

Impact of Market Share

In this case study, the influence of marketing on operational performance is investigated. Using promoting methods like an advertisement, a company can get the same number of customers within a smaller service radius, i.e., the customer density increases with a larger market share. Thus, there exists a balance between the additional cost of advertisement and the delivery cost reduction. The results are presented in Figure 17, where 5000 orders are obtained within 100 days. If these customers come from a radius of 45 miles, the total delivery cost equals $60,258; if these customers come from a radius of 10 miles, the total delivery cost equals $50,658. Therefore, the delivery cost reduction is about $35,039 each year. It is worth conducting the promotion if the advertisement fee is less than $35,039 each year from the viewpoint of the company's profit. Meanwhile, the customers' satisfaction can be improved by this way since the percent of customers who can get the product within 3 hours increases to 86.2% under advertisement scenario from 28.9% without advertisement.

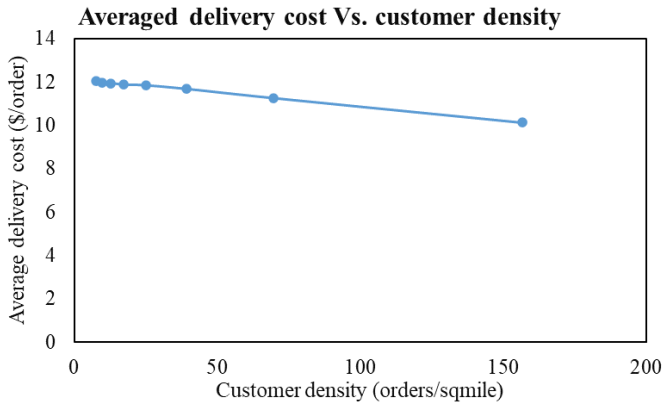

Figure 17. Average delivery cost in different customer density

Multiple Delivery Vehicles

In this case study, the influence of the different numbers of vehicles is investigated. It is assumed that the number of orders is positively related to the service area. In this case study, more trucks are engaged in the delivery. It is assumed that when one truck is not feasible to deliver all the orders, another truck is engaged to help with the rest of the orders. The results are shown in Figure 18. It is observed that using the same number of trucks, the average delivery cost decreases with

the increase of service radius. When it is necessary to add a truck, the average delivery cost increase. The average cost is around $10 to $20 at the service limit for different numbers of vehicles involved.

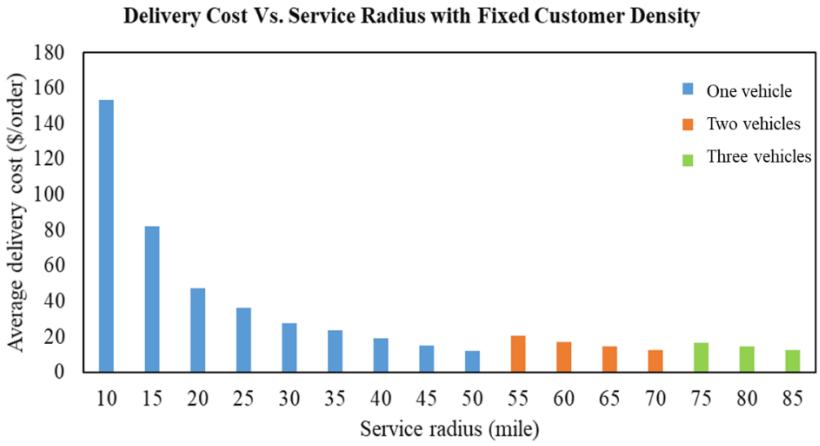

Figure 18. Average delivery cost using multiple delivery trucks

3.3 GHG Emission Modeling of the AM Integrated PIT Supply Chain

Similar to the cost modeling, when three separate supply chain stages, i.e., production, inventory, and transportation, are integrated into one, complex issues such as delivery sequencing/scheduling and route planning arise which requires extensive research efforts and thus will be investigated in future studies. In this model, without loss of generality, the following assumptions are made: 1) the delivery sequence is solely based on the sequence of received orders and is not impacted by the delivery distance, production time, or any other factors; 2) the delivery truck is equipped with a number of 3D printers that can satisfy the average demand of rush orders(localized supply chain); 3) the 3D printers that are used by the manufacturer are assumed to be well maintained so they have a high level of reliability and fabrication quality; and 4) the truck driver has been professionally trained to use the 3D printers.

3.3.1 GHG Modeling on Traditional Manufacturing Supply Chain

A TM supply chain consists of multiple stages including raw material acquisition, the fabrication of semi-finished products, the fabrication/assembly of finished products, and the

transportation/delivery of the final products [95]. This section it is considered that these stages in the modeling of GHG emissions are associated with TM. Specifically, a local supply chain of a type of consumer product with a high customization level is studied. The total GHG emissions E_{TM} include the GHG emissions from production PE_{TM} and the GHG emissions from delivery DE_{TM}.

$$E_{TM} = PE_{TM} + DE_{TM} \tag{47}$$

In this section, a scenario is considered where customers submit their customized orders to retailers, and then retailers submit received orders to the manufacturer on a fixed schedule. After the manufacturer finishes the production of the orders, the finished products are stored in inventory and then delivered to retailers on a fixed schedule. In practice, orders with a high level of customization often need rework based on the feedback received from customers. Therefore, it is assumed that the manufacturer also processes rework order requests. In this work, the delivery routes are generated using Dijkstra's algorithm for simplification reasons.

In general, some specific operations, e.g., burning, evaporating, and distillation may cause direct GHG emissions. In this Section, direct GHG emissions associated with these processes are not considered because these operations are not mandatory for the production of consumer products studied in this work. To simplify the calculation, the CO_{2eq}, which is defined as the equivalent amount of carbon dioxide with the same global warming potential, is considered as the GHG emissions in this work.

Greenhouse Gas Emission from Production in Traditional Manufacturing Supply Chain

Let R be the total number of retailers. J_r^t denotes the total number of the customization orders submitted to retailer r on workday t, where r represents the index of retailers, $r \in [1, R]$, and t is the index of the workday. The index of a specific order is defined as j_r^t, $j_r^t \in [1, J_r^t]$. In this section, only one consumer product that consists of multiple components is considered. Let n be the index

of the components, $n \in [1, N]$. GHG emissions associated with a specific order j_r^t include the GHG emissions related to electrical usage $EE_{TM}(j_r^t)$ and the GHG emissions related to material acquisition ME_{TM_n}.

$$PE_{TM}(j_r^t) = EE_{TM}(j_r^t) + \sum_{n=1}^{N} ME_{TM_n}(j_r^t) \tag{48}$$

GHG emissions that are associated with electricity for order j_r^t can be estimated as follows.

$$EE_{TM}(j_r^t) = I_e \times P_M \times T_{TM}(j_r^t) \tag{49}$$

In this equation, I_e is the emission intensity in the life cycle of electricity generation, and it represents the amount of CO_{2eq} emissions caused by generating one unit of electricity (kg CO_{2eq}/kWh). The power of the machine used in the production is denoted as P_M. The production time $T_{TM}(j_r^t)$ includes the pre-processing and assembling. To simplify the model, the production time of a part with no customization request is set as a basic case T_{TM_0}. The value of T_{TM_0} can be estimated according to professional experience or historical data. A factor $\varepsilon(j_r^t)$ is used to calculate the production time of a specific order. $\varepsilon_{TM,T}(j_r^t)$ is randomly picked from a certain range to represent different customization requests.

$$T_{TM}(j_r^t) = \varepsilon_{TM,T}(j_r^t) \times T_{TM_0} \tag{50}$$

GHG emissions that are related to the acquisition of material n can be formulated as follows.

$$ME_{TM_n}(j_r^t) = M_n(j_r^t) \times Unit_{CO_{2eq,n}} \tag{51}$$

In this equation, $M_n(j_r^t)$ represents the amount of the raw material n required for order j_r^t; $Unit_{CO_{2eq,n}}$ is the GHG emission in the production process per unit of the raw material n. Factor $\varepsilon_{TM,M_n}(j_r^t)$ is also used to simplify the calculation. M_{TM_n} is used as the mass of the material n used to fabricate one product as the basic case for the TM supply chain. Similarly, the value of

material consumption in the basic case in fabricating one product and the range of $\varepsilon_{TM,M_n}(j_r^t)$ for each material in TM can be estimated by practical experiences.

$$M_n(j_r^t) = \varepsilon_{TM,M_n}(j_r^t) \times M_{TM_n} \tag{52}$$

A function $\tau(j_r^t)$ is defined to indicate whether an order is a newly produced order or a rework order.

$$\tau(j_r^t) = \begin{cases} 1 & If\ order\ j_r^t\ is\ a\ rework\ order \\ 0 & otherwise \end{cases} \tag{53}$$

It is assumed that GHG emissions of rework orders are related to the original orders. Previous equations indicate that the major contributions of GHG emissions are time-related and mass-related variables. A random number δ in the range estimated by the practice is defined to calculate the rework order emission given the emission of the original order, which can be formulated as follows.

$$RPE_{TM}(j_r^t) = \delta \times PE_{TM}(j_r^t) \tag{54}$$

The total amount of GHG emissions during the period of T can be formulated as follows.

$$PE_{TM}(T) = \sum_{t\in T}\sum_{r\in R}\sum_{j\in J_r^t}[1-\tau(j_r^t)] \times PE_{TM}(j_r^t) + \tau(j_r^t) \times RPE_{TM}(j_r^t) \tag{55}$$

Greenhouse Gas Emission from Delivery in Traditional Manufacturing Supply Chain

After production, the completed orders are stored in the inventory before delivery. When a delivery is scheduled, a delivery truck picks up all of the products in the inventory and then distributes the orders to the retailers. GHG emissions that are generated in this process are mainly caused by the delivery trucks. Specifically, GHG emissions of delivering the finished orders to retailer r on day t (i.e., $DE_{TM_{r,t}}$) are related to the transportation distance ${TD_{TM}}_r^t$ on day t to retailer r (in miles), the miles per gallon MPG of the delivery truck (miles/gallon), and the vehicle

GHG emission constant c_e which can be obtained from vehicle technical specifications (kg CO_{2eq} /gallon).

$$DE_{TM_{r,t}} = \frac{TD_{TM_r}^{\ t}}{MPG} \times c_e \tag{56}$$

In this equation, $TD_{TM_r}^{\ t}$ is generated using Dijkstra's algorithm considering the given retailers and the distances from the manufacturer to the retailers. MPG denotes the average distance a truck can reach by consuming a gallon of fuel. c_e is the average GHG emission generated by consuming a gallon of fuel.

The total delivery-related GHG emissions during a certain time period T can be quantified as follows.

$$DE_{TM}(T) = \sum_{t \in T} \sum_{r \in R} DE_{TM_{r,t}} \times y_r^t \tag{57}$$

In this equation, a function y_r^t is defined to indicate whether or not delivery is scheduled to retailer r on day t in the following equation.

$$y_r^t = \begin{cases} 1 & If\ a\ delivery\ is\ scheduled\ to\ r\ on\ day\ t \\ 0 & otherwise \end{cases} \tag{58}$$

3.3.2 GHG Modeling on Additive Manufacturing Integrated PIT Supply Chain

The total GHG emission of the supply chain E_{AM} is contributed by the production GHG emission PE_{AM}, and the gas emission related to the delivery process DE_{AM}.

$$E_{AM} = PE_{AM} + DE_{AM} \tag{59}$$

The process of the supply chain is similar to traditional manufacturing. Customization orders from the customers are collected by the retailers and submitted to the manufacturers. Due to the high level of reliability and manufacturing quality, the PIT supply chain eliminates the possibility of rework orders. In this work, it is assumed that two types of orders are submitted at the request of the customers, namely the regular orders and the rush orders. The regular orders are submitted to

the manufacturers at a fixed period. At the delivery date, the trucks collect the fabricated products and deliver the products to the retailers to further assign the orders. Rush orders, as the name indicates, are submitted to the manufacturer at the time when the customers confirm. Once the rush order is received, the manufacturers start the fabrications. The delivery trucks integrated with the 3D printers for the rush order are ready to start delivering during the service time. Without losing generality, further assumptions are made for rush orders as follows. The sequence of the delivery depends on the time of receiving orders only. The delivery trucks are equipped with enough 3D printers to deal with the orders. The fabrication processes are assumed to be complete before the orders are delivered. Extra fossil consumption caused by the 3D printer installation on the trucks and direct GHG emission in the process is not considered in this work. An illustration of the supply chain is shown in Figure 19.

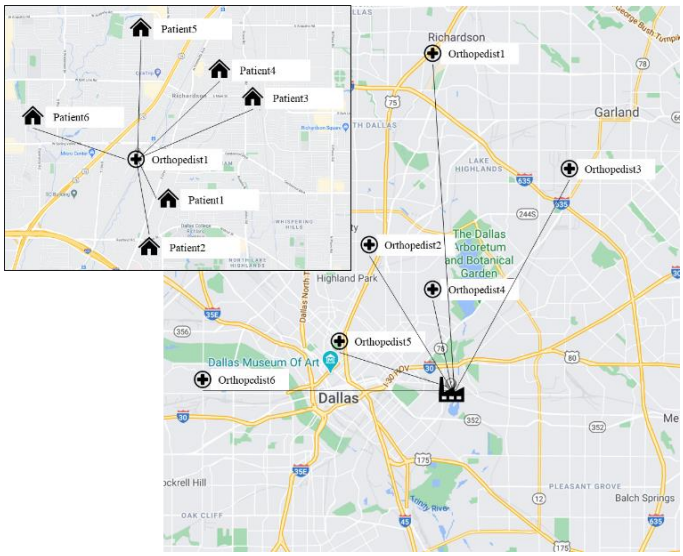

Figure 19. Illustration of the supply chain network

Greenhouse Gas Emission from Production in Additive Manufacturing Supply Chain

The production emission of a product fabricated by AM order j_r^t consists of GHG emissions of the electricity used in the production process $EE_{AM}(j_r^t)$, and the gas emission related to the raw material acquisition ME_{AM}.

$$PE_{AM}(j_r^t) = EE_{AM}(j_r^t) + ME_{AM}(j_r^t) \quad (60)$$

The GHG emission related to electricity can be formulated as follows.

$$EE_{TM}(j_r^t) = I_e \times P_{3D\ Printer} \times T_{AM}(j_r^t) \quad (61)$$

In the equation, $P_{3D\ Printer}$ denotes the power of the 3D printer utilized in the process, and $T_{AM}(j_r^t)$ is the production time of the batch of the order j_r^t. To simplify the model, a basic production time T_{AM_0} is selected according to a basic case. A random number$\varepsilon_{AM,T}(j_r^t)$ is defined to estimate the real production time for one product in AM supply chain. The value of T_{AM_0} and the range of $\varepsilon_{AM,T}(j_r^t)$ can be estimated by industrial practices. The production time can be represented as follows.

$$T_{AM}(j_r^t) = \varepsilon_{AM,T}(j_r^t) \times T_{AM_0} \quad (62)$$

Due to the advantages of the complexity and reduced amount of assembling, the products are assumed to be fabricated in one batch. The GHG emission related to the acquisition of material can be formulated as follows.to the advantages of the complexity and reduced amount of assembling, the products are assumed to be fabricated in one batch. The GHG emission related to the acquisition of material can be formulated as follows.

$$ME_{AM}(j_r^t) = M\_AM(j_r^t) \times Unit_{CO_{2eq,AM}} \quad (63)$$

In this equation, $M_{AM}(j_r^t)$ represents the amount of the raw material used in the order j_r^t; and $Unit_{CO_{2eq,AM}}$ is the GHG emission in the production process of the raw material used in the AM process. M_{AM_0} represents the mass of the material used in the basic case for AM process. A random number $\varepsilon_{AM,M}(j_r^t)$ is defined to estimate the real material consumption for the order j_r^t in AM process. The value of M_{AM_0} and the range of $\varepsilon_{AM,M}(j_r^t)$ are estimated using empirical experience in the industry.

$$M_{AM}(j_r^t) = \varepsilon_{AM,M}(j_r^t) \times M_{AM\,0} \tag{64}$$

Hence, the total GHG emission in the production process of this AM facility during a certain time period T can then be calculated as follows.

$$PE_{AM}(T) = \sum_{t\in T}\sum_{r\in R}\sum_{j\in J_r^t} PE_{AM}(j_r^t) \tag{65}$$

Greenhouse Gas Emission from Delivery in Additive Manufacturing Supply Chain

A function z_r^t is introduced to indicate whether delivery is scheduled to the retailer r on the day t in the following equation.

$$z_r^t = \begin{cases} 1 & If\ a\ delivery\ is\ scheduled\ to\ r\ on\ day\ t \\ 0 & otherwise \end{cases} \tag{66}$$

The major contribution of GHG emission in the process of delivery is considered as the emission of the delivery trucks. The delivery GHG emission is related to the transportation distance ${TD_{AM}}_r^t$ from the retailer r on the day t (mile), fossil consumption MPG of the delivery truck (mile per gallon), and the GHG emission constant c_e (kg CO_{2eq} /gallon).

$$DE_{AM_{r,t}} = \frac{{TD_{AM}}_r^t}{MPG} \times c_e \tag{67}$$

In this equation, similar to the TM supply chain, the ${TD_{AM}}_r^t$ for regular orders are generated using Dijkstra's algorithm given the locations of the retailers and distances between the retailers. As mentioned in the assumptions, the traveling route of rush orders is determined by the sequence of receiving the orders.

The delivery GHG emission of the additive manufacturer during a certain time period T can be formulated as follows.

$$DE_{AM}(T) = \sum_{t\in T}\sum_{r\in R}\left[DE_{AM_{r,t}} \times z_r^t\right] \tag{68}$$

3.3.3 Case Study Results

Comparison of Greenhouse Gas Emission from Traditional and Additive Manufacturing Supply Chain

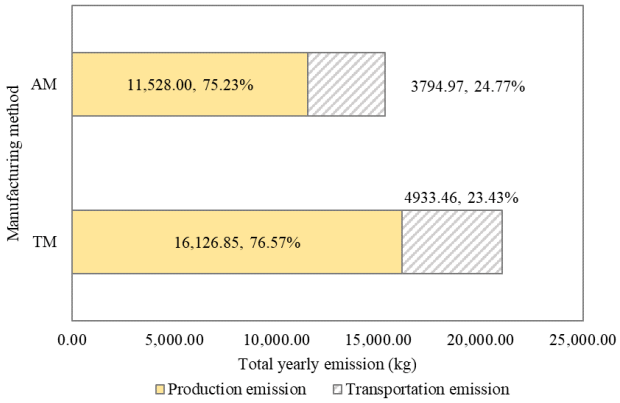

Figure 20. Supply chain GHG emission comparison for AM and TM

The model calculation results of TM and AM are shown in Figure 20. Compared with the traditional manufacturing supply chain, the total carbon emission can be saved by 26.43% by adopting the supply chain enabled by AM. The production emission of AM-enabled supply chain is estimated 27.48% less than the production emission in the traditional supply chain. The transportation emission of the AM supply chain is 23.08% less than the TM supply chain. The main reasons that cause the decrease in AM supply chain are 1) the electricity usage is less in AM supply chain, 2) the average material acquisition carbon emission is less than TM supply chain, and 3) the return rate of TM leads to extra travel of delivery trucks. There is the potential probability that the AM supply chain can save more by applying better parameters in the supply chain.

Additive Manufacturing-Enabled Supply Chain: Varying Rush Order Rates

The rate of rush order in AM is considered and calculated to compare the effect of the PIT structure integrated into the supply chain. In this case study, a new type of order is considered, i.e., rush order, in the AM-specific, integrated PIT structure. The result of different percentages of rush orders is illustrated as follows.

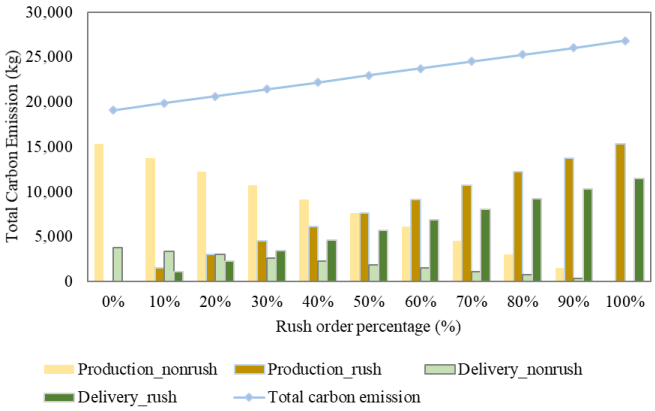

Figure 21. Carbon emission of AM with different percentage of rush order

As the figure indicates, the more rush orders in the total orders are submitted, the more emission will occur in the AM supply chain. The main reason that leads to the result is that rush orders require more travel of delivery trucks. Notably, the portion of delivery emission in regular orders is less than the portion of delivery emission in rush orders. This indicates the further possibility of reducing the carbon emission of the supply chain.

Sensitivity Analysis

In this case study, the vehicle GHG emission constant and GHG emission intensity are studied for their different influences on the supply chain GHG emissions from AM and TM supply chains. Various parameters are considered to influence the carbon emission intensity and the carbon emission constant of the vehicle. In this case study, the influence of these parameters is investigated. In the case study the rework rate of the TM supply chain is 30% and no rush order is requested in the AM supply chain.

The influence of carbon emission intensity is illustrated in Figure 22. The figure indicates that the carbon emission intensity is more significantly influencing the total emission of the manufacturing process in both TM and AM. Specifically, in AM, a 20% variation of carbon emission intensity is estimated to change the total carbon emission by 6.26%. It is notable that the setup parameters, such as tooling, cooling, lubrication, employed parameters, etc. may also influence the overall

GHG emission. The investigations on the influences of these parameters will be conducted in future research.

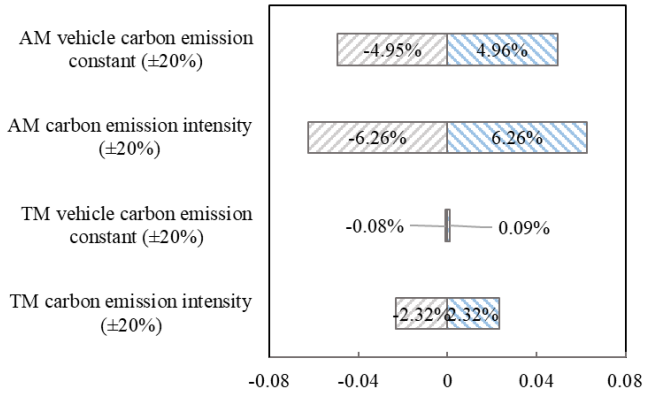

Figure 22. Sensitivity analysis on carbon emission intensity

3.4 Chapter Summary

In this Chapter, the sustainability performance for AM-enabled supply chain is evaluated by comparing its cost and GHG emission with the TM supply chain. Based on the case study results, AM-enabled PIT structure supply chain has the cost-saving potential of up to 25.75% when adopting AM compared to TM. The impact of parameters on the supply chain cost, such as order rework rate, rush order ratio, labor's hourly rate, raw material price and delivery schedule, are studied. To optimize the AM-enabled PIT supply chain, the offline and online route design problems are proposed and solved using both DP and heuristic local search-based algorithms. A potential cost saving is observed with proper design of route delivery sequence. In addition, the impact factors including service area, customer density, product complexity level, and product customization level on the delivery cost by changing one factor at a time. The results suggest that with the expansion of service or the increasing number of orders of the supply chain, more delivery vehicles are needed. Furthermore, the AM-enabled supply chain also offers potential reduction of 26.43% GHG emissions compared with TM supply chain. The sensitivity analysis of carbon emission intensity and vehicle carbon emission constant for GHG emission is performed. The

utilization of a dynamic programming approach in solving the route design problem has undergone significant enhancements. Future works will place a particular emphasis on utilizing and advancing advanced approaches to solve the dynamic problem route design problem such as, Approximate Dynamic Programming (ADP) techniques, or Reinforcement learning. The focus will be on leveraging ADP's advantages in handling complex and dynamic environments, particularly by incorporating real-time factors into the optimization process. This approach aims to optimize routes based on up-to-date information such as traffic congestion, weather conditions, and road incidents. By integrating ADP with real-time data sources and refining the dynamic programming model, future research aims to enhance the accuracy, efficiency, and adaptability of route design solutions. The model will be enhanced by incorporating additional factors and constraints relevant to the problem, such as customer demand, road conditions, delivery time windows, and vehicle capacity limitations. By expanding the scope of the model, it will become more accurate and applicable to real-world scenarios. Sensitivity analysis will also be conducted as part of future research efforts. This analysis will assess the robustness and stability of the ADP-based approach when faced with changes in input parameters. By understanding the sensitivity of the model to variations in factors like customer demand, road conditions, or fuel costs, researchers will gain insights into the system's adaptability and make more informed decisions. Another critical aspect of future works is the integration of real-time data sources into the ADP framework. This will involve incorporating data from GPS tracking systems, traffic monitoring systems, weather forecasts, and other relevant sources. The real-time data will be used to update the model dynamically and optimize routes based on the current conditions. By considering real-time factors, the ADP-based approach will be able to respond effectively to changing circumstances and provide more accurate and efficient route recommendations.

Through these future works, this dissertation seeks to advance the state-of-the-art in dynamic programming for route design. By refining the model, optimizing performance, conducting sensitivity analyses, integrating real-time data, and comparing with other algorithms, the dissertation aims to enhance the effectiveness and efficiency of route design solutions, ultimately contributing to improved transportation logistics and operational performance.

Future works also include simplifying the adopted assumptions of the model proposed in this Chapter for more comprehensive analyses, investigating different AM technologies for the unique PIT supply chain structure, study the route design problems with different parameter settings and more vehicles, integrating the impact of real-time road condition on 3D printing quality on the vehicle, influence of GHG emission for other setup parameters, such as tooling, cooling, lubrication, employee parameters, etc.

Chapter IV. Thermoplastic Waste Recycling in Additive Manufacturing: Recyclability and Cost-Benefit Analysis

Thermoplastics are popularly used as the material in extrusion-based AM including acrylonitrile butadiene styrene (ABS), polylactic acid (PLA), nylon, polypropylene (PP), etc. In the manufacturing process, thermoplastic waste can be generated from different stages such as 3D printing, use and end-of-life in various forms, which may cause potential sustainability issues. The issues can be solved by recycling these waste materials and reusing them in other manufacturing process via a mechanical process transforming the waste pellet into printable filament for extrusion-based AM. Limited research has been dedicated to investigating the effect of different combinations of printing parameters in different recycling rounds with the purpose of compensating the degradation of material during the recycling purpose.

The rest of this Chapter is presented as follows. In Section 4.1, a framework of analyzing AM material recyclability in multiple recycling rounds is proposed. The methodology is introduced in the Section. In addition, a series of experimental case studies are performed, and the results are discussed in the subsections. In Section 4.2, a cost-benefit analysis for products fabricated by AM recycled materials is presented. An optimized manufacturing plan is designed based on the cost-benefit model proposed in the Section.

4.1 Evaluation of AM Thermoplastic Recyclability

Research studies have shown the degradation in mechanical properties of thermoplastic due to the crosslinking nature. It is critical to develop methodologies to evaluate material recyclability. In this Section, material recyclability is defined as the ability of materials in terms of being recycled and reused back in 3D printing with satisfactory material properties, fabrication quality, and mechanical properties. To demonstrate the implementation of the framework, experiments are performed to characterize the potential variations of material recyclability of ABS waste

undergoing multiple recycling rounds. Different combinations of printing parameters are also explored for their impact on compensating for mechanical degradation caused by waste recycling. The potential causal relationship between molecular weight distribution and mechanical degradation is also investigated. This relationship can be utilized to determine the process parameters in different recycling rounds to compensate for material degradation. This paper serves as preliminary work for understanding the material recyclability in AM, and the results of this research will help guide high-quality waste recycling in AM towards higher material efficiency and closed-loop material flow. This research also aims to promote awareness of AM recycling and sustainable manufacturing.

4.1.1 Methodology

ABS waste recycling in extrusion-based AM is used to demonstrate the recyclability evaluation framework. This framework is implemented by quantifying some critical aspects of recyclability, which are detailed in this section. In this Section, multiple rounds of recycling are considered. A certain round of recycling starts with waste collection, and the collected waste is then converted into filament using the mechanical recycling process and used back into 3D printing. As shown in Figure 23, “Round 0” indicates the initial process of making filament from virgin ABS pellets, “Round 1” refers to the first round of recycling, converting waste generated from the 3D printing process using the filament fabricated in “Round 0” into filament, to be used in the next round for 3D printing, and so on. In each recycling round, several sets of fabricating parameters are utilized to print the specimens. The measurement of each recycling round is summarized and compared to observe the change of the material recyclability and the effect of the printing parameters during the recycling process.

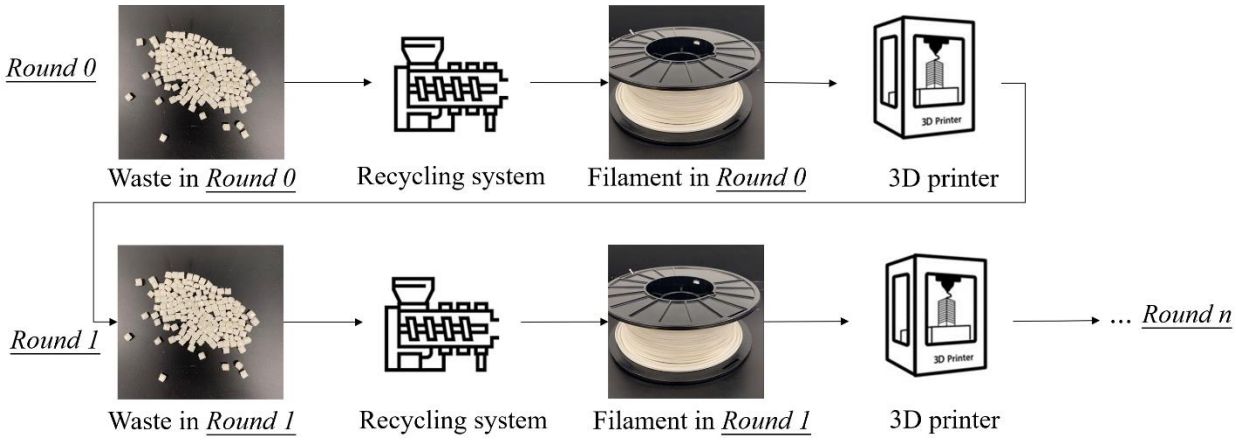

Figure 23. Illustration of multiple recycling rounds

the commercial recycling system Filabot EX6 is used to make filaments from waste pellets, as shown in Figure 24(a)-(c). This recycling system consists of three main processes, i.e., extrusion, filament path, and spooling. Specifically, the extruder includes a hopper for pellets feeding, four heating units for different heating zones, and a passage with a screw driven by a motor. The four heating units can make sure the material can be heated uniformly and the fluidity is sufficient for extrusion. In this study, the virgin pellets are the ABS pellets purchased from Filabot and they are used in received conditions. The winding path has a few fans running at the same speed to cool down the extruded material. The spooler consists of a drive wheel and a spool holder. The specific procedures of waste recycling are stated as follows. First, the temperature of each heating zone is set up; and when the target temperature is reached, and the granulated ABS pellets are fed into the hopper to initiate the process. Second, when the material is heated sufficiently, it is extruded out, following the winding path while being cooled down by the fans. Third, when the extruded material reaches the spooler holder, it is winded at a constant speed to ensure filament consistency. An appropriate selection of parameters (such as heating temperature and spooling speed) can ensure a good quality of extruded filament. In this Section, the values of these parameters are

selected based on experimental results and empirical knowledge: the temperature for each heating unit is set as 40℃, 170℃, 175℃, and 170℃; the extruder motor is set to 66 rpm; the spooling speed is around 4500 to 5000 mm/min; the fan in the winding path is set at the max speed; the position of the recycling system is fixed and aligned in a straight line. In addition, the commercial extrusion-based AM machine used in this study is the MakerGear M3-ID 3D printer, as shown in Figure 24(d). According to the specifications of this machine, the layer thickness can be changed from 0.02 mm to 0.35 mm, the raster angle can be selected from 0° to 180°, and the printing speed can be selected from 0-4000mm/min. In this study, waste is intentionally generated by printing small-sized pellets with a layer thickness of 0.3mm, a raster angle of 0 degrees, and a printing speed of 3500mm/min.

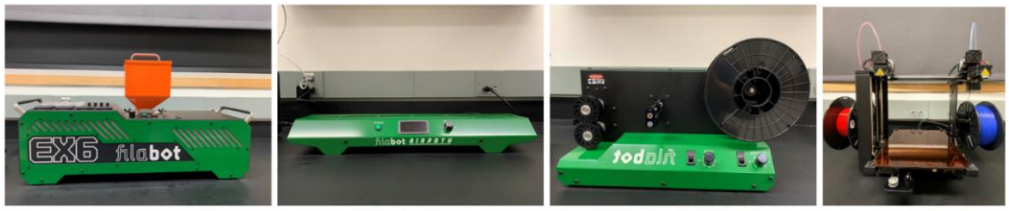

Figure 24. The recycling system that consists of (a) extruder, (b) winding path, and (c) spooler; the 3D printer (d) MakerGear M3-ID

4.1.2 Case Study Results

An Overview of Material Recyclability

The material recyclability under multiple rounds of recycling is quantified as shown in Table 5. Note that the values shown in Table 5 are the averaged values of all test specimens in that specific recycling round.

It can be observed from Table 5 that the averaged material density as well as material molecular weight decrease with more rounds of recycling. This material degradation is potentially caused by chain scission occurs during the process of the polymer extrusion [96]. It has been discovered that material degradation occurs at some temperature range for thermoplastic. The amount of chain

scission appears in the MWD shift and the polydispersity decrease. In addition, the results also suggest that the average ultra-tensile strength of the parts decreases with the increase of the recycling rounds. For the compression test, most parts do not break apart during the first two recycling rounds. The maximum strain percentage with the largest load of the machine (2000N) is used for the results of the compression test. The average strain percentage increases during the recycling rounds. These two measurements indicate that both tensile and compress strength of the specimens fabricated by the material of each round of recycling decreases correspondingly. Thermo-mechanical and thermo-oxidative degradations are responsible for the changes in the results in the mechanical tests.

Table 5. The averaged material recyclability in each recycling round

		Round 0	**Round 1**	**Round 2**	**Round 3**
Material properties	Density (g/cm^3)	0.904	0.867	0.825	0.760
	M_n $(Dalton)$	77,367	75,744	74,629	73,598
	M_w $(Dalton)$	144,425	139,337	137,894	134,571
	M_z $(Dalton)$	237,898	252,202	241,664	233,650
	Polydispersity	2.081	1.891	1.827	1.807
Fabrication quality	Averaged filament dimension (mm)	1.823	1.792	1.774	1.750
	Ra (μm)	42.095	44.196	48.121	54.531
Mechanical properties	Ultimate tensile strength (MPa)	34.181	24.830	21.273	17.043
	Ultimate compressive strain (%)	2.011	4.136	5.244	5.600

In the test results, some obvious trends are observed. For instance, the mechanical strength decreases with the increase of recycling times. Compared with the original specimens, an average of 27.36% decrease in ultimate tensile strength is observed in Round 1, a 37.76% decrease is observed in Round 2, and a 50.14% decrease is observed in Round 3. The mechanical degradation is also observed in the compression tests. In Figure 25, the changes of the tensile strength and

number average molecular weight of the specimen in each recycling round are presented. In the figure, both tensile strength and number average molecular weight decrease in the recycling process. According to the research studies [97], [98], the degradation in the mechanical test can be explained by the decrease in molecular weight. With the increase of the recycling times, the specimen is more capable to be deformed and breaking. The consistency of the filament is decreased in the recycling procedures. The density of the fabricates decreases when the material is recycled.

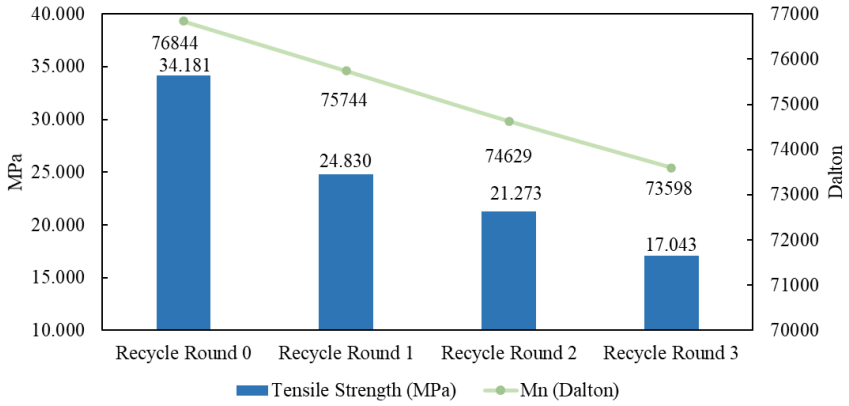

Figure 25. Changes of tensile strength and number average molecular weight in each recycling round

The MWD results indicate that the average molecular weight diminishes during recycling. The decrease in average molecular weight is inspected in the process of AM recycling. The weight average molecular weight decreases in the recycling process in each recycling round. The total degradation of weight average molecular weight after three times of recycling is 5.08%. The total decrease in number average molecular weight after three recycling rounds is 3.52%. The decrease in z average molecular weight is 21.35% after three times of recycling. The PDI of the material demotes the increase of recycling times. Decreases occur during the process of printing for each recycling round. The total degradation of PDI after three times recycling is 5.07%.

Material Property Change Under Multiple Recycling Rounds

The molecular weight for each recycling stage is listed as follows. To better illustrate the recycling process, the recycling procedure is numbered in the order of fabricating. Three samples from each round are collected to run the GPC test. The data is collected using the average of the results of the test for each recycling round. The results are summarized in Table 6. In the table, the samples are numbered in the order of the manufacturing. For example, sample 1 is the original waste. Sample 2 is the filament made from the original waste. Sample 3 is the waste printed with the filament in Round 0. Sample 4 is the filament in Round 1. Sample 5 is the waste made with the filament in Round 1. Sample 6 is the filament in Round 2. Sample 7 is waste printed with the filament for the second recycling round. Sample 8 is the filament in the third round. Sample 9 is the waste printed by the filament in Round 3.

Table 6. Summary of the GPC Results

Sample	**Mn (Dalton)**	**Mw (Dalton)**	**Mp (Dalton)**	**Mz (Dalton)**	**Mz+1 (Dalton)**	**Polydispersity**
1	63,671	143,090	123,343	374,818	1,257,002	2.2473
2	77,367	145,085	124,556	237,898	515,147	2.0813
3	76,884	144,425	123,483	302,197	738,343	1.9033
4	76,059	142,861	122,779	286,411	600,485	1.8914
5	75,744	139,337	122,764	252,202	432,873	1.8320
6	75,534	138,370	122,344	249,222	425,333	1.8269
7	74,629	137,894	122,298	241,664	401,370	1.8211
8	74,174	136,003	122,266	237,651	391,523	1.8067
9	73,598	134,571	122,200	233,650	370,842	1.7952

The number average molecular weight of the samples increases after the original wastes are made into filament and remains at the same level during the recycling process. To better view the trend

of the alteration, the change of the MWD for the filament in the different recycling rounds is shown in Figure 26.

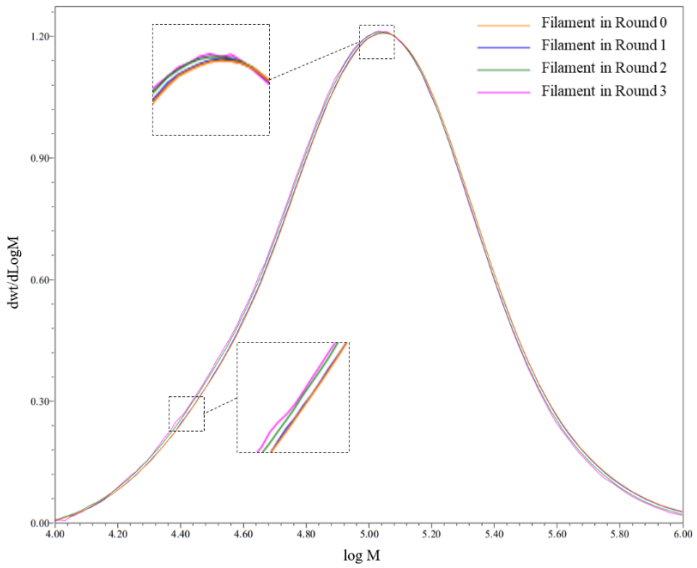

Figure 26. MWD for the filament in each recycling round

As shown in Figure 26, a slight shift to the right is observed with the increase of the times of recycling. The weight average molecular weight, z average molecular weight, and z+1 average molecular weight decrease with the procedure of recycling. The average molecular weight measures the average mass of individual chains.

The changes of the weight average molecular weight, number average molecular weight, z average molecular weight, and polydispersity (PDI) for different recycling rounds are presented in Figure 27. The results in Figure 27 (a) indicate that the number average molecular weight of the ABS decreases when the recycling proceeds for each round. The decrease before and after recycling for number average molecular weight in Round 1 is 1.07%. The decrease of the number in Round 2 is 0.28%, the decrease in Round 3 is 0.61%. Total degradation of 3.52% in weight average molecular is presented with three times of recycling. The results in Figure 27 (b) present the changes in weight average molecular weight of ABS for each recycling round. It is observed that the weight

average molecular weight decreases before and after recycling for each recycling round. In Round 1, the weight average molecular weight decreases by 1.08%. The decrease is 0.69% in Round 2 and 1.37% in Round 3. A total decrease is 5.83% after three recycling rounds. The results in Figure 27 (c) indicate the decrease of z average molecular weight of the material for each recycling round. A 5.22% decrease of z average molecular weight is presented in Round 2. The number is 1.18% in Round 2 and 1.66% in Round 3. The total degradation of z average molecular weight is 21.35% after three recycling rounds.

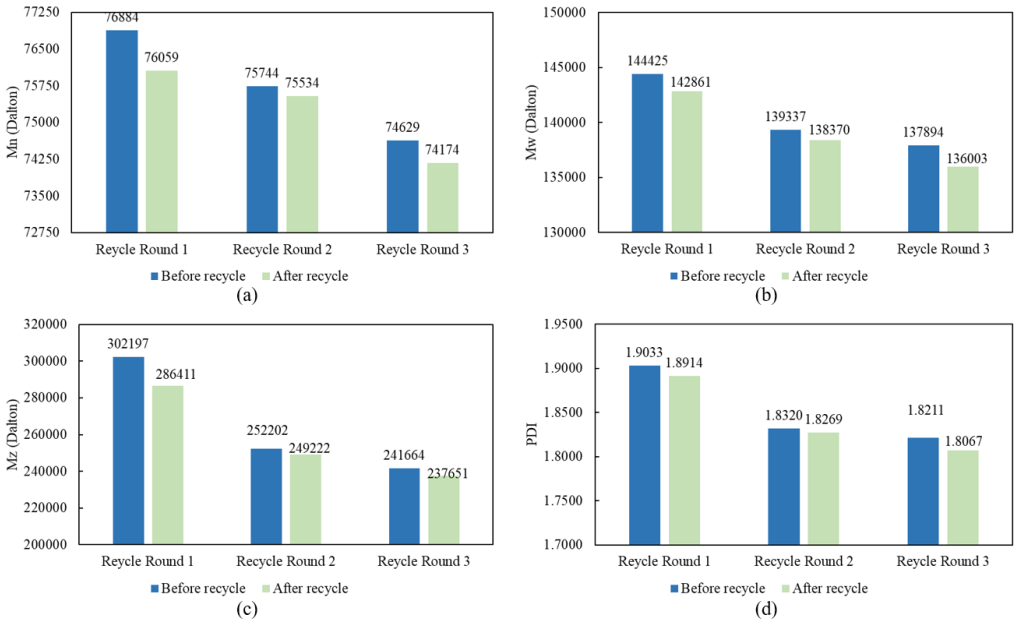

Figure 27. Calibrated results for each recycling round, (a) change of Mn; (b) change of PDI

The polydispersity index (PDI) decreases with the process of recycling. PDI is a measure of the heterogeneity of the original material. The MWD results make sense because the recycling procedure breaks the bond of the original materials. With the increase in the number of recycling, more bonds of the material are broken. The break of bonds has a negative effect on the thermal dynamic features as well as the mechanical characteristics. From the result shown in Figure 27 (d), a decrease of PDI with the number of the recycling is observed. The decrease before and after

recycling for PDI in Round 1 is 0.62%. The number in Round 2 is 0.27%. A decrease of 0.79% is observed in Round 3. The total degradation of PDI during the three times of recycling is 5.07%.

Fabrication Quality Change Under Multiple Rounds of Recycling

Results in the overview of the recyclability demonstrate that the filament diameter reduces during the process of recycling. It is reasonable because the filament fabricating system does not have a precise controlling system for the speed of extruding and the speed of wheeling. During the process of manufacturing the filament, the same set of parameters is utilized to avoid errors. Using the set of parameters declared in Section 2.2.2, the filament in each round of recycling is eligible to use in the commercial AM machine in a tolerable range. The results of the average diameter and the variance of the measurement are shown in Figure 28. The filament diameter decreases insignificantly during the process of recycling. Although the overall filament consistency is acceptable, an increase of variance for the filament diameter is observed. It can be observed that the filament consistency decreases in the process of recycling.

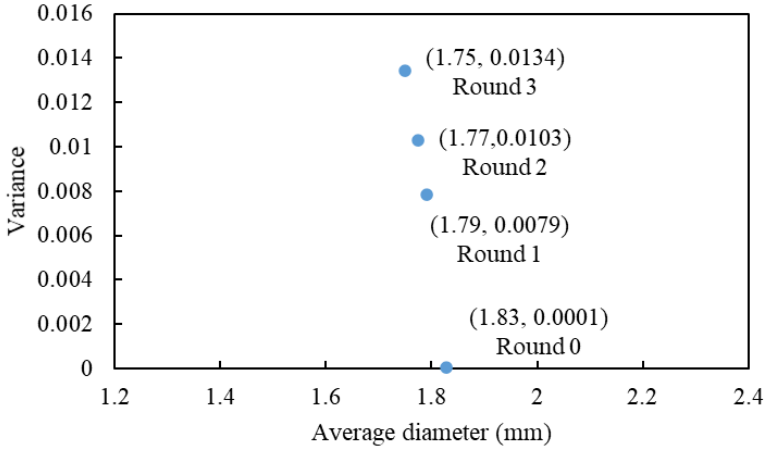

Figure 28. Average filament diameter and variance for each recycling round

The surface roughness of the specimen increases during recycling. The variation indicates a decline in surface quality occurs with the increase of the recycling times. Research studies have concluded that the surface roughness is significantly influenced by the printing parameters [99],

[100]. To eliminate the effect of printing parameters, the results in this case study are the average surface roughness of the specimens printed with different parameters using the material in the same round. Some specific surface roughness measurements of specimens from each recycling round are shown in Figure 29.

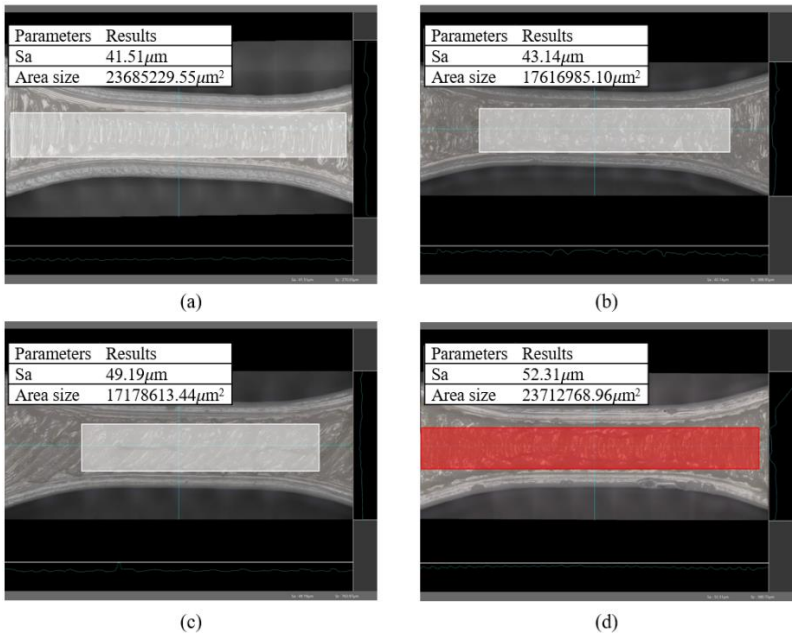

Figure 29. Surface roughness of a specimen from (a) Round 0, (b) Round 1, (c) Round 2, and (d) Round 3

Mechanical Property Change Under Multiple Rounds of Recycling and Within One Round

In this Section, a regression model is generated based on the data for each round. The results of the tensile test are analyzed using the design of experiments (DOE) methodology. The printing parameters are set up as the input. The response variable is the average ultimate tensile strength for each group. In this case study, tensile strength is set as the measurement of the specimen quality. The print parameters are set up as two-level factors. The definition of the level is stated as follows. The 3500 mm/s print speed is the high level, and the 2000 mm/s print speed is the low level. The 0.3mm layer thickness is set as the high level and the 0.1mm layer thickness is set as the low level. The high level for raster angel is 90° and the low level is 0°. The model proposed in this section

can be effective within the range of the selected parameters, specifically, the print speed should be selected from 2000 mm/s to 3500 mm/s, layer thickness should be selected from 0.1mm to 0.3mm, and raster angle should be selected from 0° to 90°.

For the parts printed by the filament in Round 0, the results are presented in Table 7. The source means the source of the effect. The estimate means the effect of the source. The t value is the ratio of the difference between the mean of the source and the given number to the standard error of the mean. The column Pr > |t| is the p-value. It is the two-tailed probability computed using the T distribution. P-value measures the significance of the source. In this work, the source is considered significant if the p-value is less than 0.01.

In the results, it is observed all the effects are presented to be significant in the test results. The final model of the filament in Round 0 is presented as follows. The main effects of the printing speed and the layer thickness are both showing dominant effects in the model for Round 0.

$$\begin{aligned} UTS = {} & -1.648 \times Printing\ Speed - 1.724 \times Layer\ thickness \\ & + 0.974 \times Printing\ Speed \times Layer\ thickness \\ & - 0.614 \times Raster\ angle \\ & + 1.447 \times Printing\ Speed \times Raster\ angle \\ & - 0.860 \times Layer\ thickness \times Raster\ angle \\ & + 0.954 \times Layer\ thickness \times Printing\ Speed \times Raster\ angle \\ & + 28.484 \end{aligned} \tag{69}$$

For the parts printed by the filament in Round 1, the results are as in Table 7. The results indicate that the main effects of the printing speed, the layer thickness, and the raster angle are significant. The interaction effect of printing speed and layer thickness is significant. Other interaction effects

are insignificant. The estimate for the UTS is shown in (70). The interaction effect of the layer thickness with the printing speed presents the dominant effect in the model.

$$UTS = -1.271 \times Printing\ Speed - 1.879 \times Layer\ thickness - 3.981 \times Printing\ Speed \times Layer\ thickness - 0.615 \times Raster\ angle + 23.918 \quad (70)$$

Results for the parts printed by the filament in Round 2 are shown in Table 7. The results imply that the main effects and the interaction effects of the layer thickness with the printing speed and the printing speed with the raster angle are significant. The model for the estimate of UTS for the specimen in Round 2 is shown in (71). The main effect of the layer thickness presents the dominant effect in the model.

$$UTS = -1.148 \times Printing\ Speed - 3.262 \times Layer\ thickness - 1.862 \times Printing\ Speed \times Layer\ thickness - 1.542 \times Raster\ angle + 0.951 \times Printing\ Speed \times Raster\ angle + 21.446 \quad (71)$$

The results for the specimen in Round 3 are presented in Table 7. In the results, all the effects are significant except for the interaction effect of the three parameters. The estimate of UTS for the fabricates with filament in Round 3 is presented as follows. It means the value of UTS for the specimen printed in the Round 3 can be predicted using the equation and the printing parameters given as follow. The main effect of the layer thickness presents the dominant effect in the model.

Table 7. Summary of DOE results for each recycling round

Source	Round 0			Round 1			Round 2			Round 3		
	Estimate	**t Value**	**Pr > |t|**	**Estimate**	**t Value**	**Pr > |t|**	**Estimate**	**t Value**	**Pr > |t|**	**Estimate**	**t Value**	**Pr > |t|**
Intercept	28.484	88.65	<.0001	23.918	103.59	<.0001	21.446	61.13	<.0001	17.181	58.81	<.0001
PS	-1.648	5.13	<.0001	-1.271	5.51	<.0001	-1.148	3.27	0.0016	-1.062	3.64	0.0005
LT	-1.724	5.36	<.0001	-1.879	8.14	<.0001	-3.262	9.3	<.0001	-3.993	13.67	<.0001
PS×LT	0.974	3.03	0.0034	-3.981	-17.24	<.0001	-1.862	-5.31	<.0001	-1.991	-6.82	<.0001
RA	-0.614	-8.14	<.0001	-0.615	-2.66	0.0096	-1.542	-4.4	<.0001	-0.979	-3.35	0.0013
PS×RA	1.447	-4.5	<.0001	-0.273	1.18	0.2404	0.951	-2.71	0.0084	-0.785	2.69	0.009
LT×RA	-0.86	2.68	0.0092	-0.268	1.16	0.2503	-0.622	1.77	0.0804	-1.599	5.47	<.0001
PS×LT×RS	0.954	2.97	0.0041	0.192	0.83	0.408	0.37	1.05	0.2915	0.37	1.05	0.0516
Number of observations		80			80			80			80	
R-square value		0.868			0.906			0.88			0.776	

In this table, PS represents for Printing speed, LT represents Layer thickness, and RA represents Raster angle

$$UTS = -1.062 \times Printing\ Speed - 3.993 \times Layer\ thickness \quad (72)$$
$$- 1.991 \times Printing\ Speed \times Layer\ thickness$$
$$- 0.979 \times Raster\ angle$$
$$- 0.785 \times Printing\ Speed \times Raster\ angle$$
$$- 1.599 \times Layer\ thickness \times Raster\ angle + 17.181$$

Using the DOE methodology, the effects of printing parameters on the mechanical properties are analyzed. Models (69)(70)(71)(72) show the change of the relationships between the fabricate quality and the printing parameters during the recycling procedure. With the increase of the times of recycling, the effect of printing speed reduces. The effect of layer thickness increases when the material is recycled. The effect of the raster angle decreases with the recycling procedure. With the increase of recycling rounds, the layer thickness has a dominating effect on the tensile strength of the specimen fabricated. The models generated above instruct on adjusting the printing parameters to improve the tensile strength for each round of recycling.

To investigate the effect of recycling rounds, an additional model was developed by including the number of recycling rounds as a factor to generate the model. The obtained results were subsequently analyzed and presented in Table 8. It is noticed that the recycling round has a dominating negative effect on the tensile strength of the specimen if it is considered a factor in the experiments. The model generated based on the results is shown in (73). Upon analyzing the results, a significant and negative effect of the recycling round factor on the tensile strength of the specimen was observed. Specifically, as the number of recycling rounds increased, the tensile strength of the specimen decreased considerably.

$$UTS = -4.068 \times Recycling\ round - 2.751 \times Raster\ angle + 1.796 \times Printing\ speed - 2.146 \times Raster\ angle \times Printing\ speed + 0.509 \times Layer\ thickness \times Recycling\ round - 0.767 \times Recycling\ round \times Raster\ angle + 0.908 \times Printing\ speed \times Recycling\ round \times Raster\ angle + 1.051 \times Layer\ thickness \times Recycling\ round \times Raster\ angle \quad (73)$$

Table 8. Summary of DOE results including the number of recycling round

Source	Estimate	t Value	Pr > |t|
Intercept	32.746	67.790	<.0001
RR	-4.068	-23.060	<.0001
LT	1.123	2.320	0.021
RA	-2.751	-5.700	<.0001
PS	1.796	3.720	0.000
LT×RA	-0.761	-1.580	0.116
LT×PS	-0.314	-0.650	0.516
RA×PS	-2.146	-4.440	<.0001
LT×RA×PS	0.179	0.370	0.711
PS×RR	-0.278	-1.580	0.116
LT×RR	0.509	2.890	0.004
RA×RR	0.767	4.350	<.0001
PS×LT×RR	-0.238	-1.350	0.179
PS×RA×RR	0.908	5.150	<.0001
LT×RA×RR	1.051	5.960	<.0001
PS×LT×RA×RR	0.341	1.930	0.054
Number of observations		320	
R-square value		0.855	

In this table, RR represents for Recycling round, PS represents for Printing speed, LT represents Layer thickness, and RA represents Raster angle

According to the results of DOE, the effect of the layer thickness is dominant in the tensile strength of the specimen during each recycling round. The increase in the layer thickness will result in lower UTS according to the models. With the increase in the number of recycling, the effect of the printing speed and the raster angle appears the decline. The effect of layer thickness increases with

the number of recycling. It is estimated that selecting the proper layer thickness has a considerable contribution to improving the tensile strength of the fabricates manufactured by recycled material. In addition, 3D printers and recycling machines used in the studies have different specifications. The effect of the recycling round is dominant on the tensile strength of the fabrication. With the increase of the recycling round, the tensile strength of the specimens decreases. In summary, the improvement of tensile strength for the specimens can be easier achieved by adjusting the layer thickness with the increase of the recycling times. To keep the same tensile strength of the specimen fabricated by the recycled material, it is recommended to decrease the layer thickness when the recycling time of the material increases. The effect of the printing speed is lower than the layer thickness but higher than the raster angle. The conclusion matches the results in the literature [101], [102]. The models generated in the literature may be different from the models generated in this work. The potential reason why the models generated are different is that the types and definitions of the parameters are different.

4.2 Cost-Benefit Analysis of AM Products Fabricated from Recycled Materials

In this Section, a mechanical recycling facility that processes 3D printing thermoplastic wastes is studied. The objective of this research is to obtain the optimum daily recycling plans (or sequences) for this facility to achieve maximum profit.

The AM thermoplastic recycling process is illustrated in Figure 30. In Figure 30 (a), 3D printing wastes such as failed parts, support structures, wasted filaments, and abandoned parts are generated, possibly due to machine errors, inappropriate geometry designs, or improper process parameter settings. These wastes are collected, cleaned, and cut into uniform-sized pellets in Figure 30 (b). The waste pellets are then heated, extruded, and cooled to form filaments via the extruder in Figure 30 (c), the air path in Figure 30 (d), and the spool in Figure 30 (e). The recycled filament is then used back in AM for fabricating parts.

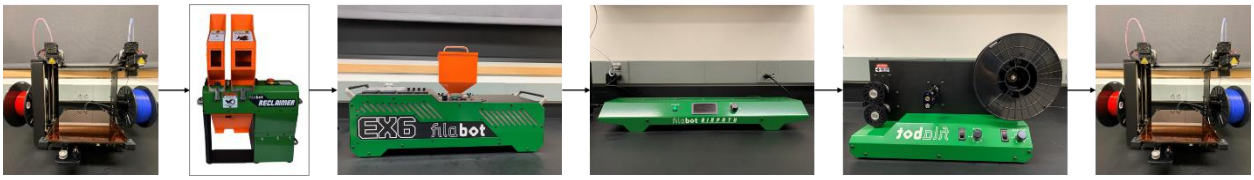

(a) (b) (c) (d) (e) (f)

Figure 30. Illustration of AM thermoplastic recycling process

Existing research studies show a certain level of mechanical degradation in parts fabricated using recycled filament, in comparison with parts fabricated using new filament. Also, the mechanical degradation caused by recycling becomes worse with an increasing number of recycling times.

4.2.1 Recycling Cost Model Formulation

To model the recycling cost, a few assumptions are adopted in this Section.

(1) The recycling facility offers the fabrication of new filament (using virgin material pellets) and the fabrication of recycled filament (using collected wastes). At the recycling facility, four types of filaments can be made, including new filament F0, first-time recycled filament F1, second-time recycled filament F2, and third-time recycled filament F3. Any recycling times that are greater than three are not considered in this research due to the unsatisfactory quality and consistency of the recycling and the 3D printing.

(2) The recycling facility accepts two types of orders. i.e., picking up waste from customers and delivering filaments to customers. When a customer places an order, this customer can choose to just place a pick-up order, a delivery order, or both.

(3) Customers are responsible for correctly labeling the 3D printing as “new waste” (waste generated from new filament), “first-time recycled waste”, “second-time recycled waste”, and “third-time recycled waste”. The third-time recycled waste will not be recycled at the facility, but rather, it will be disposed of strictly following all relevant regulations.

(4) Customers pay the facility for filament purchase and delivery, depending on the order filament type and the delivery speed. Orders with different required delivery speeds will be

assigned a different level of priority. On the other hand, customers receive incentives when they order waste pickup, depending on the waste type.

(5) For the utility, the material used to fabricate each type of filament is sufficient, assuming the manufacturer has run the service for a long time and the inventory is relatively steady.

(6) The study focuses on the fabrication plan at the manufacturer site. The delivery process is not considered because it is performed beyond the range of the manufacturer site.

Total cost in a time T of includes electricity cost EC, overhead cost OC, labor cost LC, and material cost MC.

$$TC(T) = EC(T) + OC(T) + LC(T) + MC(T) \tag{74}$$

Let $\boldsymbol{i} \in \{\boldsymbol{W0}, \boldsymbol{W1}, \boldsymbol{W2}, \boldsymbol{W3}, \boldsymbol{F0}, \boldsymbol{F1}, \boldsymbol{F2}, \boldsymbol{F3}\}$ is the index of the type of material or filament. Let $\boldsymbol{t} \in [\boldsymbol{1}, \boldsymbol{T}]$ be the index of the workday. $\boldsymbol{p} \in [\boldsymbol{1}, \boldsymbol{3}]$ is the index of the priority level. $\boldsymbol{j} \in [\boldsymbol{1}, \boldsymbol{J}]$ is the index of the order to be manufactured in a workday. $\boldsymbol{MT}$ is the index of the manufacturing date of the order.

Material Cost

The material cost includes the total cost of virgin material, the total cost of the first-time recycled waste, the total cost of the second-time recycled waste, and the total cost of the third-time recycled waste.

$$MC(T) = \sum_{MT(i_j^{t,p})=1}^{T} \sum_{j=1}^{J} \sum_{i \in \{W0, W1, W2, W3\}} W(j_i^{t,p}) \times MC_i \tag{75}$$

In this equation, MC_{W0} is the material unit cost for the pellets to fabricate the new material (USD/kg). MC_{W1} (USD/kg), MC_{W2} (USD/kg), and MC_{W3} (USD/kg) are the material cost of purchasing the waste from the customers. W is the weight of the corresponding material.

Electricity Cost

Electricity cost includes the power used to extrude the filament and the power used to granulate the waste material. In this study, it is assumed that the extruding machine and the granulating machine work on the rated power. The time to fabricate a unit of each material is fixed but varies from each other. The time to granulate the same amount of each material is also the same but varies from each other. It is also assumed that the unit cost of the electricity is the same during the T days.

$$EC(T) = C_{Elec} \times \sum_{MT(j_i^{t,p})=1}^{T} \sum_{j=1}^{J} \sum_{i\in\{F0,F1,F2,F3\}} W(j_i^{t,p}) \times (P_{Recy} \times u_i + P_{Gran} \times T_{Gran,i}) \tag{76}$$

In this equation, C_{Elec} is the unit cost of electricity (USD/kWh). P_{Extr} is the power of the recycling machine. u_i is the time to recycle 1kg of material i (kW). P_{Gran} is the power of the granulating machine. $T_{Gran,i}$ is the time to granulate 1kg of material i (h). These parameters are defined to calculate the total fabricating time.

Labor Cost

Labor cost includes the workers' wages on the manufacturing site. In specific, labor cost is calculated by the workers' hourly pay multiplied by the total process time. As stated in section 4.2.1, the time to manufacture or granulate the same amount of one type of material is the same but varies depending on the material type.

$$LC(T) = C_{work} \times \Big(\sum_{MT(j_i^{t,p})=1}^{T} \sum_{j=1}^{J} \sum_{i\in\{F0,F1,F2,F3\}} W(j_i^{t,p}) \times \left(u_i + T_{Gran,i}\right) + \sum_{MT(j_i^{t,p})=1}^{T} \sum_{j=1}^{J} \sum_{i\in\{W0,W1,W2,W3\}} W(j_i^{t,p}) \times T_{Prep} \Big) \tag{77}$$

In this equation, C_{work} is the worker's hourly pay (USD/h). T_{Prep} is the preparation time for recycling 1kg of material, which includes cleaning the machine, setting up the machine, and pre-processing the materials (h).

Overheads

Overhead cost is the average facility cost per fabrication. It includes the average cost of the granulating machine and the extruding machine. Machines are assumed to have limited working lives. The facility cost is also included in the overhead cost. The overhead cost is summarized as follows.

$$OC(T) = \left(\frac{C_{Gran}}{LS_{Gran}} + \frac{C_{Extr}}{LS_{Extr}}\right) \times \sum_{MT(j_i^{t,p})=1}^{T} \sum_{j=1}^{J} \sum_{i \in \{F0,F1,F2,F3\}} W(j_i^{t,p}) + C_{Faci} \times T \quad (78)$$

In this equation, C_{Gran} is the cost of the granulating machine (USD). LS_{Gran} is the life span of the granulating machine (min). C_{Extr} is the cost of the recycling machine (USD). LS_{Extr} is the life span of the recycling machine (min). C_{Faci} is the rent cost for the facility (USD/day).

Incentive

The incentive includes the incentive of the filament with each quality level and different order priority. It is assumed that the unit price for each type of filament is different. In addition, the price is higher for orders with higher priority.

$$I(T) = \sum_{MT(j_i^{t,1})=1}^{T} \sum_{j=1}^{J} \sum_{i\in\{F0,F1,F2,F3\}} W(j_i^{t,2}) \times MP_i \times Cr_2$$

$$+ \sum_{MT(j_i^{t,1})=1}^{T} \sum_{j=1}^{J} \sum_{i\in\{F0,F1,F2,F3\}} W(j_i^{t,1}) \times MP_i \times Cr_1 \quad (79)$$

$$+ \sum_{MT(j_i^{t,0})=1}^{T} \sum_{j=1}^{J} \sum_{i\in\{F0,F1,F2,F3\}} W(j_i^{t,0}) \times MP_i$$

In the equation, MP_i is the price for the material i (USD/kg). Cr_p is the price change ratio for urgent orders that priority level is p. In this study, $Cr_p \in [1,2], for\ p = 1,2$.

4.2.2 Optimization Problem Formulation

The problem aims to find a recycling plan to maximize the profit during the period T. The mathematical model can be expressed as follows.

Objective: Max $P(T)$

$$P(T) = I(T) - TC(T) \quad (80)$$

The equation indicates the relationship between the profit in T days with the total cost and the incentive in T days. The aforementioned problem is modeled in the discrete-time control system perspective and further is formulated as an optimal control problem to obtain the best daily production strategy which will: (i) the plan keeps track of the daily inventory; (ii) it meets all customers' requests with different levels of emergency; and (iii) it maximizes the utility of the production line in terms of energy cost, producing time, etc.

The daily inventory is denoted as (i.e., $In_i(ct^t)$ for each category of material waste and filament, $i \in \{F_0, F_1, F_2, F_3, W_0, W_1, W_2, W_3\}$) as the state variable of interest, $x(t) \in \mathbb{R}^8$ with the first four for filament inventory and the rest for waste inventory, with $t = 0, 1, \dots, T$. Hence, the inventory can be expressed as follows.

$$x(t+1) = Ax(t) + Bu(t) + CO(t) \tag{81}$$

$$A = I_8 \tag{82}$$

$$B = \begin{bmatrix} \mu_1 & 0 & 0 & 0 \\ 0 & \mu_2 & 0 & 0 \\ 0 & 0 & \mu_3 & 0 \\ 0 & 0 & 0 & \mu_4 \\ -1 & 0 & 0 & 0 \\ 0 & -1 & 0 & 0 \\ 0 & 0 & -1 & 0 \\ 0 & 0 & 0 & -1 \end{bmatrix} \tag{83}$$

$$C = \begin{bmatrix} -1 & 0 & 0 & 0 & 0 & 0 & 0 & 0 \\ 0 & -1 & 0 & 0 & 0 & 0 & 0 & 0 \\ 0 & 0 & -1 & 0 & 0 & 0 & 0 & 0 \\ 0 & 0 & 0 & -1 & 0 & 0 & 0 & 0 \\ 0 & 0 & 0 & 0 & 1 & 0 & 0 & 0 \\ 0 & 0 & 0 & 0 & 0 & 1 & 0 & 0 \\ 0 & 0 & 0 & 0 & 0 & 0 & 1 & 0 \\ 0 & 0 & 0 & 0 & 0 & 0 & 0 & 1 \end{bmatrix} \tag{84}$$

A, B, and C are constant matrices, $O(t) \in \mathbb{R}^8$ records the order information characterized for day t based on delivery time $DT(j^{t,p})$, and $u(t) \in \mathbb{R}^4$ denotes our daily resumption for each type of material due to daily production that will be determined in an optimal manner. In this study, the inventory is restricted due to practical needs, such as the capacity and actual demand of the customers' orders. The constraint can be rewrite as the lower and upper bounds for the state variable $x(t)$ and targeted input $u(t)$ as follows.

$$x_{Lower} \leq Dx(t) \leq x_{upper} \tag{85}$$

$$u_{Lower} \leq Eu(t) \leq u_{upper} \tag{86}$$

In particular, equation (83) and equation (84) leads to $x_{Lower} = 0$ and $u_{Lower} = 0$, respectively. Equation (84) provides the upper-bound for the state, i.e., $D = [1 \quad 1 \quad 1 \quad 1 \quad 1 \quad 1 \quad 1 \quad 1]$ and $x_{upper} = CapIn$. The equations gives the production limit due to time, i.e., $E = [u_{F1}\mu_1 \quad u_{F2}\mu_2 \quad u_{F3}\mu_3 \quad u_{F4}\mu_4]$ and $u_{upper} = \max t - 3CT$.

The goal is to come up with an optimal $u(t)$ such that the total profit is maximized, where the incentive $I(x,u,T)$ is determined by the order information $O(t)$ and the cost including electricity, overhead, labor, and material are considered.

Now, the desired problem is transferred into the equations as follows.

$$\max_{u} P(x,u,T) = I(x,u,T) - TC(x,u,T) = \sum_{t=0}^{T} lu(t)$$

$$\sum_{t=0}^{T} \begin{bmatrix} \mu_1(MP_1 - MC_1 - u_{F1}C_{Elec}P_{Recy} - C_{Elec}P_{Gran}T_{Gran,1} - \frac{C_{Recy}}{LS_{Recy}}P_{Recy}u_{F1} - \frac{C_{Gran}}{LS_{Gran}}P_{Gran}T_{Gran,1}) \\ \mu_2(MP_2 - MC_2 - u_{F2}C_{Elec}P_{Recy} - C_{Elec}P_{Gran}T_{Gran,2} - \frac{C_{Recy}}{LS_{Recy}}P_{Recy}u_{F2} - \frac{C_{Gran}}{LS_{Gran}}P_{Gran}T_{Gran,2}) \\ \mu_3(MP_3 - MC_3 - u_{F3}C_{Elec}P_{Recy} - C_{Elec}P_{Gran}T_{Gran,3} - \frac{C_{Recy}}{LS_{Recy}}P_{Recy}u_{F3} - \frac{C_{Gran}}{LS_{Gran}}P_{Gran}T_{Gran,3}) \\ \mu_4(MP_4 - MC_4 - u_{F4}C_{Elec}P_{Recy} - C_{Elec}P_{Gran}T_{Gran,4} - \frac{C_{Recy}}{LS_{Recy}}P_{Recy}u_{F4} - \frac{C_{Gran}}{LS_{Gran}}P_{Gran}T_{Gran,4}) \end{bmatrix}^{T} u(t)$$

$$\text{s.t. } x(t+1) = Ax(t) + Bu(t) + CO(t),$$

$$x(t) \geq 0, u(t) \geq 0 \text{ and } Dx(t) \leq x_{upper};\ Eu(t) \leq u_{upper}.$$

$$I(x,u,T) = [MP_1 \quad MP_2 \quad MP_3 \quad MP_4 \quad 0 \quad 0 \quad 0 \quad 0]^T x(t)$$

$$TC(x,u,T) = EC(x,u,T) + OC(x,u,T) + LC + MC\ (u)$$

$$EC(x,u,T) = C_{Elec} \cdot \begin{bmatrix} \mu_1(P_{Recy} \times u_{F1} + P_{Gran} \times T_{Gran,1}) \\ \mu_2(P_{Recy} \times u_{F2} + P_{Gran} \times T_{Gran,2}) \\ \mu_3(P_{Recy} \times u_{F3} + P_{Gran} \times T_{Gran,3}) \\ \mu_4(P_{Recy} \times u_{F4} + P_{Gran} \times T_{Gran,4}) \end{bmatrix}^{T} u(t)$$

$$OC(x,u,T) = \begin{bmatrix} \mu_1(\frac{C_{Recy}}{LS_{Recy}} \times P_{Recy} \times u_{F1} + \frac{C_{Gran}}{LS_{Gran}} \times P_{Gran} \times T_{Gran,1}) \\ \mu_2(\frac{C_{Recy}}{LS_{Recy}} \times P_{Recy} \times u_{F2} + \frac{C_{Gran}}{LS_{Gran}} \times P_{Gran} \times T_{Gran,2}) \\ \mu_3(\frac{C_{Recy}}{LS_{Recy}} \times P_{Recy} \times u_{F3} + \frac{C_{Gran}}{LS_{Gran}} \times P_{Gran} \times T_{Gran,3}) \\ \mu_4(\frac{C_{Recy}}{LS_{Recy}} \times P_{Recy} \times u_{F4} + \frac{C_{Gran}}{LS_{Gran}} \times P_{Gran} \times T_{Gran,4}) \end{bmatrix}^T u(t)$$

$$LC = C_{work} \times T \times T_{workday}$$

$$MC(x,u,T) = [\mu_1 MC_1 \quad \mu_2 MC_2 \quad \mu_3 MC_3 \quad \mu_4 MC_4]u(t)$$

Now, from Pontryagon's Maximum Principle, we define the Hamiltonian associated to this system as:

$$H(x,u,t) = lu + \lambda^T(Ax + Bu + Co), \tag{87}$$

where $\lambda(t) \in \mathbb{R}^8$ denotes the co-state that satisfies the following recursive law:

$$\lambda(t) = A^T\lambda(t+1), \;\; \lambda(T) = 0. \tag{88}$$

Hence, $\lambda(t) \equiv 0, \forall t = 0,1,\dots,T$, and then $H = lu$, which is linear with respect to the decision variable u. As a result, u is chosen as the largest possible value for each day, that is $u(t)$ must satisfy the equation as follows.

$$Dx(t) = x_{upper} \text{ and } Eu(t) = u_{upper} \tag{89}$$

Inventory constraints

The total inventory includes the spaces for both raw materials and different types of filaments. The constraint limits the storage spaces for production. The constraints can be expressed using the following equations.

$$In_i(Maxt^{MT\left(j_i^{t,p}\right)})$$

$$= In_i(Maxt^{MT\left(j_i^{t,p}\right)-1}) + Ma_i^{MT(j_i^{t,p})} \quad (90)$$

$$- W\left(j_i^{t,p}\right), forMT(j_{ji}^t) \in \{2,3, \dots T\}, i \in \{F0, F1, F2, F3\}$$

The equation expresses the relationship between the inventory of the filament between two adjunct days.

$$In_i(Maxt^{MT\left(j_i^{t,p}\right)})$$

$$= In_i(Maxt^{MT\left(j_i^{t,p}\right)-1}) - Ma_i^{MT(j_i^{t,p})} + W(j_i^{t,p}), for\ t \quad (91)$$

$$\in \{2,3, \dots T\}, i \in \{W0, W1, W2, W3\}$$

The equation is the relationship of the inventory for waste between two adjunct days.

$$In_i(Maxt^{MT\left(j_i^{t,p}\right)-1}) \geq \sum_{MT(i_j^t)=1}^{J} W\left(j_i^{t,p}\right), for\ t \in \{2,3, \dots T\}, i \quad (92)$$

$$\in \{F0, F1, F2, F3\}$$

The constraint indicates that the inventory for each type of filament is enough for the orders to be delivered on the next day.

$$In_{Fn}(Maxt^{t-1}) + \mu_n \times In_{Wn}(Maxt^{t-1}) \geq Ma_{Fn}^t, n \in \{0,1,2,3\} \quad (93)$$

The constraint indicates that the waste inventory on day t is enough to manufacture the amount of respective filament in the plan on day t.

$$\sum_{i=F0,F1,F2,F3,W0,W1,W2,W3} In_i(ct^t) \leq CapIn \quad (94)$$

The constraint indicates that the inventory cannot excess a capacity amount of inventory $CapIn$.

Time constraint in a workday

Two-time constraints are considered in this study. The first one is that the total manufacturing time of each day has an upper bound. The constraint indicates that the total manufacturing time of the plant has a limit $Maxt$ for each day, which is expressed in (95).

$$\Omega(t1) \leq Maxt, t1 \in \{1,2, \dots T\} \tag{95}$$

The second time constraint considered in this study is that there are three delivery priority levels, indicating the day to deliver an order cannot exceed a specific number of days depending on the delivery priority. Three priority levels are considered in this study.

$$DT(j^{t,p}) \leq \begin{cases} t+7, p=0 \\ t+2, p=1 \\ t, p=2 \end{cases} \tag{96}$$

The constraint indicates that an order should be delivered within several days after it is submitted depends on the priority. $\Omega(t1)$ is defined as the total manufacturing time (min) in day $t1$

$$\Omega(t1) = \sum_{MT(j_i^{t,p})=t1} \tau\left(j_i^{t,p}\right) + \sum_{k=2}^{K} \theta(k) \times CT\,, j_i^{t,p} \in Se(t1) \tag{97}$$

In the equation, CT is the time to process the machine when material is changed. $\theta(k)$ is a binary value defined as follows.

$$\theta(k) = \begin{cases} 1, if\ i_k \neq i_{k-1} \\ 0, if\ i_k = i_{k-1} \end{cases}, j_k{}_{i_k}^{t_k,p_k} \in Se(t1) \tag{98}$$

4.2.3. Results and Discussion

In this Section, three case studies are performed to investigate the optimized recycling plan for AM thermoplastics. The first case study presents the parameters and their values applied in this study. It compares the order-driven recycling plan and the optimization recycling plan with two methods. The second case study demonstrates the optimization results based on the different order information. In the third case study, the profits of the optimized recycling plan applying different

pricing strategies are discussed. The sensitivity analysis is performed on the pricing strategies considered in this study.

Baseline Case

In this case study, the daily production amount and the inventory level change in 180 days are calculated. The results are set as a baseline case. In specific, one recycling system is considered in this case study. The price of each type of filament is based on the market price. The total profits in 180 days of three production plans are calculated in this case. The first plan is the optimized production plan for daily profit. The recycling plan maximizes the daily profit. The second plan is to manufacture based on the number of orders. The third plan is the optimized production plan for 10-day profit. The recycling plan maximizes the 10-day profit. Based on the results, production plans with optimization have higher profits than the plan that manufactures the number of orders. The reason is that the optimization offers a recycling plan that maximizes profit. The daily optimization plan has a similar profit to the 10-day optimization. The profit of filament 0 in daily optimization is less than the one in 10-day optimization. The reason is that in one-day optimization, all the idle time is used to produce filament 0, which makes the cost of manufacturing filament 0 high. In the 10-day optimization, idle time is used to manufacture the filament that has the highest profit in the previous 10 days. Filaments other than filament 0 are possible to be manufactured during idle time because of this mechanism. In this case, filament 1 in the 10-day optimization has less profit than in the daily optimization. The reason is that the idle time of some days in the 10-day optimization is used to fabricate filament 1. Profits of other filaments are similar in the two optimized recycling plans. The values of the parameters are presented in Table 9.

Table 9. Values of parameters used in the case study

Symbol	Value	Data source	Symbol	Value	Data source
T_{Recy}	30 (min)	[103]	C_{Recy}	14,217.00 ($)	[104]
u_{F1}	22 (min/kg)	[23]	LS_{Recy}	5 (yr)	
u_{F2}	20 (min/kg)		C_{work}	14.31 ($/hour)	[93]
u_{F3}	18 (min/kg)		C_{Gran}	7979.00 ($)	[105]
u_{F4}	16 (min/kg)		LS_{Gran}	20 (yr)	
C_{Elec}	6.44 (cents/kWh)	[106]	T	180 (day)	Assumed in this study
MC_{w0}	3.31($/kg)	[107]	μ_1	0.98	Assumed in this study
MC_{w1}	3.14($/kg)		μ_2	0.96	Assumed in this study
MC_{w2}	2.98($/kg)		μ_3	0.95	Assumed in this study
MC_{w3}	2.84($/kg)		μ_4	0.93	Assumed in this study
MP_{F0}	21.99($/kg)		$CapIn$	2000 (kg)	Assumed in this study
MP_{F1}	20.89($/kg)		CT	15 (min)	Assumed in this study
MP_{F2}	19.85($/kg)		T_{Prep}	20 (min)	Assumed in this study
MP_{F3}	18.85($/kg)		$T_{workday}$	8 (hour)	Assumed in this study

The production plan for 180 days is considered. The start inventory of each type of filament is 100 kg. The inventory capacity is 2000 kg in this case. The daily recycling plan is based on the order information. With fulfilling the number ordered by the customer, the idle time of the machine is used to manufacture the filament to optimize the total profit. It is assumed that 20 customers submit random orders. In each order, the maximum amount of each type of filament is 12, 10, 8, and 6 kg for filament 0, 1, 2, and 3, respectively. The filament suffers from less level of degradation with

less recycling times. The maximum amounts are assumed because customers tend to select virgin filaments because they have a wider range of applications.

In Figure 31, compared with the other two recycling plans, order-driven manufacturing has less profit during the 180 days. The profit of the daily profit-driven recycling plan is 31.02% higher than the order-driven plan. And the profit of the 10-day profit-driven plan is 27.89% higher than the order-driven plan. The reason is that the latter two fabrication plans manufacture the filament in idle time, which leads to the potential inventory values. In this case, the profit of the daily profit-driven recycling plan is higher than it of the 10-day profit-driven plan. However, the different order amounts will lead to a change in profit, and this will be discussed in the case study.

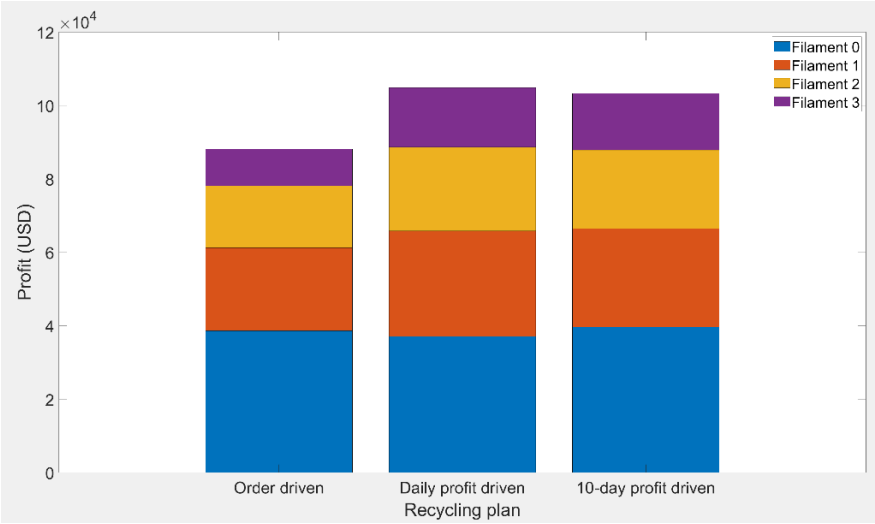

Figure 31. Profit of each recycling plant

To compare the daily profit driven and the 10-day profit-driven plan, the recycling plan for each day is presented in Figure 32. 60 days of the plan are presented in Figure 33, It is noticed that in the daily profit-driven plan, the preference in the build-ahead production for filament 0 is higher than other types of the filament. The reason is that filament 0 has a higher unit profit than other types of filament. If the inventory capacity is not reached, making as much filament 0 as possible will maximize the daily profit. However, when the inventory capacity is almost reached, some

types of other filaments are made during the left-over time. In the 10-day profit-driven plan, it is presented that the preference of the build-ahead production changes every 10 days. It is also noticed that the profit of filament 0 for the daily profit-driven recycling plan is less than the number in the 10-day profit-driven plan. The reason is that when the plan decides to fabricate more of a specific type of filament, the total cost of that type of filament increases, which decreases the average profit of the type. It is noticed that the product diversity of the 10-day profit plan is better than the daily profit-driven recycling plan because of the change of preference for build-ahead production every 10 days. Product diversity refers to the variety of products that a company offers. There are different ways to calculate product diversity, but one common approach is to use a measure called the Herfindahl-Hirschman Index (HHI). The HHI is a widely used measure of market concentration that is also applicable to measuring product diversity, which is calculated by the equation (99). The HHI of the daily profit-driven recycling plan is 0.27, and the number of the 10-day profit-driven recycling plan is 0.30, which indicates that the product diversity of the 10-day profit-driven recycling plan is better.

$$HHI = \sum_{i=F0,F1,F2,F3} \frac{Profit(i)}{Totalprofit}^{2} \tag{99}$$

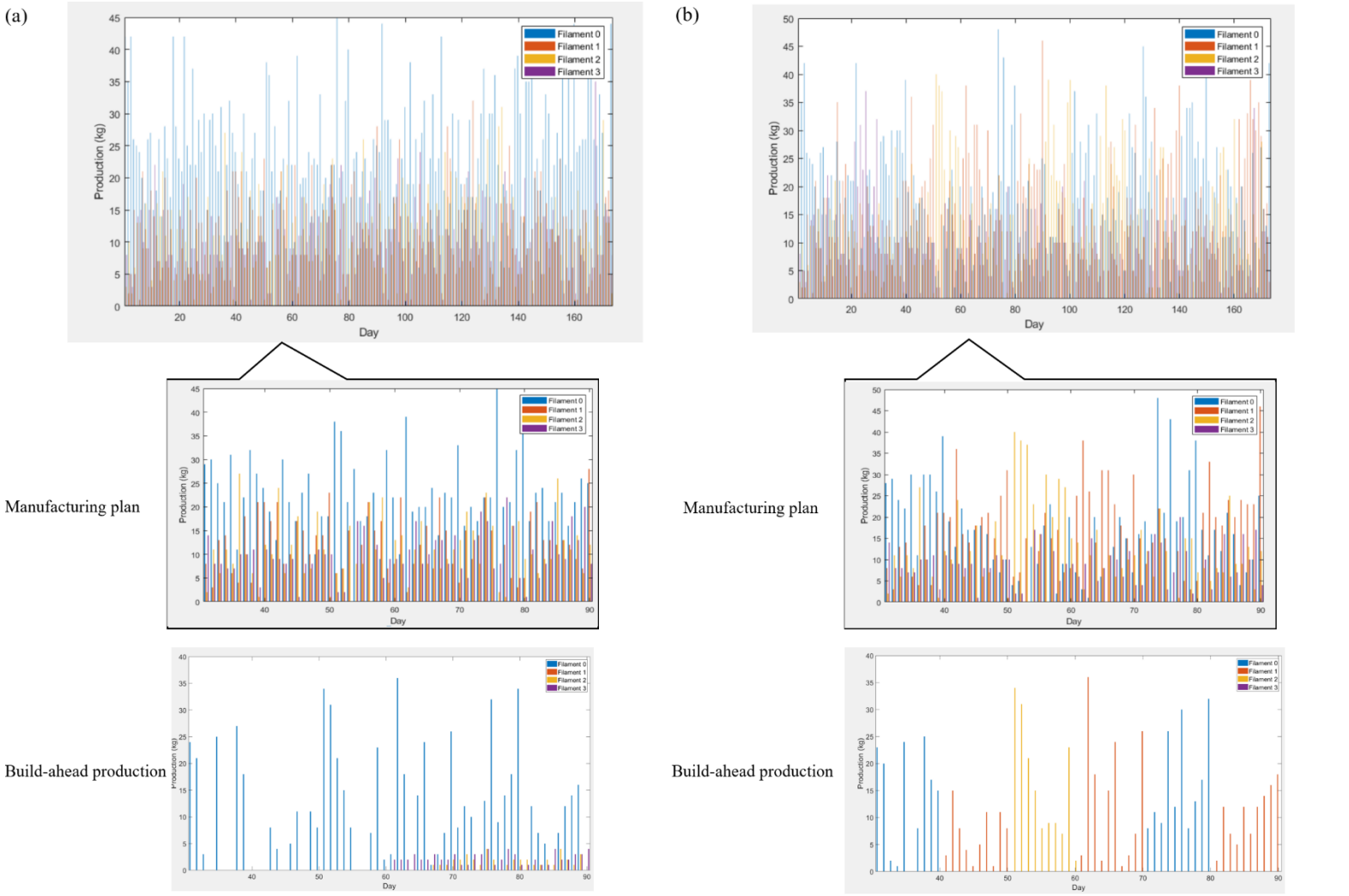

Figure 32. Production plan for each type of filament, (a) daily profit-driven recycling plan, (b) 10-day profit-driven recycling plan

Profit for Different Order Information

In this case, the influence of the order information pattern on the total profit is investigated. It is noticed that in some cases, the profit of a daily profit-driven recycling plan does not guarantee optimized profit over a period of days because it only considers the profit earned in each individual day, without taking into account any potential interdependencies or long-term effects such as inventory cost, customer preferences, and changes in the product quality, etc.

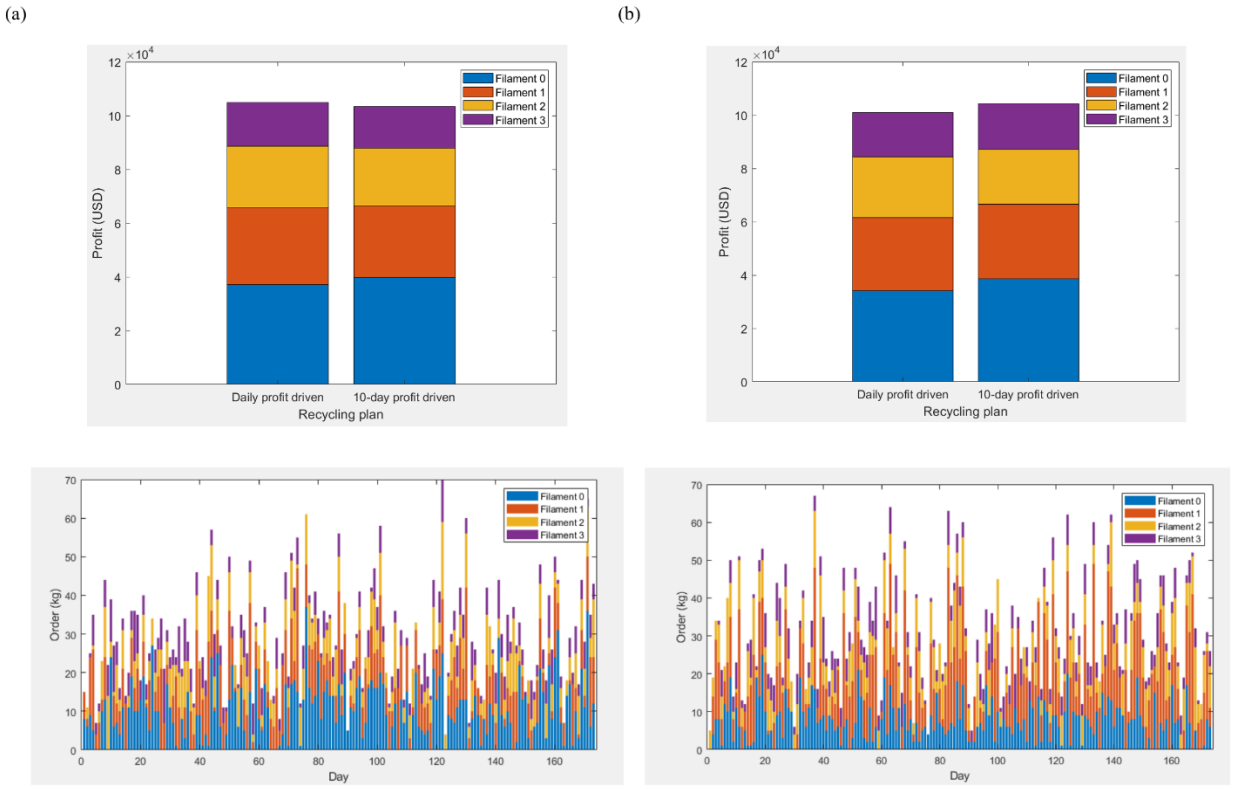

Figure 33. Profit for different order information

Figure 33 presents the profit comparison of the two methods based on two different order information. It is observed that in Figure 33 (a), the daily profit-driven recycling plan has a higher profit than the 10-day profit-driven. However, in Figure 33 (b), the 10-day profit-driven recycling plan has the higher profit. By comparing the order information, it is noticed that the order amount for filament 0 in Figure 33 (a) is higher than the number in Figure 33 (b). The increased order

amount for filament 0 will lead to the generation of revenue for the build-ahead productions. As discussed in the previous case study, the daily profit drive recycling plan has the preference of fabricating the filament 0. If in the order, the number of filament 0 dominates, it is recommended to select a daily profit-driven recycling plan. However, if customers prefer to order more recycled filaments, selecting 10-day profit-driven manufacturing will result in higher profit.

Profit for Different Pricing Strategies

In this case study, profit analyses are performed based on different pricing strategies. Four pricing strategies are considered in this case study. The first strategy is applying the market price. The price of the filaments is set based on the prevailing market conditions and the prices that competitors are charging for similar products or services. The second pricing strategy is using the profit margin price. It includes the cost of producing or acquiring the product, as well as any other expenses associated with delivering it to customers. The third pricing strategy is applying the bulk price. The strategy offers discounts to customers who purchase products or services in large quantities. The last strategy is the value-based pricing strategy. In this section, the transportation speed is selected as the value of the service. The strategy involves setting prices based on the perceived value that customers place on the speed of transportation. Some customers may be willing to pay more for faster shipping or transportation options. In this strategy, customers pay more if the order is delivered in less time. In this section, 10-day profit-driven recycling plan is considered for each pricing strategy.

Figure 34 presents the results of profit for each pricing strategy and the result where the number of orders increased by 40%. Specifically, with the amount of the order increasing by 40%: the profit in market price increases by 43.61%; the profit of the profit margin pricing strategy increases by 44.53%; the profit of the bulk price strategy increases by 36.59%; and the profit of value-based

increases by 43.91%. The reason why the profit bulk pricing strategy increases less than other strategies is that more amount of orders leads to more discount for bulk pricing strategies.

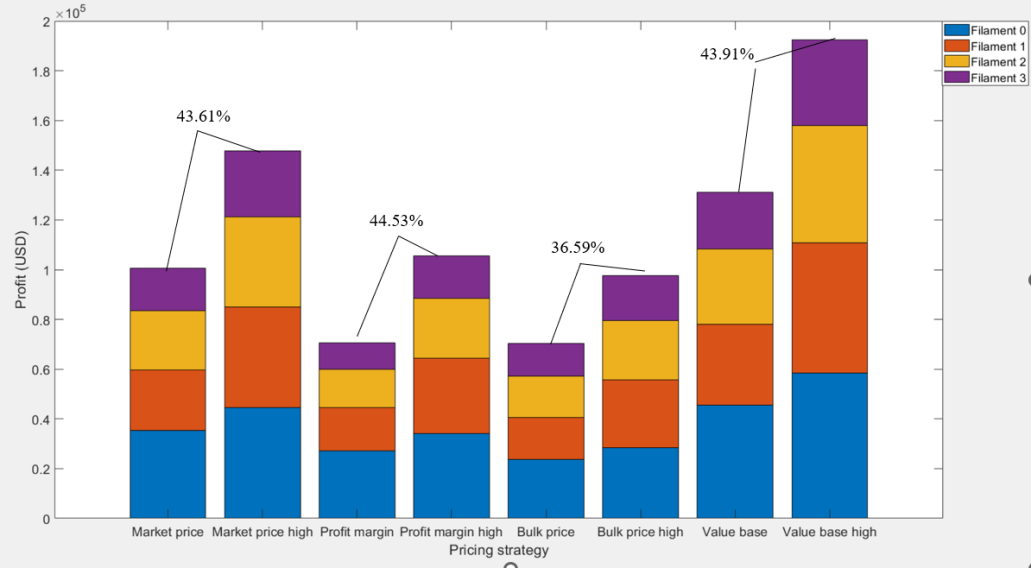

Figure 34. Profit from each pricing strategy

In addition, sensitivity analysis for material cost is performed for each pricing strategy. As shown in Figure 35, t is observed that by changing the material cost by 20%, the profit change for each pricing strategy is 3.62%, 9.19%, 12.79%, and 6.41%, correspondingly. The results indicate that the profit margin pricing strategy is more sensitive to the material price.

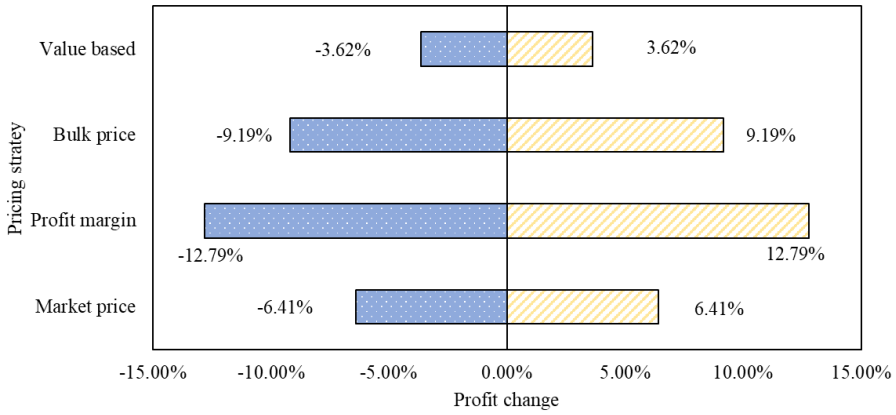

Figure 35. Sensitivity analysis on material cost

The sensitivity analysis on the electricity cost is presented in Figure 36. It indicates that the profit changes for each pricing strategy by changing the electricity cost by 20%. The results show that the profit margin pricing strategy is still more sensitive to the energy cost compared with other pricing strategies, where a 20% change in electricity unit price results in a 5.58% change in the profit.

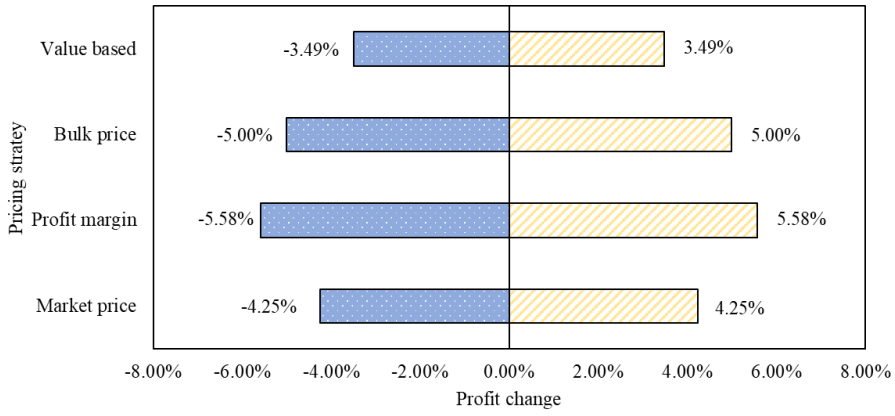

Figure 36. Sensitivity analysis on energy cost

4.3 Chapter Summary

In this Chapter, the framework for assessing the recyclability is proposed to analyze multiple recycling rounds with multiple sets of parameters, and an optimization algorithm is utilized to maximize profits in the production process for recycling the AM materials. In this Chapter, a series of tests are executed to investigate the changes in the recyclability of ABS during multiple rounds of recycling. Different AM process parameters are applied during the recycling process. The effects of layer thickness, printing speed, and raster angle on the printing quality in different recycling rounds are investigated. Case studies are designed to investigate the recyclability changes according to different rounds of recycling and the recyclability changes according to the parameters. Based on the results, the degradation of recyclability occurs during multiple recycling rounds. The degradation can be compensated by changing the printing parameters. In addition, it

is observed that the main effect influencing the printing quality is layer thickness according to DOE results of the case studies. The detailed results are summarized as follows.

1. The average ultimate tensile strength of the fabricate printed by virgin material is 34.181MPa, and the number decreases to 17.043 MPa using the filament in the third recycling round. The average ultimate compressive strain percentage is 2.011% for the fabricates printed with virgin material, and the number promotes to 5.600% in the third recycling round.

2. The surface quality of the parts printed using the recycling materials increases when the number of recycling round increase. The average Ra of the specimens printed by virgin material is 42.095 μm, and the number increases to 54.531 μm in the third recycling round.

3. The density of the parts fabricated by the materials decreases with the increase of the times of recycling, from 0.904 g/cm^3 as an average for the virgin material to 0.760 g/cm^3 as an average in the third recycling round.

4. With the increase of the recycling round, the average molecular weight decreases. The average number average molecular weight of the virgin material is 77,367 Dalton, and the average number decreased to 73,598 Dalton in the third recycling round. PDI of the material decreases when the time of recycling increases. A tendency for the degradation of PDI is observed in the results.

5. Based on the results of the case studies, it is recommended to apply the recycling plan that contains the build-ahead productions. The profit of the daily profit-driven recycling plan can be 31.02% higher than the order-driven recycling plan and the profit of the 10-day profit-driven can be 27.89% higher. It is noticed that if the amount order of filament is 0 dominants, selecting the daily profit-driven manufacturing will result in higher overall profit. If the demand for

recycled filaments increases, selecting a 10-day profit-driven recycling plan may lead to higher profit.

6. Different pricing strategies are compared in the case study. Among the pricing strategies, the profit margin price is more sensitive to the material price. Results also indicate that the profit margin pricing strategy is more sensitive to the electricity price compared with other pricing strategies.

The key lessons envisioned from the study results are stated as follows. Firstly, the degradation of the fabrication occurs consistently in multiple recycling rounds. The degradation is reflected in multiple aspects, including tensile strength, surface quality, density, and molecular weight distribution. Secondly, changing the layer thickness is more effective in enhancing the mechanical properties than other printing parameters in multiple recycling rounds. To compensate for the degradation of the AM fabricated parts in multiple recycling processes, selecting the proper layer thickness is more effective.

The limitations of this study are mainly threefold. First, in this research, only 3 rounds of recycling were performed due to the time-intensive data collection process, where multiple measurements need to be taken for each round of recycling with different sets of process parameters and replications. The results of this study will be more comprehensive if more times of recycling can be conducted. Second, this research only studied the material recyclability of ABS. The findings may be different for other AM thermoplastics such as Nylon and PLA. Third, a specific FDM printer was used in experiments with limitations on process parameter settings. More process parameters with broader ranges of values should be investigated for more comprehensive results. As

The results of this study can be used in multiple aspects. The profitability analysis identifies the key cost drivers in the manufacturing process, including the cost of raw materials, labor, equipment, and energy. This information can be used to optimize the production process and reduce costs. It helps to identify the key cost drivers in the manufacturing process, including the cost of raw materials, labor, equipment, and energy. The information can be used to optimize the production process and reduce costs. The results can be used to evaluate the performance of the recycling plan against established targets and benchmarks. It can help identify areas of improvement and optimize the production process for maximum profitability. By understanding the costs of production, the pricing strategy can be developed to ensure profitability while remaining competitive in the market. The cost-benefit analysis provides decision-makers with a clear understanding of the financial implications of different decisions related to the recycling plan. This can help ensure that decisions are based on sound financial considerations and can optimize profitability.

To extend this research, future studies will be conducted to explore recycling other types of AM thermoplastics such as PLA and Nylon, considering wider ranges of printing parameters, and investigating additional recycling rounds. The general model to predict the material recyclability of each recycling round and different printing parameters will be generated using other methodologies such as multi-objective neural networking, multiple linear regression, data mining, etc. The optimization studies will be performed with the generated model to maximize the recyclability of the thermoplastics in AM. Future work should also be focused on the potential areas of research and development that can further enhance the effectiveness and sustainability of the production process. The cost model now has multiple assumptions to simplify the calculations. Future works can be applied to the model with more real-world data and nonlinear relationships to better simulate the situations.

Chapter V. Academic Contributions

AM has been applied in different industry fields for decades since its advantages compared with conventional manufacturing. With the growing interest in developing AM, some potential sustainability issues have been presented. Three research questions are proposed in this dissertation based on the potential sustainability issues. To enlarge the advantages of AM technologies applied in the supply chain, a cost model is established to analyze the sustainability of an AM-integrated supply chain. Results indicate that the overall cost of AM integrated supply chain is 31.46% less than the TM supply chain. To further optimize the cost of the AM-integrated PIT supply chain structure, the offline and the online route design problem are formulated and solved using both DP and heuristic algorithms. For the route design problem in AM supply chain, the DP approach is better when the amount of orders is small. However, the heuristic method performs better when the number of orders increases. The results of route design problems also indicate that the optimized sequence saves the average cost per order by 4.80% to 14.04% depending on the order received per day. The proposed algorithm also delivers orders with a single vehicle during work hour compared with FOFD order. To analyze the environmental impact of AM technologies adopted in the supply chain, a GHG emission model of the AM-integrated PIT supply chain structure is established. AM integrated PIT supply chain structure saves GHG emissions by 26.43%. In addition, a framework to estimate the recyclability of the AM material in multiple recycling rounds is proposed. Results indicate that UTS degradation after each recycling round varies from 27% to 50%, surface roughness increases by 29.54% after three rounds of recycling, and molecular weight distribution of recycling presents an obvious shift after recycling rounds. With the results, it is possible to compensate for the material degradation during recycling with proper adjusting fabricating parameters.

The investigation of a unique PIT supply chain structure, where an AM machine is installed on a truck, presents a novel approach that integrates production, inventory, and transportation into one streamlined process. This innovative concept challenges traditional supply chain paradigms by enabling on-demand production at the point of need, eliminating the need for large, centralized manufacturing facilities. By leveraging the mobility of the AM machine, products can be manufactured directly at the location where they are required, minimizing lead times and reducing transportation costs. This novel supply chain structure not only offers increased flexibility and responsiveness but also has the potential to revolutionize the way goods are produced and distributed.

Furthermore, the novelty extends to the infrastructure of analyzing recyclability and developing recycling plans for 3D printing materials. As AM gains prominence, there is a growing need to address the sustainability aspect of the technology. The ability to assess the recyclability of 3D printing materials and establish effective recycling processes is a significant advancement in promoting circular economy principles within the AM industry. By developing innovative techniques and strategies for material recycling, the environmental impact of 3D printing can be minimized, reducing waste and contributing to a more sustainable supply chain.

The results of this dissertation can be used by decision-makers in the manufacturing industry when considering replacing new AM technologies or updating the current production line toward sustainable AM. The investigation of both the unique supply chain structure with an AM machine installed on a truck and the infrastructure for analyzing recyclability and developing recycling plans for 3D printing materials represents a pioneering contribution to the field. These novel approaches have the potential to reshape traditional manufacturing and supply chain practices, driving efficiency, sustainability, and adaptability in an increasingly dynamic and environmentally

conscious world. Some business-related factors such as order delivery schedule, rush order percentage, and other material-oriented factors are studied and their impact on the total supply chain cost as well as the total supply chain GHG emission is discussed in the case studies. This will help the manufacturers of AM better evaluate the sustainability of the AM supply chain. The result of the waste recycling data can be referred to determine the proper printing parameters for AM material in different recycling conditions. The models generated by DOE are feasible for AM manufacturers to evaluate the recyclability of the material according to its material properties and process data. For material designers, the outcome can be used to develop sustainable recyclable 3D printing materials based on their chemical properties. Additionally, the results of the dissertation can be used to promote awareness of sustainability practices in the advanced manufacturing industry. The results of this work can help develop the culture of public sustainability.

Publications

Journal Papers

1. **Di, L.**, Yang, Y., 2022, Towards closed-loop Material flow in additive manufacturing: Recyclability analysis of thermoplastic waste. *Journal of Cleaner Production*, 132427. (**IF=11.072**)
2. **Di, L.**, Yang, Y., 2022, Greenhouse Gas Emission Analysis of Integrated Production-Inventory-Transportation Supply Chain Enabled by Additive Manufacturing. *Journal of Manufacturing Science and Engineering*. (**IF=3.952**)
3. **Di, L.**, Yang, Y., 2020, Cost Modeling and Evaluation of Direct Metal Laser Sintering with Integrated Dynamic Process Planning. *Sustainability* 2021, 13, 319. (**IF=3.889**)
4. **Di, L.**, Wang, S., Yang, Y., 2023, Additive Manufacturing Thermoplastic Recycling: Profit-driven Planning and Optimization, *Journal of Cleaner Production.* (**IF=11.072**), under review
5. Cui, W., Yang, Y., **Di, L.**, Dababneh, F., 2021, Additive manufacturing-enabled supply chain: Modeling and case studies on local, integrated production-inventory-transportation structure. *Additive Manufacturing*, Vol.48. (**IF=11.632**)
6. Cui, W., Yang, Y., **Di, L.**, 2021, Hybrid Statis-Dynamic Delivery Route Design in Additive Manufacturing-Enabled Supply Chain, *International Journal of Production Economics*, 247, 132427. (**IF=11.251**)
7. Yang, Y., Zhao, J., **Di, L.**, Md Humaun, K., 2023, Driving Additive Manufacturing Towards Circular Economy: State-of-the-Art and Future Research Directions, *3D Printing and Additive Manufacturing.* (**IF=5.355**), under review.
8. Dababneh, F., Yang, Y., **Di, L.**, Hussein, R., 2021, Investigation of Third-Party Electric Vehicle Battery Remanufacturing Supply Chains: Modeling and Case Studies, *Journal of Cleaner Production*. (**IF=11.072**), Under Review.

Conference Proceedings

1. Ali, S., Yang, Y., **Di, L.,** Design of 3D Printable LED Heat Sink Inspired by Firefly Wings *2023 MSEC Manufacturing Science & Engineering Conference*. Under review.
2. Aman, M., Yang, Y., **Di, L.**, Experimental Study of Microscopic Morphology and Material Property for Recycled Polyamide 12 Powder in Selective Laser Sintering, *2022 MSEC Manufacturing Science & Engineering Conference*.
3. **Di, L.**, Manish, G., Yang, Y., Cui, W., 2021. Greenhouse Gas Emission Analysis of Integrated Production-Inventory Transportation Supply Chain Enabled by Additive Manufacturing, *2021 MSEC Manufacturing Science & Engineering Conference*.
4. Kan, C., Ye, Z., Yang, Y., **Di, L.**, Shah, D., Multi-Extrusion Additive Manufacturing for Error Compensation: A Demonstrative Case Study, *ASME 2020 15th International Manufacturing Science and Engineering Conference*.
5. Wang. S., Sarrafan A., Hoang T., **Di. L**, Yang Y., An Optimal Control Approach for Additive Manufacturing Production with Waste Recycling Process, *IEEE Conference on Decision and Control*, Singapore, under review (2023).

References

[1] S. Ford and M. Despeisse, "Additive manufacturing and sustainability: An exploratory study of the advantages and challenges," *Journal of Cleaner Production*, 2015. doi: 10.1016/j.jclepro.2016.04.150.

[2] T. D. Ngo, A. Kashani, G. Imbalzano, K. T. Q. Nguyen, and D. Hui, "Additive manufacturing (3D printing): A review of materials, methods, applications and challenges," *Composites Part B: Engineering*. 2018. doi: 10.1016/j.compositesb.2018.02.012.

[3] B. Durakovic, "Design for additive manufacturing: Benefits, trends and challenges," *Periodicals of Engineering and Natural Sciences*, 2018, doi: 10.21533/pen.v6i2.224.

[4] Wohler's Associates, "Wohler's Report 2022: 3D Printing and Additive Manufacturing Global State of the Industry," 2022.

[5] "3D printing scales up: Digital manufacturing: There is a lot of hype around 3D printing. But it is fast becoming integrated with mainstream manufacturing," *Economist (United Kingdom)*, 2013.

[6] S. A. M. Tofail, E. P. Koumoulos, A. Bandyopadhyay, S. Bose, L. O'Donoghue, and C. Charitidis, "Additive manufacturing: scientific and technological challenges, market uptake and opportunities," *Materials Today*. 2018. doi: 10.1016/j.mattod.2017.07.001.

[7] H. Moens, N. Neophytou, and F. Flamigni, "KIC Added-value Manufacturing: Exploiting synergies and complementarities with EU policies and programmes," *EIT Infoday*, no. February, 2016.

[8] L. Chen, Y. He, Y. Yang, S. Niu, and H. Ren, "The research status and development trend of additive manufacturing technology," *International Journal of Advanced Manufacturing Technology*. 2017. doi: 10.1007/s00170-016-9335-4.

[9] F. Wang, S. Fathizadan, F. Ju, K. Rowe, and N. Hofmann, "Print Surface Thermal Modeling and Layer Time Control for Large-Scale Additive Manufacturing," *IEEE Transactions on Automation Science and Engineering*, 2021, doi: 10.1109/TASE.2020.3001047.

[10] K. M. M. Billah *et al.*, "Large-scale additive manufacturing of self-heating molds," *Addit Manuf*, 2021, doi: 10.1016/j.addma.2021.102282.

[11] H. Shen, L. Pan, and J. Qian, "Research on large-scale additive manufacturing based on multi-robot collaboration technology," *Addit Manuf*, 2019, doi: 10.1016/j.addma.2019.100906.

[12] K. Oettmeier and E. Hofmann, "Impact of additive manufacturing technology adoption on supply chain management processes and components," *Journal of Manufacturing Technology Management*, 2016, doi: 10.1108/JMTM-12-2015-0113.

[13] K. Marchese, C. Haley, and J. Crane, "3D opportunity for the supply chain. Additive manufacturing delivers.," *Deloitte University Press*, 2015.

[14] M. Attaran, "The rise of 3-D printing: The advantages of additive manufacturing over traditional manufacturing," *Bus Horiz*, vol. 60, no. 5, pp. 677–688, 2017, doi: https://doi.org/10.1016/j.bushor.2017.05.011.

[15] D. Thomas, "Costs, benefits, and adoption of additive manufacturing: a supply chain perspective," *International Journal of Advanced Manufacturing Technology*, 2016, doi: 10.1007/s00170-015-7973-6.

[16] United States Environmental Protection Agency, "Sources of Greenhouse Gas Emissions," *Climate Change*, 2019.

[17] W. Cui, Y. Yang, L. Di, and F. Dababneh, "Additive Manufacturing-Enabled Supply Chain: Modeling and Case Studies on Local, Integrated Production-Inventory-Transportation Structure," *Addit Manuf*, vol. 48, p. 102471, 2021.

[18] L. Di and Y. Yang, "Greenhouse Gas Emission Analysis of Integrated Production-Inventory-Transportation Supply Chain Enabled by Additive Manufacturing," *J Manuf Sci Eng*, vol. 144, no. 3, Aug. 2021, doi: 10.1115/1.4051887.

[19] Z. D. Kenger, C. Koc, and E. Ozceylan, "Integrated Disassembly Line Balancing and Routing Problem with Mobile Additive Manufacturing," *Int J Prod Econ*, vol. 235, p. 108088, 2021.

[20] DHL, "3D Printing and the Future of Supply Chains," *DHL Customer Solutions & Innovation*, 2016.

[21] M. Attaran, "Additive Manufacturing: The Most Promising Technology to Alter the Supply Chain and Logistics," *Journal of Service Science and Management*, 2017, doi: 10.4236/jssm.2017.103017.

[22] J. V. L. Silva and R. A. Rezende, "Additive manufacturing and its future impact in logistics," in *IFAC Proceedings Volumes (IFAC-PapersOnline)*, 2013. doi: 10.3182/20130911-3-BR-3021.00126.

[23] F. A. Cruz Sanchez, H. Boudaoud, S. Hoppe, and M. Camargo, "Polymer recycling in an open-source additive manufacturing context: Mechanical issues," *Addit Manuf*, 2017, doi: 10.1016/j.addma.2017.05.013.

[24] J. Hopewell, R. Dvorak, and E. Kosior, "Plastics recycling: Challenges and opportunities," *Philosophical Transactions of the Royal Society B: Biological Sciences*. 2009. doi: 10.1098/rstb.2008.0311.

[25] D. J. Byard, A. L. Woern, R. B. Oakley, M. J. Fiedler, S. L. Snabes, and J. M. Pearce, "Green fab lab applications of large-area waste polymer-based additive manufacturing," *Addit Manuf*, 2019, doi: 10.1016/j.addma.2019.03.006.

[26] D. Strong, M. Kay, B. Conner, T. Wakefield, and G. Manogharan, "Hybrid manufacturing – integrating traditional manufacturers with additive manufacturing (AM) supply chain," *Addit Manuf*, 2018, doi: 10.1016/j.addma.2018.03.010.

[27] C. Feldmann and A. Pumpe, "A holistic decision framework for 3D printing investments in global supply chains," in *Transportation Research Procedia*, 2017. doi: 10.1016/j.trpro.2017.05.451.

[28] E. Özceylan, C. Çetinkaya, N. Demirel, and O. Sabırlıoğlu, "Impacts of Additive Manufacturing on Supply Chain Flow: A Simulation Approach in Healthcare Industry," *Logistics*, 2017, doi: 10.3390/logistics2010001.

[29] M. C. Chiu and Y. H. Lin, "Simulation based method considering design for additive manufacturing and supply chain An empirical study of lamp industry," *Industrial Management and Data Systems*, 2016, doi: 10.1108/IMDS-07-2015-0266.

[30] A. S. Mhapsekar, "A Methodology to Estimate Supply Chain Cost of Low Demand Parts," 2015.

[31] A. S. Mhapsekar and A. S. Mhapsekar, "A Methodology to Estimate Supply Chain Cost of Low Demand Parts A METHODOLOGY TO ESTIMATE DEMAND PARTS Master of Science in Industrial Engineering Thesis Committee : Dr . Scott Grasman," 2015.

[32] A. Emelogu, M. Marufuzzaman, S. M. Thompson, N. Shamsaei, and L. Bian, "Additive manufacturing of biomedical implants: A feasibility assessment via supply-chain cost analysis," *Addit Manuf*, 2016, doi: 10.1016/j.addma.2016.04.006.

[33] J. Holmström, J. Partanen, J. Tuomi, and M. Walter, “Rapid manufacturing in the spare parts supply chain: Alternative approaches to capacity deployment,” *Journal of Manufacturing Technology Management*, vol. 21, no. 6, pp. 687–697, 2010, doi: 10.1108/17410381011063996.

[34] M. Khorram Niaki and F. Nonino, “Additive manufacturing management: a review and future research agenda,” *Int J Prod Res*, vol. 55, no. 5, pp. 1419–1439, 2017.

[35] O. Jumaah, D. Candidate, and P. Szary, “A Study on 3D Printing and its Effects on the Future of Transportation,” no. September, 2018.

[36] S. Zanoni, M. Ashourpour, A. Bacchetti, M. Zanardini, and M. Perona, “Supply chain implications of additive manufacturing: a holistic synopsis through a collection of case studies,” *International Journal of Advanced Manufacturing Technology*, vol. 102, no. 9–12, pp. 3325–3340, 2019, doi: 10.1007/s00170-019-03430-w.

[37] B. Mohajeri, S. H. Khajavi, T. Nyberg, and S. H. Khajavi, “Supply chain modifications to improve additive manufacturing cost-benefit balance,” *25th Annual International Solid Freeform Fabrication Symposium &#65533; An Additive Manufacturing Conference, SFF 2014*, no. Figure 1, pp. 1304–1314, 2014.

[38] A. I. Pettersson and A. Segerstedt, “To Evaluate Cost Savings in a Supply Chain : Two Examples from Ericsson in the Telecom Industry,” *Operations and Supply Chain Management: An International Journal*, vol. 6, no. 3, pp. 94–102, 2014, doi: 10.31387/oscm0150094.

[39] R. Cassia, M. Nocioni, N. Correa-Aragunde, and L. Lamattina, “Climate change and the impact of greenhouse gasses: CO2 and NO, friends and foes of plant oxidative stress,” *Frontiers in Plant Science*. 2018. doi: 10.3389/fpls.2018.00273.

[40] M. Meinshausen *et al.*, “Greenhouse-gas emission targets for limiting global warming to 2°C,” *Nature*, 2009, doi: 10.1038/nature08017.

[41] C. Oertel, J. Matschullat, K. Zurba, F. Zimmermann, and S. Erasmi, “Greenhouse gas emissions from soils—A review,” *Chemie der Erde*. 2016. doi: 10.1016/j.chemer.2016.04.002.

[42] M. C. Heller and G. A. Keoleian, “Greenhouse Gas Emission Estimates of U.S. Dietary Choices and Food Loss,” *J Ind Ecol*, 2015, doi: 10.1111/jiec.12174.

[43] United States Environmental Protection Agency, “Sources of Greenhouse Gas Emissions,” 2020. https://www.epa.gov/ghgemissions/sources-greenhouse-gas-emissions

[44] W. R. Moomaw, “Industrial emissions of greenhouse gases,” *Energy Policy*. 1996. doi: 10.1016/s0301-4215(96)80360-0.

[45] E. L. Plambeck, “Reducing greenhouse gas emissions through operations and supply chain management,” *Energy Econ*, 2012, doi: 10.1016/j.eneco.2012.08.031.

[46] EPA, “Greenhouse Gases Equivalencies Calculator - Calculations and References,” *Energy and the Environment*, 2017.

[47] C. Jira and M. W. Toffel, “Engaging supply chains in climate change,” *Manufacturing and Service Operations Management*, 2013, doi: 10.1287/msom.1120.0420.

[48] M. Ö. Arıoğlu Akan, D. G. Dhavale, and J. Sarkis, “Greenhouse gas emissions in the construction industry: An analysis and evaluation of a concrete supply chain,” *J Clean Prod*, 2017, doi: 10.1016/j.jclepro.2017.07.225.

[49] E. L. Plambeck, “Reducing greenhouse gas emissions through operations and supply chain management,” *Energy Econ*, 2012, doi: 10.1016/j.eneco.2012.08.031.

[50] B. Sundarakani, R. De Souza, M. Goh, S. M. Wagner, and S. Manikandan, "Modeling carbon footprints across the supply chain," in *International Journal of Production Economics*, 2010. doi: 10.1016/j.ijpe.2010.01.018.

[51] N. M. Modak, D. K. Ghosh, S. Panda, and S. S. Sana, "Managing green house gas emission cost and pricing policies in a two-echelon supply chain," *CIRP J Manuf Sci Technol*, 2018, doi: 10.1016/j.cirpj.2017.08.001.

[52] D. J. M. Flower and J. G. Sanjayan, "Green house gas emissions due to concrete manufacture," *Int J Life Cycle Assess*, 2007, doi: 10.1007/s11367-007-0327-3.

[53] X. Tao, C. Mao, F. Xie, G. Liu, and P. P. Xu, "Greenhouse gas emission monitoring system for manufacturing prefabricated components," *Autom Constr*, 2018, doi: 10.1016/j.autcon.2018.05.015.

[54] B. He, Y. Liu, L. Zeng, S. Wang, D. Zhang, and Q. Yu, "Product carbon footprint across sustainable supply chain," *J Clean Prod*, 2019, doi: 10.1016/j.jclepro.2019.118320.

[55] S. Parashar, G. Sood, and N. Agrawal, "Modelling the enablers of food supply chain for reduction in carbon footprint," *J Clean Prod*, 2020, doi: 10.1016/j.jclepro.2020.122932.

[56] E. D. R. Santibanez-Gonzalez, "A modelling approach that combines pricing policies with a carbon capture and storage supply chain network," *J Clean Prod*, 2017, doi: 10.1016/j.jclepro.2017.03.181.

[57] G. Leonzio and E. Zondervan, "Analysis and optimization of carbon supply chains integrated to a power to gas process in Italy," *J Clean Prod*, 2020, doi: 10.1016/j.jclepro.2020.122172.

[58] B. Cheang, X. Gao, A. Lim, H. Qin, and W. Zhu, "Multiple pickup and delivery traveling salesman problem with last-in-first-out loading and distance constraints," *Eur J Oper Res*, 2012, doi: 10.1016/j.ejor.2012.06.019.

[59] M. Keskin, B. Çatay, and G. Laporte, "A simulation-based heuristic for the electric vehicle routing problem with time windows and stochastic waiting times at recharging stations," *Comput Oper Res*, 2021, doi: 10.1016/j.cor.2020.105060.

[60] S. Dash, O. Günlük, A. Lodi, and A. Tramontani, "A time bucket formulation for the traveling salesman problem with time windows," *INFORMS J Comput*, 2012, doi: 10.1287/ijoc.1100.0432.

[61] R. Baldacci, A. Mingozzi, and R. Roberti, "New state-space relaxations for solving the traveling salesman problem with time windows," *INFORMS J Comput*, 2012, doi: 10.1287/ijoc.1110.0456.

[62] K. Lian, A. B. Milburn, and R. L. Rardin, "An improved multi-directional local search algorithm for the multi-objective consistent vehicle routing problem," *IIE Transactions (Institute of Industrial Engineers)*, 2016, doi: 10.1080/0740817X.2016.1167288.

[63] M. M. Aguayo, S. C. Sarin, and H. D. Sherali, "Solving the single and multiple asymmetric Traveling Salesmen Problems by generating subtour elimination constraints from integer solutions," *IISE Trans*, 2018, doi: 10.1080/24725854.2017.1374580.

[64] L. Zhen, W. Lv, K. Wang, C. Ma, and Z. Xu, "Consistent vehicle routing problem with simultaneous distribution and collection," *Journal of the Operational Research Society*, 2020, doi: 10.1080/01605682.2019.1590134.

[65] L. Zhang, S. Wang, and X. Qu, “Optimal electric bus fleet scheduling considering battery degradation and non-linear charging profile,” *Transp Res E Logist Transp Rev*, 2021, doi: 10.1016/j.tre.2021.102445.

[66] M. Pollák, J. Kaščak, M. Telišková, and J. Tkáč, “Design of the 3D printhead with extruder for the implementation of 3D printing from plastic and recycling by industrial robot,” *TEM Journal*, 2019, doi: 10.18421/TEM83-02.

[67] F. R. Beltrán *et al.*, “Evaluation of the Technical Viability of Distributed Mechanical Recycling of PLA 3D Printing Wastes,” *Polymers (Basel)*, 2021, doi: 10.3390/polym13081247.

[68] M. A. Kreiger, M. L. Mulder, A. G. Glover, and J. M. Pearce, “Life cycle analysis of distributed recycling of post-consumer high density polyethylene for 3-D printing filament,” *J Clean Prod*, vol. 70, pp. 90–96, 2014, doi: 10.1016/j.jclepro.2014.02.009.

[69] P. Zhao, C. Rao, F. Gu, N. Sharmin, and J. Fu, “Close-looped recycling of polylactic acid used in 3D printing: An experimental investigation and life cycle assessment,” *J Clean Prod*, 2018, doi: 10.1016/j.jclepro.2018.06.275.

[70] N. Vidakis *et al.*, “Sustainable additive manufacturing: Mechanical response of polyamide 12 over multiple recycling processes,” *Materials*, 2021, doi: 10.3390/ma14020466.

[71] M. Spoerk, F. Arbeiter, I. Raguž, C. Holzer, and J. Gonzalez-Gutierrez, “Mechanical recyclability of polypropylene composites produced by material extrusion-based additive manufacturing,” *Polymers (Basel)*, 2019, doi: 10.3390/polym11081318.

[72] J. Fernandes, A. M. Deus, L. Reis, M. F. Vaz, and M. Leite, “Study of the influence of 3D printing parameters on the mechanical properties of PLA,” in *Proceedings of the*

International Conference on Progress in Additive Manufacturing, 2018. doi: 10.25341/D4988C.

[73] R. Hashemi Sanatgar, C. Campagne, and V. Nierstrasz, "Investigation of the adhesion properties of direct 3D printing of polymers and nanocomposites on textiles: Effect of FDM printing process parameters," *Appl Surf Sci*, 2017, doi: 10.1016/j.apsusc.2017.01.112.

[74] C. F. Durach, S. Kurpjuweit, and S. M. Wagner, "The impact of additive manufacturing on supply chains," *International Journal of Physical Distribution and Logistics Management*, 2017, doi: 10.1108/IJPDLM-11-2016-0332.

[75] M. Ashour Pour, S. Zanoni, A. Bacchetti, M. Zanardini, and M. Perona, "Additive manufacturing impacts on a two-level supply chain," *International Journal of Systems Science: Operations and Logistics*, vol. 6, no. 1, pp. 1–14, 2019, doi: 10.1080/23302674.2017.1340985.

[76] V. Verboeket and H. Krikke, "Additive Manufacturing: A Game Changer in Supply Chain Design," *Logistics*, 2019, doi: 10.3390/logistics3020013.

[77] Z. D. Kenger, C. Koc, and E. Ozceylan, "Integrated Disassembly Line Balancing and Routing Problem with Mobile Additive Manufacturing," *Int J Prod Econ*, vol. 235, p. 108088, 2021.

[78] "Insoles free 3d model," 2015. http://3dmag.org/en/market/item/948/

[79] AVCalc LLC, "Price of Cork, Solid."

[80] Plastics Insight, "ABS Plastic (ABS): Production, Market, Price and its Properties."

[81] Buckskin Leather Company, "Leather Price List."

[82] U.S. Bureau of Labor Statistics, "Occupational Employment and Wages, May 2019 51-6042 Shoe Machine Operators and Tenders," 2020. https://www.bls.gov/oes/current/oes516042.htm

[83] "Truck Movement in Response to Demands of COVID-19 – March 24, 2020," 2020. https://truckingresearch.org/2020/03/24/truck-movement-in-response-to-demands-of-covid-19-march-24-2020/

[84] U.S. Bureau of Labor Statistics, "Heavy and Tractor-trailer Truck Drivers," 2019. https://www.bls.gov/ooh/transportation-and-material-moving/heavy-and-tractor-trailer-truck-drivers.htm

[85] U.S. Department of Energy, "Average Fuel Economy by Major Vehicle Category." https://afdc.energy.gov/data/10310

[86] U.S. Energy Information Administration, "Weekly Retail Gasoline and Diesel Prices," 2020. https://www.eia.gov/dnav/pet/PET_PRI_GND_DCUS_STX_A.htm

[87] LoopNet, "Retail Storage Space," 2020.

[88] Simplify3D, "Filament Properties Table." https://www.simplify3d.com/support/materials-guide/properties-table/?highlight=nylon

[89] Public Utility Commission of Texas, "Public utility commission of Texas competitive markets division and retail electric service rate comparisons," 2020. https://www.puc.texas.gov/industry/electric/rates/RESrate/rate20/June20Rates.pdf

[90] T. Peng, "Energy Modelling for FDM 3D Printing from a Life Cycle Perspective," *International Journal of Manufacturing Research*, 2017, doi: 10.1504/ijmr.2017.10003722.

[91] T. Liu, L. Lei, K. Zheng, and K. Zhang, "Autonomous Platoon Control with Integrated Deep Reinforcement Learning and Dynamic Programming," *IEEE Internet Things J*, 2022, doi: 10.1109/JIOT.2022.3222128.

[92] H. Fan, P. K. Tarun, and V. C. P. Chen, "Adaptive value function approximation for continuous-state stochastic dynamic programming," *Comput Oper Res*, vol. 40, no. 4, 2013, doi: 10.1016/j.cor.2012.11.016.

[93] U.S. Bureau of Labor Statistics, "Occupational Employment and Wage Statistics," 2020. https://www.bls.gov/oes/current/oes533032.htm

[94] U.S. Energy Information Administration, "PETROLEUM & OTHER LIQUIDS," 2021. https://www.eia.gov/dnav/pet/pet_pri_gnd_dcus_stx_m.htm

[95] S. A. Rehman Khan and Z. Yu, "Introduction to supply chain management," in *EAI/Springer Innovations in Communication and Computing*, 2019. doi: 10.1007/978-3-030-15058-7_1.

[96] V. A. González-González, G. Neira-Velázquez, and J. L. Angulo-Sánchez, "Polypropylene chain scissions and molecular weight changes in multiple extrusion *," *Polym Degrad Stab*, 1998, doi: 10.1016/S0141-3910(96)00233-9.

[97] K. H. Schimmel and G. Heinrich, "The influence of the molecular weight distribution of network chains on the mechanical properties of polymer networks," *Colloid Polym Sci*, 1991, doi: 10.1007/BF00657430.

[98] R. W. Nunes, J. R. Martin, and J. F. Johnson, "Influence of molecular weight and molecular weight distribution on mechanical properties of polymers," *Polym Eng Sci*, 1982, doi: 10.1002/pen.760220402.

[99] M. Pérez, G. Medina-Sánchez, A. García-Collado, M. Gupta, and D. Carou, "Surface quality enhancement of fused deposition modeling (FDM) printed samples based on the selection of critical printing parameters," *Materials*, 2018, doi: 10.3390/ma11081382.

[100] D. Wu, Y. Wei, and J. Terpenny, "Predictive modelling of surface roughness in fused deposition modelling using data fusion," *Int J Prod Res*, 2019, doi: 10.1080/00207543.2018.1505058.

[101] V. D. Sagias, K. I. Giannakopoulos, and C. Stergiou, "Mechanical properties of 3D printed polymer specimens," *Procedia Structural Integrity*, vol. 10, pp. 85–90, 2018, doi: 10.1016/j.prostr.2018.09.013.

[102] M. Samykano, S. K. Selvamani, K. Kadirgama, W. K. Ngui, G. Kanagaraj, and K. Sudhakar, "Mechanical property of FDM printed ABS: influence of printing parameters," *International Journal of Advanced Manufacturing Technology*, vol. 102, no. 9–12, pp. 2779–2796, 2019, doi: 10.1007/s00170-019-03313-0.

[103] K. Mikula *et al.*, "3D printing filament as a second life of waste plastics—a review," *Environmental Science and Pollution Research*, vol. 28, no. 10, pp. 12321–12333, 2021, doi: 10.1007/s11356-020-10657-8.

[104] Filabot, "FILABOT EX6 FILAMENT EXTRUDER - STANDARD SERIES," 2014. https://www.filabot.com/collections/filabot-core/products/filabot-ex6-filament-extruder?gclid=Cj0KCQjwhLKUBhDiARIsAMaTLnF63QQ0MfuaR9mR8K9iA2_nHCnk_we6NONoOUs4ZSgnHGqpmCAyiR0aAoQzEALw_wcB

[105] Filabot, "FILABOT RECLAIMER." https://www.filabot.com/products/filabot-reclaimer-1?variant=33063213039691&currency=USD&utm_medium=product_sync&utm_source=google&utm_content=sag_organic&utm_campaign=sag_organic&gclid=CjwKCAjwrJ-

hBhB7EiwAuyBVXVHYFUEQI2yKkKfezIDv6ja2QtZHmKS5yYABqvDaJDg0ftcGFgbI8RoC1yQQAvD_BwE

[106] EIA, “Electric Power Monthly,” 2022. https://www.eia.gov/electricity/monthly/epm_table_grapher.php?t=epmt_5_6_a

[107] I. Kauppila, “The Best Pellet 3D Printers & Extruderse,” 2022. https://all3dp.com/1/cheaper-3d-printing-with-pellets/